AD-755 551

OPEN-WIRE TRANSMISSION LINES APPLIED TO THE MEASUREMENT OF THE MACROSCOPIC ELECTRICAL PROPERTIES OF A FOREST REGION

John Taylor, et al

Stanford Research Institute

Prepared for:

Army Electronics Command
Advanced Research Projects Agency

October 1971

DISTRIBUTED BY:

NTIS
National Technical Information Service
U. S. DEPARTMENT OF COMMERCE
5285 Port Royal Road, Springfield Va. 22151

TR ECOM-0220-42
Special Technical Report 42

Reports Control Symbol
OSD-1366

OPEN-WIRE TRANSMISSION LINES APPLIED TO THE MEASUREMENT OF THE MACROSCOPIC ELECTRICAL PROPERTIES OF A FOREST REGION

By: JOHN TAYLOR CHING CHUN HAN CHUNG LIEN TIEN GEORGE HAGN

Prepared for:

U.S. ARMY ELECTRONICS COMMAND
FORT MONMOUTH, NEW JERSEY 07703

CONTRACT DAAB07-70-C-0220

Sponsored by:

ADVANCED RESEARCH PROJECTS AGENCY (ARPA Order 371)
U.S. ARMY ELECTRONICS COMMAND

STANFORD RESEARCH INSTITUTE
Menlo Park, California 94025 · U.S.A.

NOTICES

Disclaimers

The findings in this report are not to be construed as an official Department of the Army position, unless so designated by other authorized documents.

The citation of trade names and names of manufacturers in this report is not to be construed as official Government indorsement or approval of commercial products or services referenced herein.

Disposition

Destroy this report when it is no longer needed. Do not return it to the originator.

UNCLASSIFIED

Security Classification

DOCUMENT CONTROL DATA - R & D

(Security classification of title, body of abstract and indexing annotation must be entered when the overall report is classified)

1. ORIGINATING ACTIVITY (Corporate author) Stanford Research Institute 333 Ravenswood Avenue Menlo Park, California 94025	2a. REPORT SECURITY CLASSIFICATION Unclassified 2b. GROUP N/A

3. REPORT TITLE

OPEN-WIRE TRANSMISSION LINES APPLIED TO THE MEASUREMENT OF THE MACROSCOPIC ELECTRICAL PROPERTIES OF A FOREST REGION

4. DESCRIPTIVE NOTES (Type of report and inclusive dates)

Special Technical Report 42

5. AUTHOR(S) (First name, middle initial, last name)

John Taylor Ching Chun Han Chung Lien Tien George Hagn

6. REPORT DATE	7a. TOTAL NO. OF PAGES	7b. NO. OF REFS
June 1972	150	16

8a. CONTRACT OR GRANT NO. DAAB07-70-C-0220 b. PROJECT NO. c. d.	9a. ORIGINATOR'S REPORT NUMBER(S) Special Technical Report 42 SRI Project 8663 9b. OTHER REPORT NO(S) (Any other numbers that may be assigned this report)

10. DISTRIBUTION STATEMENT

This document has been approved for public release and sale. It's distribution is unlimited.

11. SUPPLEMENTARY NOTES This work was initiated under Contract DA36-039 AMC-00040(E) (SRI Project 4240) and completed under the contract referenced in line 8a above.	12. SPONSORING MILITARY ACTIVITY Advanced Research Projects Agency and U.S. Army Electronics Command Fort Monmouth, New Jersey 07703

13. ABSTRACT

The theoretical capabilities of two-conductor, open-wire transmission lines (OWLs) as probes to measure the macroscopic electrical properties of a forest are examined under the premise that a forest can be represented as a lossy dielectric slab. A laboratory experiment with a line inserted in a relatively homogeneous, isotropic slab of Styrofoam was performed to verify certain approximations in the analysis of such a line when a void (hole) exists in the slab near the line. The effective sensing radius for a 300-ohm line is shown to be about one and one-half line spacings. The limitations of a transmission-line probe for inhomogeneous and anisotropic dielectrics are discussed.

The forest also is considered as a synthetic dielectric composed of lossy scatterers. The equivalent circuit of a short scatterer (length small relative to the RF wavelength) as a load on the transmission line is shown to be a lossy capacitor. The values of capacitance and resistance for isolated trees were measured and observed to depend on (among other things) tree height, diameter, conductivity, and distance from the line. A forest was simulated in the laboratory with wooden bars and also with metal rods positioned at random along a transmission line. The complex dielectric constant of the synthetic forest was deduced from the propagation constant of the line as determined from impedance bridge readings. The results were in reasonable

DD FORM 1 NOV 65 1473 (PAGE 1)

S/N 0101-807-6801

Ia

Unclassified

Security Classification

13. Abstract (concluded)

agreement with values obtained from a computer program for a transmission line loaded randomly with lossy shunt capacitors of a size and distribution similar to that of the simulated forest. The computer model was used to investigate the effect of the number of scatterers per wavelength along the line, and the electric susceptibility (ϵ_r - 1) was seen to increase linearly with the number of scatterers per wavelength. A brief investigation of the macroscopic electrical properties of a volume containing living vegetation in South Carolina produced results in general agreement with those already obtained in California, Washington, and Thailand.

It is concluded that a forest can be considered to act as a lossy dielectric slab whose electrical properties can be inferred from measurements with OWL probes--even when significant scatterers (e.g., tree trunks) are present; however, the results of such measurements (and particularly in other cases where anisotropy may be significant) must be interpreted with care. A future experiment is recommended where the measured OWL equivalent circuits of single trees are used--along with forest mensuration data (e.g., tree height, diameter and spacing distributions, etc.)--in the random scatterer computer program to estimate the effective electrical properties of an equivalent forest slab. If the results of these suggested experiments are positive, then a significant step will have been taken toward relating the type of forest descriptions currently being made by environmental scientists to the needs of researchers in the field of radio propagation and communications.

Ib

STANFORD RESEARCH INSTITUTE
Menlo Park, California 94025 · U.S.A.

TR ECOM-0220-42
October 1971
Special Technical Report 42

Reports Control Symbol
OSD-1366

OPEN-WIRE TRANSMISSION LINES APPLIED TO THE MEASUREMENT OF THE MACROSCOPIC ELECTRICAL PROPERTIES OF A FOREST REGION

By: JOHN TAYLOR CHING CHUN HAN CHUNG LIEN TIEN GEORGE HAGN

Prepared for:

U.S. ARMY ELECTRONICS COMMAND
FORT MONMOUTH, NEW JERSEY 07703

CONTRACT DAAB07-70-C-0220

SRI Project 8663

Approved by:

R. F. DALY, *Director*
Telecommunications Department

E. J. MOORE, *Executive Director*
Engineering Systems Division

Sponsored by:

ADVANCED RESEARCH PROJECTS AGENCY (ARPA Order 371)
U.S. ARMY ELECTRONICS COMMAND

II

ABSTRACT

The theoretical capabilities of two-conductor, open-wire transmission lines (OWLs) as probes to measure the macroscopic electrical properties of a forest are examined under the premise that a forest can be represented as a lossy dielectric slab. A laboratory experiment with a line inserted in a relatively homogeneous, isotropic slab of Styrofoam was performed to verify certain approximations in the analysis of such a line when a void (hole) exists in the slab near the line. The effective sensing radius for a 300-ohm line is shown to be about one and one-half line spacings. The limitations of a transmission-line probe for inhomogeneous and anisotropic dielectrics are discussed.

The forest also is considered as a synthetic dielectric composed of lossy scatterers. The equivalent circuit of a short scatterer (length small relative to the RF wavelength) as a load on the transmission line is shown to be a lossy capacitor. The values of capacitance and resistance for isolated trees were measured and observed to depend on (among other things) tree height, diameter, conductivity, and distance from the line. A forest was simulated in the laboratory with wooden bars and also with metal rods positioned at random along a transmission line. The complex dielectric constant of the synthetic forest was deduced from the propagation constant of the line as determined from impedance bridge readings. The results were in reasonable agreement with values obtained from a computer program for a transmission line loaded randomly with lossy shunt capacitors of a size and distribution similar to that of the simulated forest. The computer model was used to investigate the effect of the number of scatterers per wavelength along the line, and the electric susceptibility (ϵ_r - 1) was seen to increase linearly with the number of

scatterers per wavelength. A brief investigation of the macroscopic electrical properties of a volume containing living vegetation in South Carolina produced results in general agreement with those already obtained in California, Washington, and Thailand.

It is concluded that a forest can be considered to act as a lossy dielectric slab whose electrical properties can be inferred from measurements with OWL probes--even when significant scatterers (e.g., tree trunks) are present; however, the results of such measurements (and particularly in other cases where anisotropy may be significant) must be interpreted with care. A future experiment is recommended where the measured OWL equivalent circuits of single trees are used--along with forest mensuration data (e.g., tree height, diameter and spacing distributions, etc.)--in the random scatterer computer program to estimate the effective electrical properties of an equivalent forest slab. If the results of these suggested experiments are positive, then a significant step will have been taken toward relating the type of forest descriptions currently being made by environmental scientists to the needs of researchers in the field of radio propagation and communications.

CONTENTS

ILLUSTRATIONS

TABLES

Preceding page blank

SYMBOLS

ϵ	Dielectric Constant
ϵ_r	Complex Relative Dielectric Constant
ϵ_r'	Real Part of ϵ_r
ϵ_r''	Imaginary Part of ϵ_r
ϵ_o	Relative Dielectric Constant of Air
μ_r	Complex Relative Permeability
μ_r'	Real Part of μ_r
μ_r''	Imaginary Part of μ_r
μ_o	Relative Permeability of Air
Z_c	Characteristic Impedance of a Transmission Line
R_c	Real Part of Z_c
X_c	Imaginary Part of Z_c
Z_{co}	Characteristic Impedance of a Transmission Line in Air
Z_{sc}	Input Impedance of a Transmission Line Terminated in a Short Circuit
Z_{oc}	Input Impedance of a Transmission Line Terminated in an Open Circuit
Z_o	Intrinsic Impedance of Free Space
γ	Propagation Constant of a Transmission Line
α	Attenuation Constant--Real Part of γ
β	Phase Constant--Imaginary Part of γ
α_c	Attenuation Constant Due to Conductor Losses
δ	Loss Tangent
P	Fraction of Power Flowing in Void Region
λ	Wavelength

ζ	Impedance of the Medium
ζ_o	Impedance of Free Space (120π)
WC	Water Content
X_e	Electric Susceptibility
f	Wave Frequency
ω	Angular (radian) Wave Frequency
G	Real Part of Equivalent Shunt Admittance
B	Imaginary Part of Equivalent Shunt Admittance
R	Equivalent Shunt Resistance of Scatterer
C	Equivalent Shunt Capacitance of Scatterer
k_o	Wave Number in Air
℄	Center Line of Conductor or Scatterer
a	Radius of Conductors
b	Half the Distance between Conductors
c	Half the Distance between Bipolar Centers of the Conductors
r	Radius of Circle from Center of Bipolar Coordinate System (or Center of Conductor)

I INTRODUCTION

In the study of the propagation of radio waves through a forest, a model has been suggested and demonstrated as feasible in which the forest is represented by one or more layers of dielectric above a flat earth.[1-6*] The purpose of the investigation at the University of South Carolina (the results of which are reported here) was to develop the theory pertaining to the use of open-wire transmission-line (OWL) probes for measuring and calculating the equivalent dielectric constant and loss tangent (or conductivity) of the forest region for use in this propagation model. Preliminary results from this study were reported in Ref. 7.

Many different techniques for the measurement of the dielectric constant and the loss tangent of a continuous medium have been developed. These techniques generally fall into two categories: those which use transmission through a sample and those which use the reflection from the sample. The open-wire transmission-line method discussed in this report belongs to the first category; it has been used to measure the effective macroscopic electrical properties of forest regions in the United States[8,9,10] and in Thailand.[11,12,13] However, when the open-wire line is used for this purpose, several questions arise which must be answered before the validity of the measuring technique can be established. One such question concerns how well a group of randomly spaced, discrete scatterers can be represented in the model by a single parameter (the complex dielectric constant) and whether or not this parameter has the same significance for plane-wave propagation that it does for a TEM wave--or quasi-TEM wave--on a transmission line. In regard to the measurement of this parameter with a transmission line, several other questions arise. For example, how does the support structure for the line affect the accuracy of the measurement and what is the relative effect of scatterers at different distances from the line?

---

*References are listed at the end of the report.

One support structure considered for use on this project consisted of a two-wire line covered with a fiberglass cylinder.[8] This type of line could be inserted conveniently into dense vegetation while still maintaining the tolerance on conductor spacing. Unfortunately, since the protective fiberglass cylinder excluded vegetation from the immediate vicinity of the line, the following questions arose: How must the computational formulas be modified to take into account the absence of the forest medium in the immediate vicinity of the line? How is the accuracy of the measurement affected? These questions have been considered and are answered in some detail in this report.

The effect of scatterers near a two-wire transmission line was investigated experimentally in the laboratory and in the field. Dry and wet wooden bars and aluminum rods were used individually and in groups to simulate in the laboratory the effects of tree trunks and/or branches. The measurements on individual scatterers yielded equivalent circuits of the scatterers (as seen by the transmission line) as lumped-constant loads at the location of the scatterer along the line. These equivalent circuits then were used to compute the effects of a random distribution of such scatterers and to infer the effective macroscopic electrical properties of a volume containing these scatterers. Measurements were made on random distributions of these scatterers for comparison with the computed values. Measurements on freshly cut vegetation (tree branches) and living vegetation were made to check the reasonableness of the simulation.

This report is organized so that the development of most of the various formulas and equations used are presented in the appendices. Some of these are rather standard and are reproduced for the convenience of the reader. Others were not found in the literature, at least in the form in which they are used here. In Sec. II the theory of determining the dielectric constant and loss tangent from transmission-line measurements is reviewed, and the formulas for computation are explained. Section III is concerned with the power-density distribution in the wave around a two-wire line and the relative effect of inhomogeneities at different positions as a consequence of the distribution. The effect of the fiberglass support structure is considered in this context. In Sec. IV we consider the power densities in two orthogonal polarizations and the limitations of the measuring line for resolving anisotropic properties of the medium as a result of these distributions. Section V presents measured data which show that individual scatterers of the type we are considering can be represented as lossy capacitors on the transmission line. In Sec. V we also consider the representation of the macroscopic effect of distributions of these scatterers (including small trees) by a single parameter, the complex dielectric constant. Section VI presents the conclusions from this study and the recommendation of an experiment to test the hypothesis: that one can determine the OWL equivalent circuit of a single tree as a function of tree type and geometry (tree diameter, height, branch configuration, distance from line, etc.) by measurement; and, knowing the statistics of a given forest (tree type, height and spacing distributions, etc.), one can compute the effective macroscopic electric constants for that forest considered as a lossy dielectric slab.

II THEORY OF THE USE OF TRANSMISSION LINES FOR MEASURING THE MACROSCOPIC ELECTRICAL PROPERTIES OF HOMOGENEOUS, ISOTROPIC DIELECTRICS

A. General Comments

The macroscopic electrical properties of homogeneous, isotropic dielectrics can be adequately described for our purposes by two parameters, the complex relative dielectric constant, ϵ_r, and the complex relative permeability, μ_r. The two parameters can be computed from the characteristic impedance, Z_c, and the propagation constant, γ, of a transmission line in which the space between the conductors is filled with the material in question. We will write:

$$\epsilon_r = \epsilon'_r - j\epsilon''_r = \epsilon'_r(1 - j\delta)$$

$$\mu_r = \mu'_r - j\mu''_r$$

$$\gamma = \alpha + j\beta$$

$$Z_c = R_c + jX_c \quad .$$

For an open two-wire line in a dielectric:*

$$Z_c = \frac{1}{\pi}\sqrt{\frac{\mu}{\epsilon}}\cosh^{-1}\left(\frac{b}{a}\right)$$

and,

$$\gamma = j\omega\sqrt{\mu\epsilon}$$

---

*It has not been considered necessary to separate equations involving complex variables into real and imaginary parts. The facility with which complex numbers and functions can be handled by modern compilers (such as Fortran IV) makes the complex form of the equation more convenient for computational purposes than are the two component equations.

where a is the radius of the conductors and b is half the distance between the conductors. For the same transmission line in air, Z_c becomes

$$R_{co} = \frac{1}{\pi}\sqrt{\frac{\mu_o}{\epsilon_o}}\cosh^{-1}\left(\frac{b}{a}\right)$$

and γ becomes

$$jk_o = j\omega\sqrt{\mu_o\epsilon_o} \quad .$$

Therefore,

$$\frac{Z_c}{R_{co}} = \sqrt{\frac{\mu_r}{\epsilon_r}}$$

and,

$$\frac{\gamma}{k_o} = j\sqrt{\mu_r\epsilon_r} \quad .$$

Solving these two equations for ϵ_r and μ_r, we obtain

$$\epsilon_r = -j\frac{\gamma}{k_o}\frac{R_{co}}{Z_c}$$

$$\mu_r = -j\frac{\gamma}{k_o}\frac{Z_c}{R_{co}} \quad .$$

For the special case where

$$\mu_r = 1$$

we can find ϵ_r (both ϵ_r' and U) either from

$$\epsilon_r = \frac{R_{co}^2}{Z_c^2}$$

or from

$$\epsilon_r = -\frac{\gamma^2}{k_o^2} \quad .$$

From the foregoing we see that the dielectric constant can be easily computed from the measured characteristic impedance and propagation constant of a two-wire line which has been inserted into the material under consideration. There are many methods for determining these parameters, but since impedance bridges are much more convenient to use in the frequency range of interest than are slotted lines, we will restrict our attention to bridge methods. Two commonly used methods are considered in the following section.

B. The Short-Circuit Termination--Open-Circuit Termination Method

If we denote the input impedance of a section of transmission line terminated in a short circuit by Z_{sc} and that of the same section terminated in an open circuit by Z_{oc} then we can write

$$Z_{sc} = Z_c \tanh \gamma \ell$$

and

$$Z_{oc} = Z_c \coth \gamma \ell$$

where ℓ is the length of the section of line. From these two equations we obtain

$$Z_c = \sqrt{Z_{sc} Z_{oc}}$$

and

$$\gamma = \frac{1}{\ell} \tanh^{-1} \left(\frac{Z_{sc}}{Z_{oc}} \right)^{\frac{1}{2}} \quad .$$

Two other forms of the formula for computing γ, either of which may be more convenient to use, are:

$$\gamma = \frac{1}{l} \tanh^{-1} \left(\frac{Z_{sc}}{Z_c} \right)$$

and

$$\gamma = \frac{1}{2l} \ln \left[\frac{1 + \left(\frac{Z_{sc}}{Z_{oc}} \right)^{\frac{1}{2}}}{1 - \left(\frac{Z_{sc}}{Z_{oc}} \right)^{\frac{1}{2}}} \right] .$$

In using this method one usually finds that a line approximately an eighth of a wavelength long yields good results since for this length the magnitude of both the hyperbolic tangent and hyperbolic cotangent are approximately unity and hence the magnitudes of Z_{oc} and Z_{sc} are of the order of $|Z_c|$, a range in which the accuracy of most bridges is high.

C. Variable-Length--Fixed-Termination Method of Measuring the Characteristic Impedance and Propagation Constant of a Transmission Line

Another method, based on impedance bridge measurements, of finding the characteristic impedance and propagation constant of a transmission line consists of making two measurements of the input impedance; for both measurements the line section is terminated in the same impedance, but the length of the section is changed between the measurements. In theory, any termination and any two lengths will suffice, but of course the accuracy will be very dependent on the choice of both length and termination since the chosen lengths and the chosen termination affect the input impedance at the bridge terminals. We will illustrate the method with an open-circuit termination and two lengths which are in ratio of 1 to 2. This is a convenient combination and the accuracy should be good when the shorter length is about three-sixteenths of a wavelength long. In this case write $Z(l)$ for the input impedance of the shorter section and $Z(2l)$ for the input impedance of the longer section.

Then,

$$Z(\ell) = Z_c \coth \gamma\ell$$

and

$$Z(2\ell) = Z_c \coth (2\gamma\ell) \quad .$$

Using the identity

$$\coth 2X = \frac{1}{2} (\coth X + \tanh X)$$

we obtain

$$\frac{Z(2\ell)}{Z_c} = \frac{1}{2}\left[\frac{Z(\ell)}{Z_c} + \frac{Z_c}{Z(\ell)}\right]$$

which leads to

$$Z_c = \sqrt{Z(\ell)\left[2Z(2\ell) - Z(\ell)\right]}$$

and

$$\gamma = \frac{1}{2\ell} \ln \left\{ \frac{\sqrt{\dfrac{Z(\ell)}{Z(2\ell) - Z(\ell)}} + 1}{\sqrt{\dfrac{Z(\ell)}{Z(2\ell) - Z(\ell)}} - 1} \right\} \quad .$$

III INHOMOGENEITY LIMITATIONS OF TRANSMISSION-LINE METHODS

A. Relative Power Density around a Two-Wire Transmission Line

In the preceding section we assumed that the transmission-line probe would be inserted into a homogeneous, isotropic dielectric. We desire to use this probe, however, to measure the average value of the dielectric constant in an inhomogeneous material. One might ask, then, over how large a volume are we averaging when we make one measurement, or what is the effective volume of the sample measured by the transmission-line probe? To answer these questions we must consider how the power carried in the transmission-line wave is distributed about the line.

A contour plot of the relative power density around the transmission line in a plane normal to the line is shown in Fig. 1 (see Appendices A and B for derivation). The point midway between the conductors was chosen as a reference (0 dB). The coordinates are normalized so that the bipolar centers are at the points $x = \pm 1$, $y = 0$. With these normalizations the contours are independent of the characteristic impedance of the line. For a line with a particular characteristic impedance we can draw circles with the appropriate centers and radii to show where the conductors would be. These circles will enclose the bipolar centers. All contours or parts of contours which fall within these circles should be disregarded. We see, then, that the effect of increasing the characteristic impedance for a line with fixed spacing is to add high power-density contours in the region very near the conductors and thus to increase the fraction of the power in this region. The high power-density contours for a line with high characteristic impedance are very nearly circles concentric with the conductor surfaces. For a line of any characteristic impedance the low power-density contours, -15 dB or less, are also almost circular; the latter are concentric about the mid-point between the conductors. This near circularity leads to the concept of "radius of effect" or "sensing radius" discussed below.

Preceding page blank

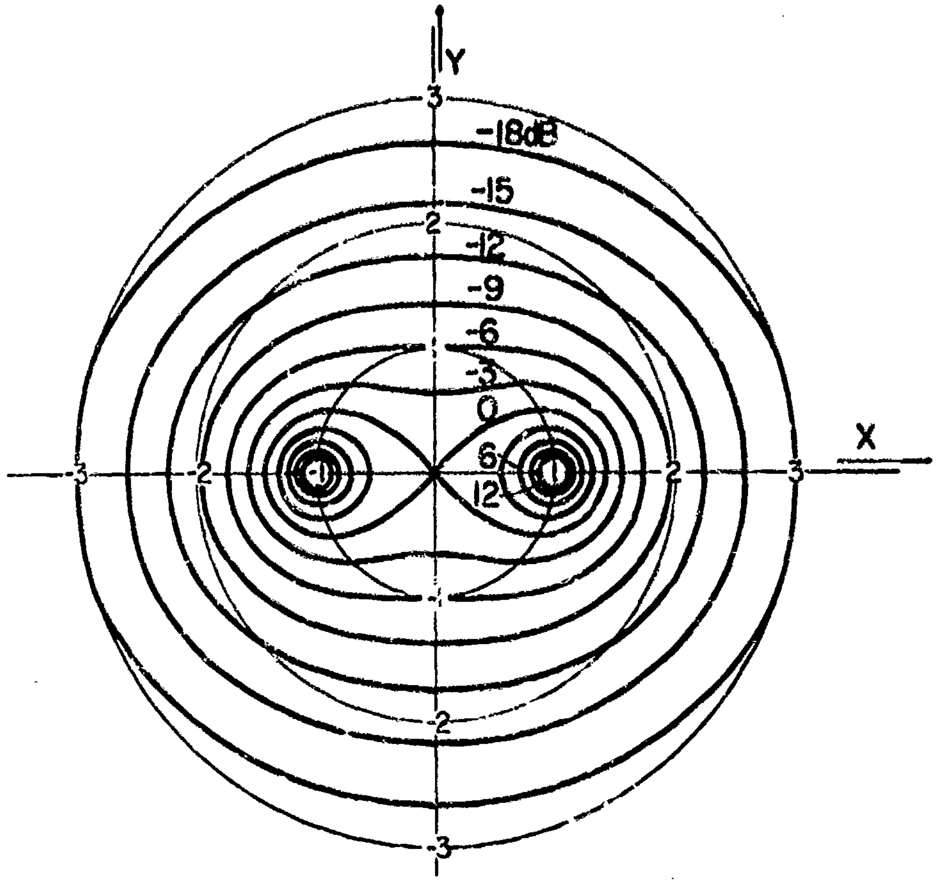

FIG. 1 RELATIVE POWER DENSITY AROUND AN OPEN-WIRE TRANSMISSION LINE

Figure 2 shows the fraction of the power flowing through a circle centered midway between the two conductors of a 300-ohm line versus the radius of the circle, r, normalized by half the distance between the conductor centers, b. Figure 3 is a similar plot with the characteristic impedance of the line as a parameter, except that the radius is normalized by half the distance between the centers of the bipolar coordinate system. In all cases the circle containing half the power passes through the bipolar centers of the conductors (in most practical cases the bipolar centers lie slightly inside but near the physical centers of the conductors). For high values of the characteristic impedance this function changes rapidly when the radius is approximately half the conductor spacing. This rapid change with distance is a consequence of the high

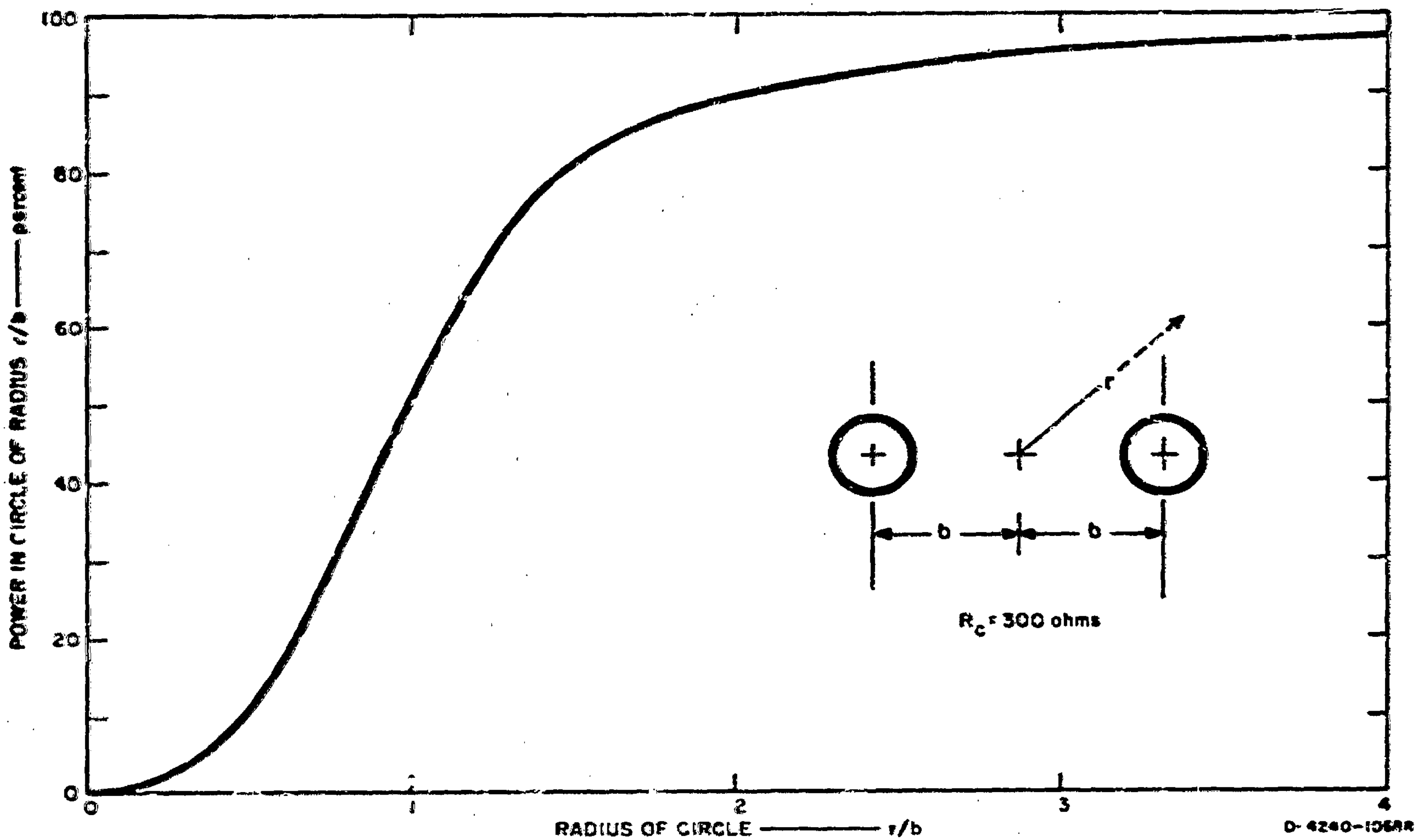

FIG. 2 RELATIVE POWER DISTRIBUTION IN THE VICINITY OF A 300-OHM OPEN-WIRE TRANSMISSION LINE

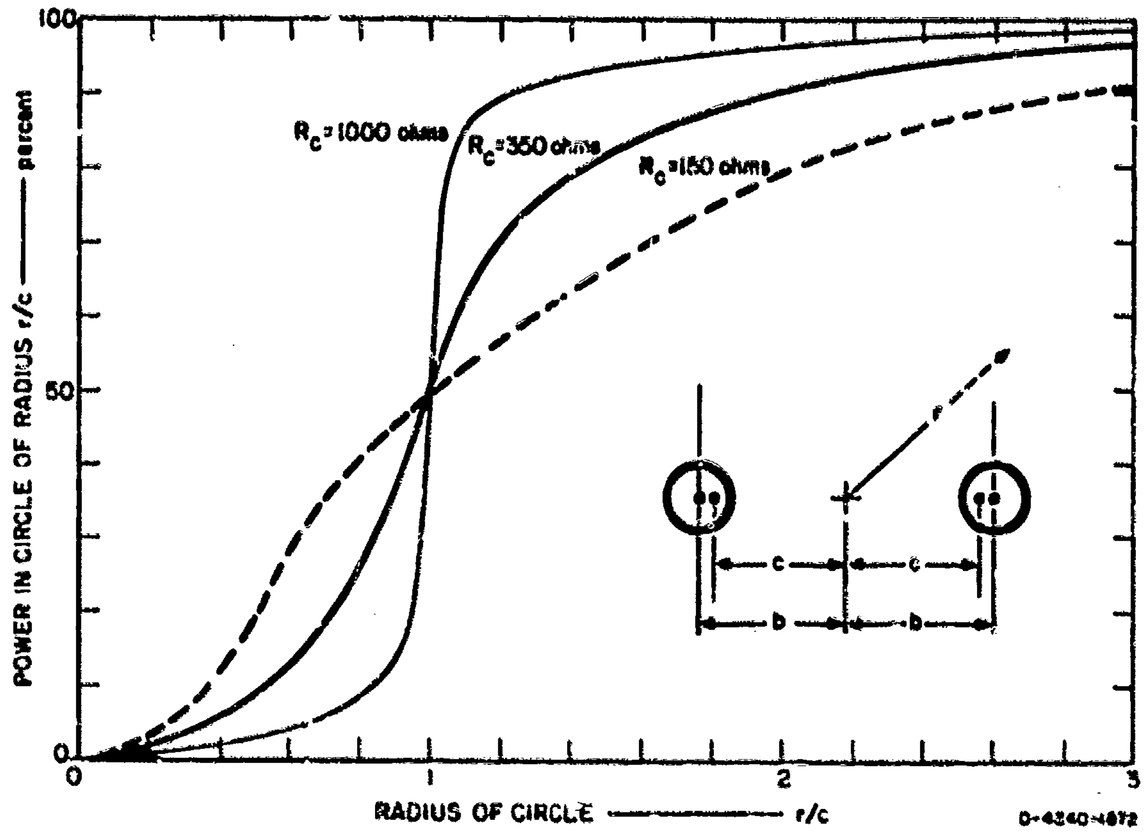

FIG. 3 RELATIVE POWER DISTRIBUTION IN THE VICINITY OF TWO-WIRE TRANSMISSION LINES OF VARIOUS CHARACTERISTIC IMPEDANCES AS A FUNCTION OF DISTANCE FROM A LINE MIDWAY BETWEEN THE CONDUCTORS

power density in the region near the conductors. For a 300-ohm line 95 percent of the power passes through a circle whose radius is 1-1/2 times the conductor spacing. For a 1000-ohm line 95 percent of the power passes through a circle whose radius is five-sixths of the conductor spacing. The power density outside the 95-percent circle is so low that a scatterer outside this circle would have negligible effect on the measurements. Therefore, one might say that the radius of this circle is the "radius of effect" or "sensing radius" of the transmission-line probe. For a 300-ohm line, since the power-density contours are also nearly circular at the 95-percent circle (passing through x = 3 on Fig. 1), the idea of a radius of effect is meaningful. For a 1000-ohm line, however, the radius of the 95-percent circle is not large enough for the power-density contours to approximate circles. The power density varies over a 9 dB range on this circle (passing through x = 1.67 on Fig. 1) on a 1000-ohm line, and the concept of radius of effect is not particularly meaningful.

Figure 4 shows the fraction of the power flowing through two circles of equal radius centered at the conductor centers versus the radius of the circles. To simplify the computations, circles centered at the bipolar centers were used (see Table I), but for the range of values of characteristic impedance shown, the approximation to circles centered at the conductor centers is excellent. For a characteristic impedance of 300 ohms 50 percent of the power flows through the two circles whose

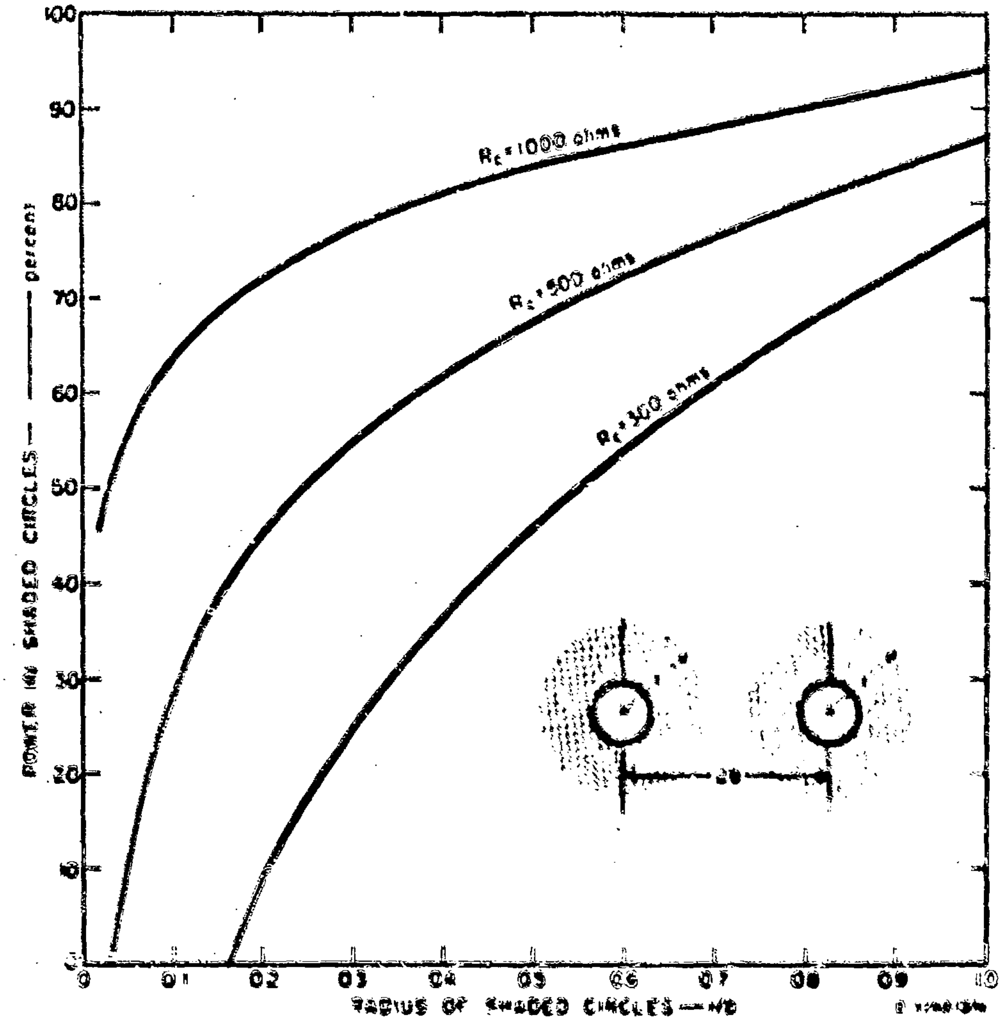

FIG. 4 RELATIVE POWER IN THE VICINITY OF THE CONDUCTORS OF A TWO-WIRE TRANSMISSION LINE AS A FUNCTION OF RADII ABOUT EACH CONDUCTOR

Table I

POWER IN CIRCLES OF RADIUS r, CENTERED AT BIPOLAR CENTERS OF TWO-WIRE TRANSMISSION LINE

r/b \ R_c	250	300	350	400	450	500	750	1000
0.05	0.0000	0.0000	0.0000	0.0000	0.0165	0.1149	0.4099	0.5574
0.10	0.0000	0.0000	0.0000	0.1020	0.2017	0.2816	0.5210	0.6408
0.15	0.0000	0.0000	0.1134	0.2242	0.3104	0.3794	0.5862	0.6897
0.20	0.0000	0.0818	0.2130	0.3113	0.3879	0.4491	0.6327	0.7245
0.25	0.0000	0.1724	0.2806	0.3793	0.4483	0.5034	0.6690	0.7517
0.30	0.0963	0.2469	0.3545	0.4352	0.4979	0.5481	0.6988	0.7741
0.35	0.1725	0.3104	0.4090	0.4828	0.5403	0.5863	0.7242	0.7931
0.40	0.2392	0.3660	0.4566	0.5245	0.5773	0.6196	0.7464	0.8098
0.45	0.2987	0.4156	0.4991	0.5617	0.6104	0.6493	0.7662	0.8247
0.50	0.3525	0.4604	0.5375	0.5953	0.6403	0.6763	0.7842	0.8381
0.55	0.4019	0.5016	0.5728	0.6262	0.6677	0.7010	0.8006	0.8505
0.60	0.4477	0.5397	0.6055	0.6548	0.6932	0.7238	0.8159	0.8619
0.65	0.4905	0.5755	0.6361	0.6816	0.7170	0.7453	0.8302	0.8726
0.70	0.5310	0.6091	0.6650	0.7068	0.7394	0.7655	0.8437	0.8827
0.75	0.5694	0.6411	0.6924	0.7308	0.7608	0.7847	0.8565	0.8923
0.80	0.6061	0.6717	0.7186	0.7538	0.7612	0.8030	0.8687	0.9015
0.85	0.6414	0.7012	0.7439	0.7759	0.8005	0.8207	0.8805	0.9104
0.90	0.6757	0.7297	0.7683	0.7973	0.8198	0.8378	0.8919	0.9189
0.95	0.7090	0.7575	0.7921	0.8181	0.8383	0.8545	0.9030	0.9272
1.00	0.7416	0.7847	0.8154	0.8385	0.8564	0.8708	0.9139	0.9354

radius is 0.275 of the line spacing and 76 percent of the power flows through the two circles whose radius is one-half of the line spacing. For a 1000-ohm line the 50-percent radius is 0.015 of the line spacing, and the 64-percent radius is 0.05 of the line spacing.

B. Two-Wire Line above a Lossy Half-Space

When we measure the dielectric constant of the forest region there are two obvious inhomogeneities, the effects of which we do not want to include in our average. These are the regions above and below the forest--the air and the ground. The interface at the forest top would usually be far from the measuring line, but even if it were only a distance of one line spacing away, one would expect it to have negligible effect since the relative dielectric constant of the forest is near that of air. The interface at the ground, however, could be expected to have considerable effect since the dielectric constant and loss tangent of the ground are large. For this reason measurements were made in the laboratory to determine how far above a lossy half-space the line must be for the effect of the lossy region to be negligible. First, a 300-ohm line (3-3/4-inch spacing) was erected above a wooden table top in a plane parallel to the table, and the open-circuit/short-circuit method was used to determine the propagation constant and the characteristic impedance as a function of height of the line above the table. The tests were then repeated over an aluminum plate 8 ft by 3 ft. The results of these tests are shown in Figs. 5, 6, and 7. Notice that the characteristics of the line are relatively independent of height for heights greater than about one line spacing (i.e., r/b > 2), indicating

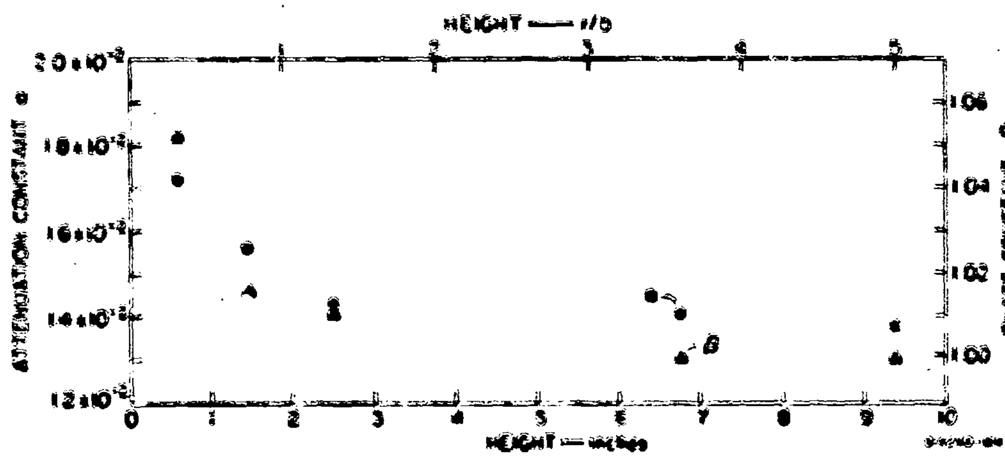

FIG. 5 PROPAGATION CONSTANT vs. HEIGHT ABOVE WOODEN TABLE

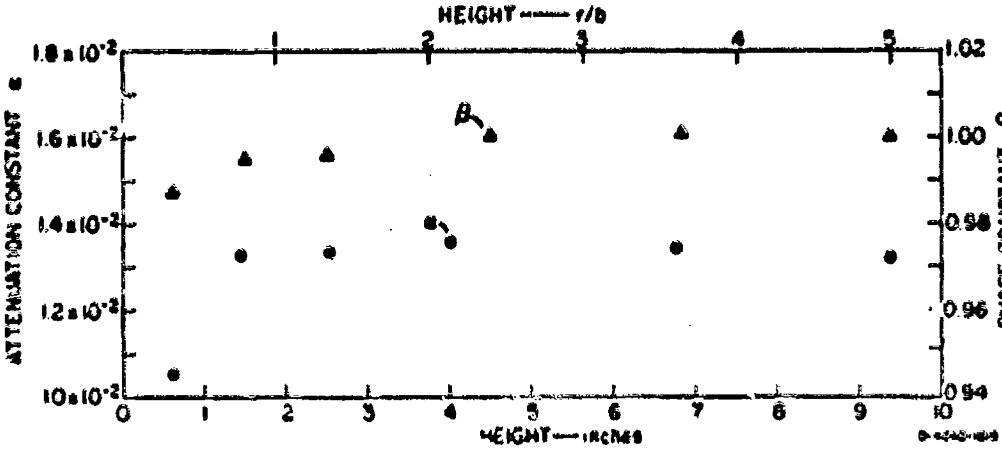

FIG. 6 PROPAGATION CONSTANT vs. HEIGHT ABOVE ALUMINUM PLATE

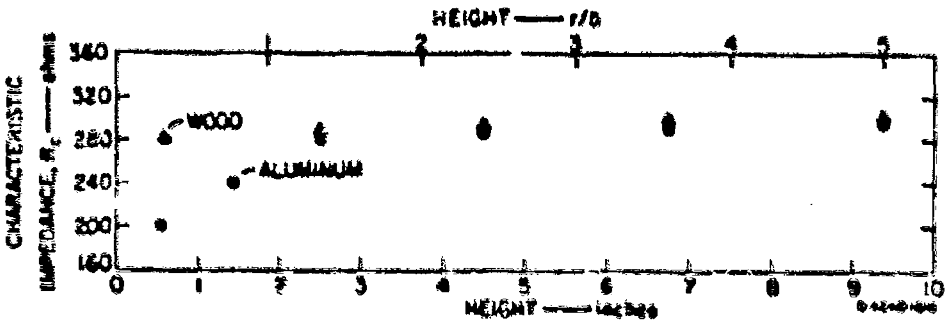

FIG. 7 CHARACTERISTIC IMPEDANCE vs. HEIGHT ABOVE WOODEN TABLE AND ALUMINUM PLATE

that forest measurements made with a line placed from one to one-and-a-half line spacings above the ground would be relatively independent of ground effects. These results are in agreement with the results of field tests with a 300-ohm line over actual ground* and also with conclusions about the "radius of effect" of such a line as deduced in the previous section.

*H. W. Parker, private communication.

C. Effect of Air Space around Line Inserted in Otherwise Homogeneous, Isotropic Dielectric

Several practical considerations lead us to consider the effect of excluding the dielectric of interest from the immediate vicinity of the line (i.e., placing the line in proximity to a two-medium region--see Fig. 8). First, it is important to maintain a constant line spacing when inserting the measuring line into vegetation, and, second, we need a line which is convenient to carry and can be easily and quickly set up for measurements. One method suggested for protecting the line during field use was to encase it in a thin-walled dielectric tube of low permittivity.[5] This technique has the disadvantage of excluding vegetation from the high-field region near the line--particularly the region between the conductors.

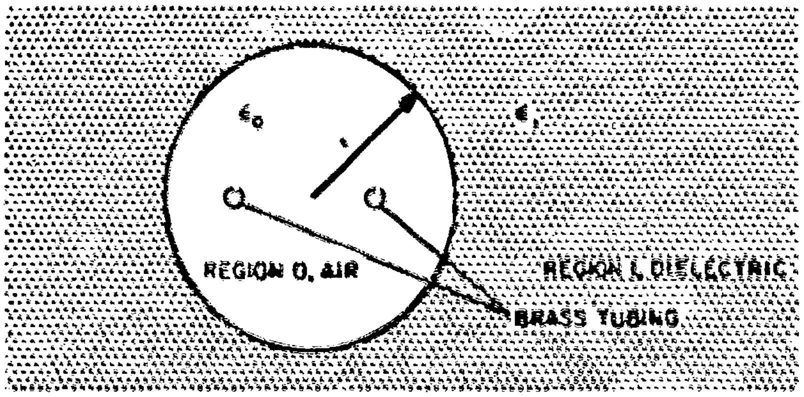

FIG. 8 OPEN-WIRE TRANSMISSION LINE IN TWO-MEDIUM REGION

In order to see the effect of this air space on the propagation constant and phase velocity, these two parameters were computed as functions of the hole diameter using the approximation developed in Appendix B. The results are shown in Fig. 9, where the phase velocity relative to that of free space is plotted against the hole diameter normalized to the half-spacing of the line. As can be seen from the curves, one could use the measured phase velocity and the known hole diameter to compute ϵ_r. Note, however, that when the hole is large

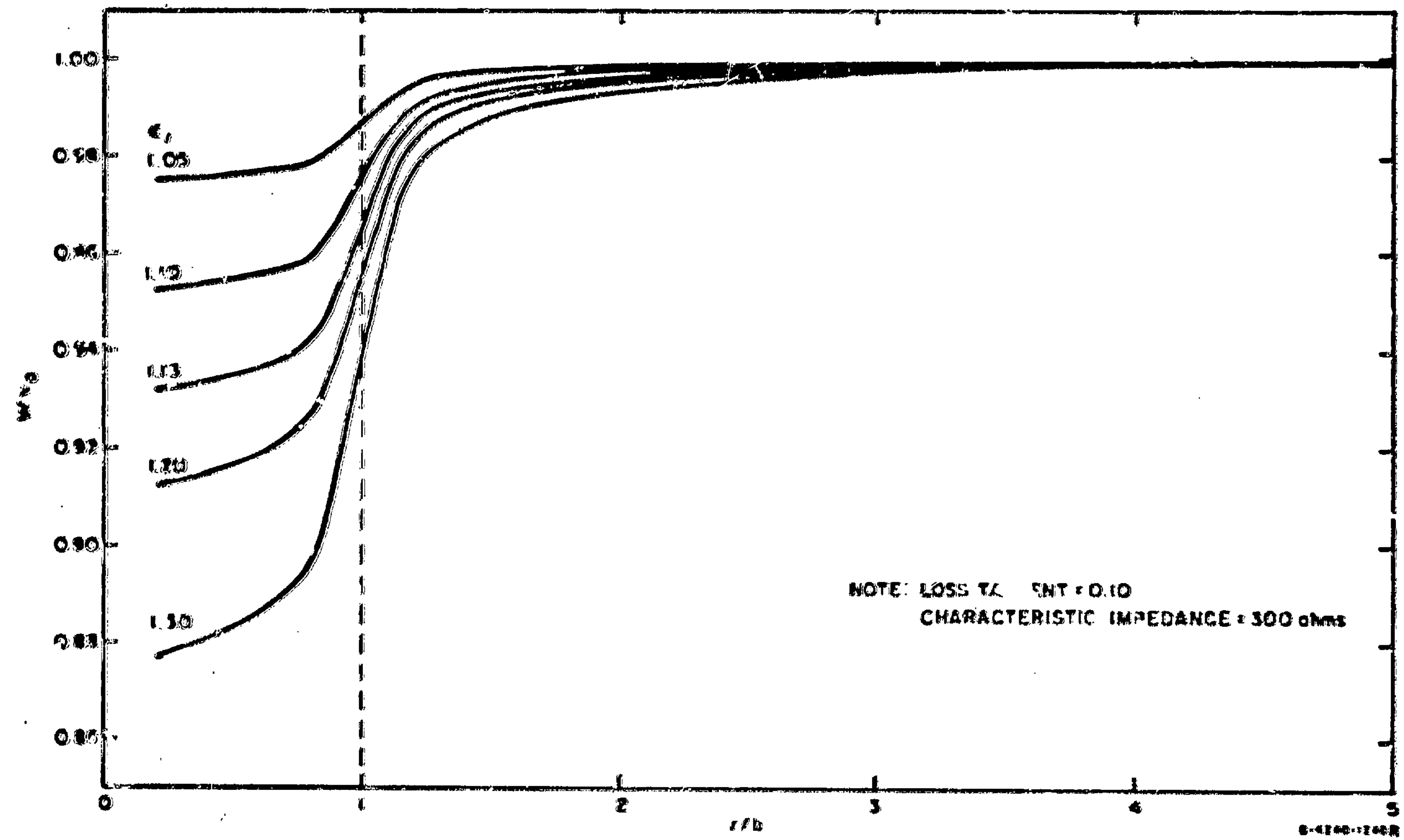

FIG. 9 FRACTIONAL PHASE VELOCITY FOR DIFFERENT AIR SPACES AROUND AN OPEN-WIRE TRANSMISSION LINE

enough to enclose the conductors ($r/b > 1$) the curves become quite close together, indicating that a small error in measuring the phase velocity or propagation constant would result in a much larger error in the electric susceptibility ($X_e = \epsilon_r - 1$). We therefore recommend that the space between and around the conductors be as uniformly filled with a representative sample of the medium as is practical. But if one must correct for a void region parallel to the axis of the line, the appropriate formula is (see Appendix B):

$$\epsilon_r = \frac{-\gamma^2(1-P)}{1+\gamma^2 P}$$

where

ϵ_r = the complex relative dielectric constant

γ = normalized propagation constant

P = fraction of power flowing in the void region.

As a check on the effect of an air space in the center region of a two-wire line, the phase velocity and propagation constant were determined from measured impedance data on a one-eighth wavelength section of line around which polyurethane foam had been poured. A rectangular cavity was cut in the foam (see Fig. 10) and was enlarged after each measurement.* Instead of a two-wire line, however, a single brass conductor of 5/8-in diameter was used over an aluminum image plane to facilitate the 17-MHz measurements with an unbalanced bridge (General Radio, GR 1606). An aluminum plate 1-1/2 ft by 3 ft was bolted to the image plane for use as a short-circuit termination.

The short-circuited and open-circuited impedances of the line were measured in air and found to be

$$Z_{sc} \approx + j178.0$$

$$Z_{oc} \approx - j133.6 \quad .$$

---

*The use of a rectangular hole in the foam to check the theory for the geometry of Fig. 9 is valid (see Appendix C).

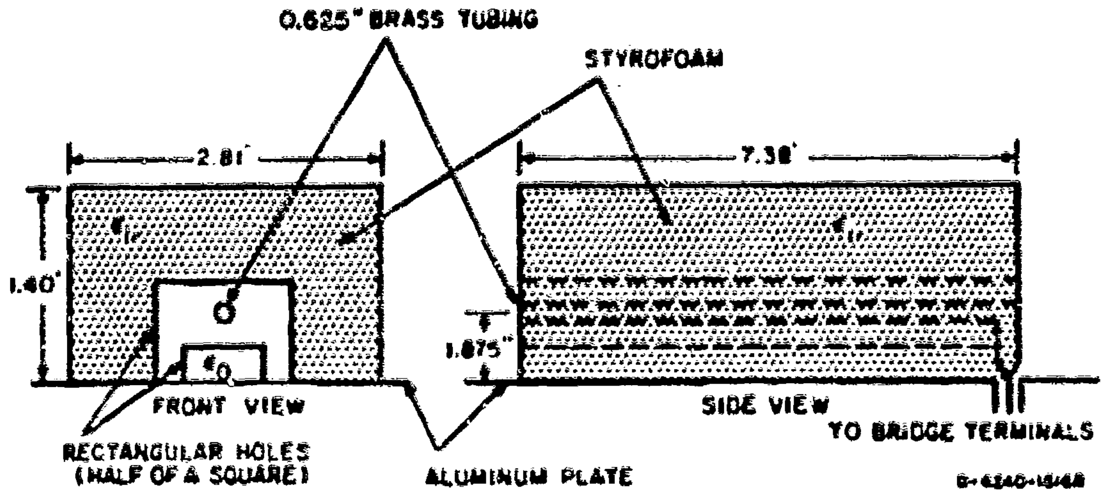

FIG. 10 SCHEMATIC MEASUREMENT SETUP OF IMAGE-PLANE LINE

From these measured values, the characteristic impedance in air is calculated as

$$Z_c = \left(Z_{oc} Z_{sc}\right)^{1/2} \approx 154.5 \text{ ohms} \quad .$$

This result is only slightly higher than the value calculated from theory: 150 ohms (i.e., one-half of the value for a 300-ohm line).*

The results of the foam measurements are summarized in Table II, and they are shown--together with the computed curves of phase velocity versus hole size--in Fig. 11. The measured points indicate a dielectric constant for the foam of 1.07. A small sample of the foam, when used as the dielectric of a coaxial capacitor, exhibited a dielectric constant of 1.08.

*It has been found experimentally in Thailand by Withan Makarabhiromya that values of Z_c measured with this method are slightly higher for short lines than the values computed from theory, but that the difference between theoretically derived and measured values decreases with increasing line length until the length is about three wavelengths.

Table II

RESULTS OF FOAM MEASUREMENTS WITH IMAGE-PLA LINE

Hole Dimension (square inches)	r_o (0/0)	Z_{sc}	Z_{oc}	α	β	Vp	ϵ_r'	δ
No hole	0	0.36 + j189.4	0.35 - j125.9	0.0013	1.0334	0.9677	1.0678	0.0026
1 × 2	14.80	2.75 + j187.94	0.20 - j127.53	0.0016	1.0275	0.9732	1.0660	0.0037
1-7/8 × 3-3/4	58.08	1.22 + j183.01	0.05 - j129.41	0.0020	1.0157	0.9846	1.0788	0.0093
3-3/4 × 7-1/2	92.06	1.24 + j178.98	0.04 - j131.76	0.0021	1.0041	0.9959	1.1112	0.0578
5-5/8 × 11-1/4	96.48	1.26 + j176.90	0.00 - j132.84	0.0020	1.0014	0.9986	1.0708	0.1249
10 × 20	98.55	1.39 + j178.84	0.00 - j133.90	0.0022	1.0012			

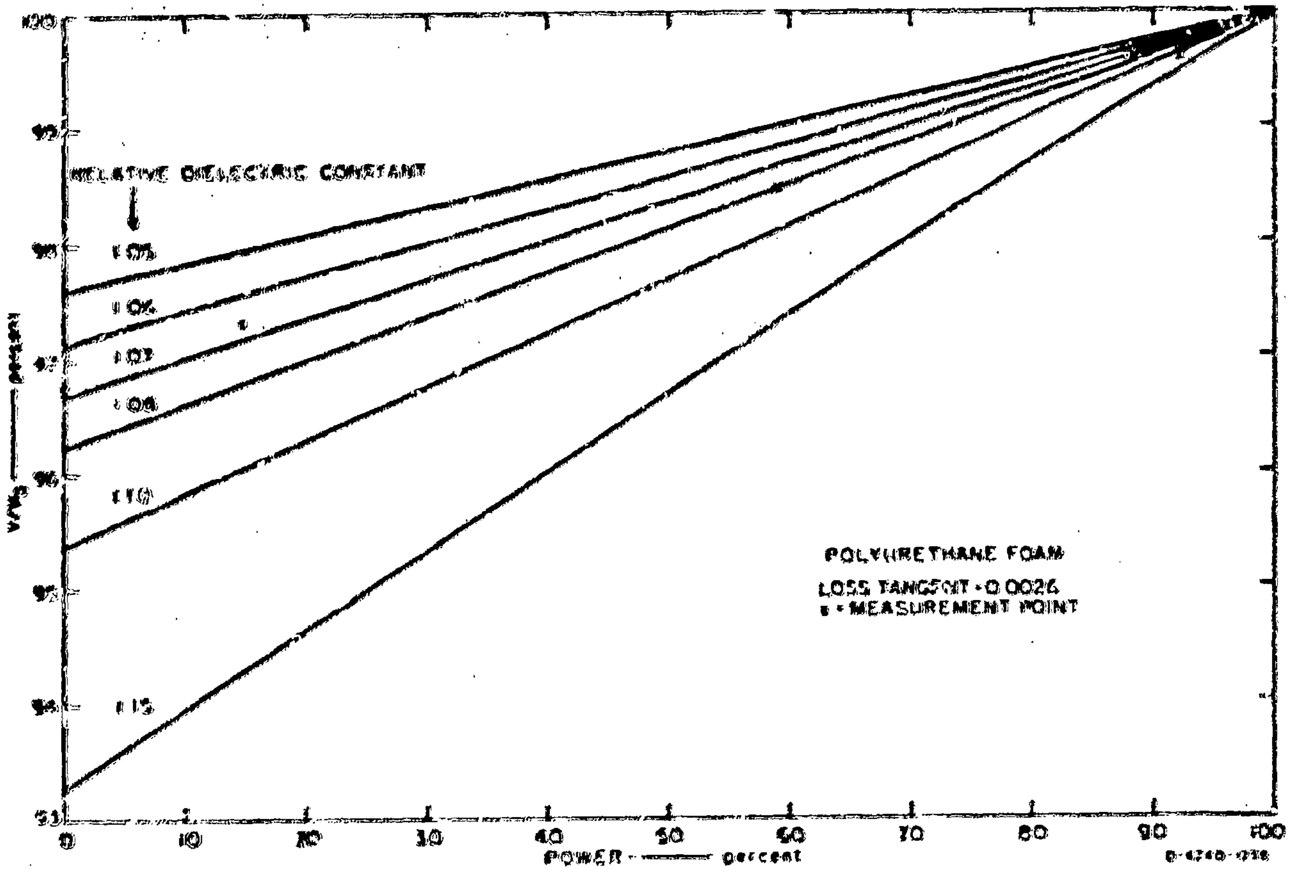

FIG. 11 FRACTIONAL PHASE VELOCITY AS A FUNCTION OF POWER THROUGH AIR SPACE AROUND THE OPEN-WIRE TRANSMISSION LINE

IV ANISOTROPY LIMITATIONS

A. Relative Power Density for Two Orthogonal Polarizations

In the preceding section we considered a transmission-line probe as a measuring instrument for determining the electrical properties of inhomogeneous but isotropic dielectrics and pointed out some of its limitations. In that discussion we disregarded anisotropic effects. We will now consider a transmission-line probe as an instrument for measuring anisotropic dielectric properties and show that it is not satisfactory for this purpose.

One would expect to be able to resolve anisotropic effects if the field about the probe were predominantly linearly polarized and most of the power was contributed by the component which pointed in a particular direction. The field about a two-wire line is linearly polarized everywhere but varies in direction from point to point. The power densities in two orthogonal polarizations and the fraction of the total power carried in each of them as a function of position around the line is not immediately obvious. It is obvious from the symmetry of the field, however, that if there is a polarization which carries more of the power than any other, then it must be either that in the plane of the conductors or that perpendicular to this plane, since the two orthogonal polarizations at 45° to the plane of the conductors carry equal power. With this fact in mind we computed the power densities and the fraction of the power carried by the two orthogonal polarizations, one in the plane of the conductors and the other perpendicular to it (see Appendix D).

Figure 12 is a plot of contours of constant power density in the x- and in the y-polarizations where the conductors are on the x axis. Only the first quadrant has been plotted. The contours in other quadrants can be obtained by noting that the curves are symmetric with respect to the x and y axes. This figure shows that in the region between the two conductors and in the vicinity of the two axes, more of the power is contributed by the x-polarized electric field; and away from these regions more of the power is contributed by the y-polarized electric field.

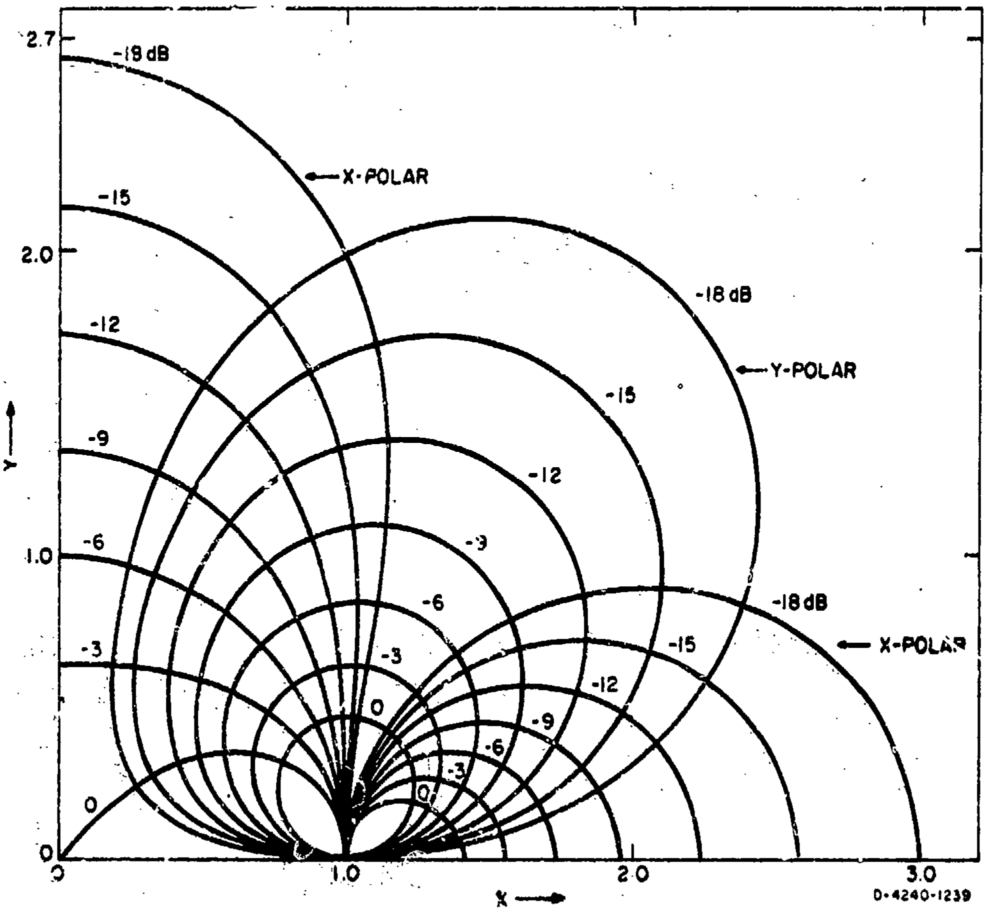

FIG. 12 RELATIVE POWER DENSITY IN X- AND Y-POLARIZATION AROUND AN OPEN-WIRE TRANSMISSION LINE

B. Integrated Relative Power Density for Two Orthogonal Polarizations

The relative power-density expressions for the x (in the plane of the line) and the y (normal to the plane of the line) components, as depicted in Fig. 12, have been integrated to determine the relative power carried in each of these polarizations. In addition, for each polarization the power inside and outside a circle centered midway between the conductors and passing through the centers of the bipolar coordinate system was computed. Table III summarizes the results of the integration for lines of characteristic impedance between 100 and 1000 ohms. It is seen again that half the power is carried within the circle $r/c = 1$, and that more of the power within that circle is stored in a polarization parallel to the plane containing the centers of the conductors.

Table III

POWER DISTRIBUTION AROUND TWO-WIRE TRANSMISSION LINES FOR ORTHOGONAL POLARIZATIONS--IN PERCENT

R_c (ohms)	Inside Circle of r/c = 1		Outside Circle of r/c = 1		Total	
	P_x	P_y	P_x	P_y	P_x	P_y
100	47.32	2.68	27.01	22.99	74.33	25.67
150	44.91	5.09	23.45	26.55	68.36	31.64
200	42.52	7.48	21.94	28.06	64.46	35.54
250	40.39	9.61	21.42	28.58	61.81	38.19
300	38.58	11.42	21.35	28.65	59.93	40.07
500	33.84	16.16	22.16	27.84	56.00	44.00
750	31.00	19.00	23.00	27.00	54.00	46.00
1000	29.5	20.50	23.50	26.50	53.00	47.00

The data of Table III indicate that more of the power about a line is flowing in a polarization parallel to the plane containing the conductors, but that the distribution becomes more even for fixed conductor size as the line spacing is increased (i.e., as the characteristic impedance is increased). Figure 13 shows the ratio of the power in the two orthogonal polarizations to the total power as a function of characteristic impedance.

C. Conclusion

It should be clear from the foregoing discussion that lines of large characteristic impedance cannot be used to resolve the degree of anisotropy of an anisotropic dielectric by simply rotating the configuration 90 degrees. Indeed, it is apparent that a balanced, two-wire transmission line constructed of cylindrical conductors is not a satisfactory instrument for determining the macroscopic anisotropic properties of dielectrics.

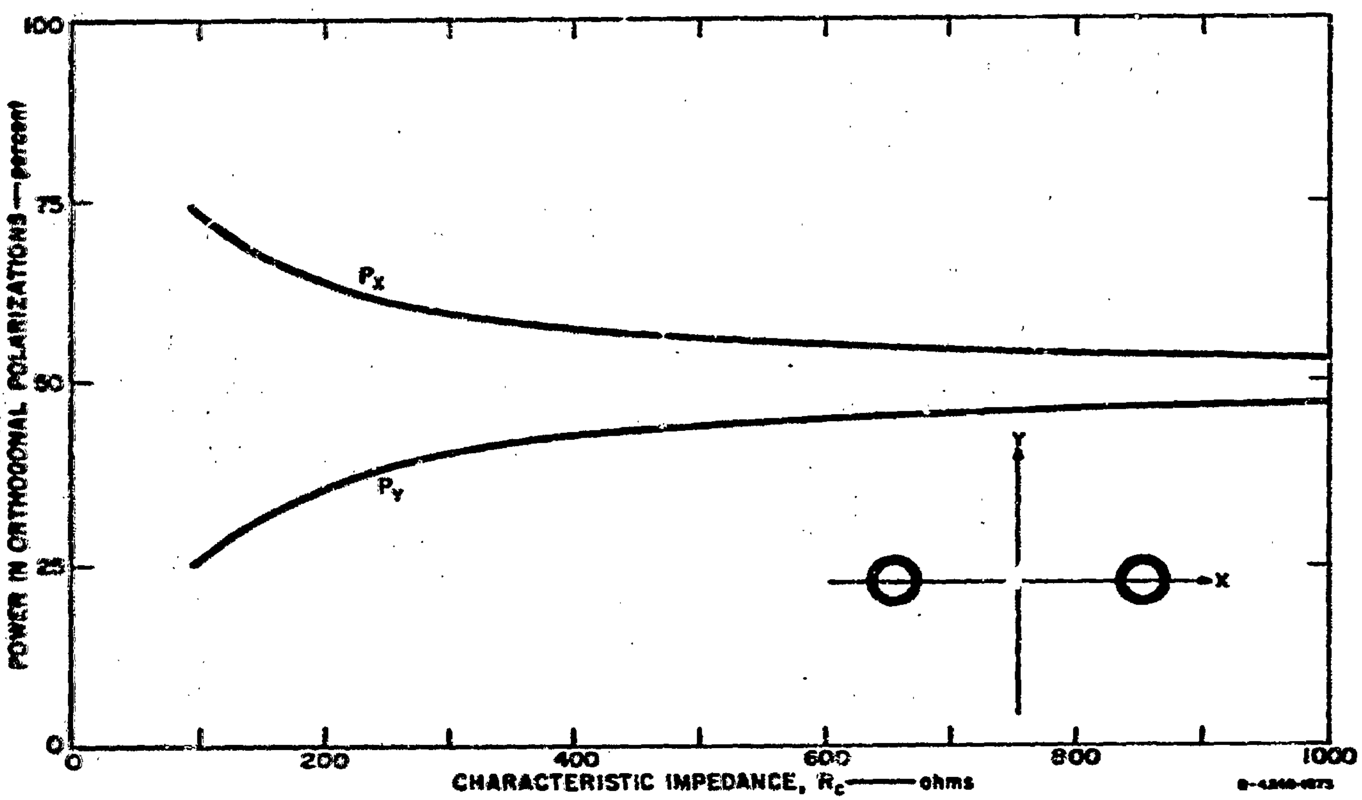

FIG. 13 POWER IN TWO ORTHOGONAL POLARIZATIONS ABOUT A TWO-WIRE TRANSMISSION LINE AS A FUNCTION OF CHARACTERISTIC IMPEDANCE

D. Recommendations

The forest is an anisotropic medium at VHF and below. A rough estimate of the anisotropy of conductivity can be obtained from measurements of the type described in Ref. 15. Further study is required, however, to develop probes useful for ground-based measurement of the macroscopic, anisotropic properties of the forest. Such probes possibly could be composed of many wires or rods (e.g., multiple-wire transmission lines designed for this purpose). Still another approach is to invert a propagation model* and do curve fitting on path-loss data versus separation between transmitter and receiver (at relatively short ranges) and versus antenna heights (at relatively long ranges) and determine what electrical constants for the forest slab are required to give a good fit when horizontal and vertical electric dipoles (or equivalent) are employed.

*The propagation model(s) employed would have to allow for anisotropy, and additional model work beyond that given in Refs. 3-5 would be required to generate the appropriate model(s) to be invented. An initial attempt at such model work was made by Dr. John Spence (currently at the University of Rhode Island) while he was with the Jansky and Bailey Division of Atlantic Research Corp in 1967. This work is summarized in an appendix to "Environmental Effects on Short Range Communication: Report of Technical Study Group," edited by Col. T. W. Doeppner, Joint Advanced Research Projects Agency and Environmental Sciences Service Administration Meeting held in Boulder, Colorado (March 1967).

V DISCRETE SCATTERERS NEAR A TRANSMISSION LINE

A. Introductory Remarks

In this report we have been considering a model for a forest region suitable for explaining and predicting how radio waves propagate through the forest and across the boundaries at the ground and at the tree tops. In our model the forest is considered to be a layor of lossy dielectric--not necessarily homogeneous or isotropic--which can be characterized by a complex relative dielectric constant, ϵ_r. If the medium is not isotropic ϵ_r will, of course, be a tensor. The present section is concerned with trees as discrete scatterers in an attempt to justify our representation of a large number of discrete scatterers by a continuous medium. In this investigation we have chosen to consider the effect of these scatterers on a wave guided by a two-wire transmission line rather than the effect on a plane wave. We have done this for two reasons: First, because the guided-wave case is a one-dimensional problem which lends itself to analysis by distributed-circuit methods and is also quite easy to study experimentally. Second, because the investigation reported here is concerned with measuring the electrical properties of the medium, and the two-wire line shows promise as a measuring instrument for this purpose. Since we have considered only the guided wave, the question arises as to whether or not the guided wave is similar enough to the plane wave that the results of our study apply to the plane-wave case; and indeed, whether or not the equivalent dielectric constant measured by transmission-line techniques is the proper value to use for plane-wave propagation. To some extent we will have to leave this question unanswered, but the study does give some insight into the usefulness and validity of our model.

We will consider, then, how the transmission-line wave is affected by scatterers in the vicinity of the line. Since we are interested in the macroscopic properties of the region containing the scatterers, we will assume that the line spacing is wide enough that a reasonable sample of scatterers is in the region near the line where the field is strong

Preceding page blank

and that there is appreciable probability that a few scatterers (trees) are included in the region between the conductors. The upper frequency limit on the measurement of our macroscopic parameters is then determined by the condition that the line spacing must be very small compared to the wavelength. Under these conditions let us look at the effect of a single one of the scatterers and find its equivalent circuit as a load on the transmission line. Then let us look at pairs of scatterers to see if the equivalent circuit is still valid or if we need to modify it to account for mutual coupling effects. Finally, we will consider random distributions of scatterers loading the line and infer the effective macroscopic electrical properties of the volume containing the scatterers as a function of the average number of scatterers per wavelength along the line.

B. Measurement Equipment

Two different lines were used for the measurements reported in this section. One was a balanced two-wire line (Fig. 14) with 5/8-in-diameter brass tubing for conductors. The line spacing could be varied in fixed increments to give characteristic impedances with air as a dielectric as

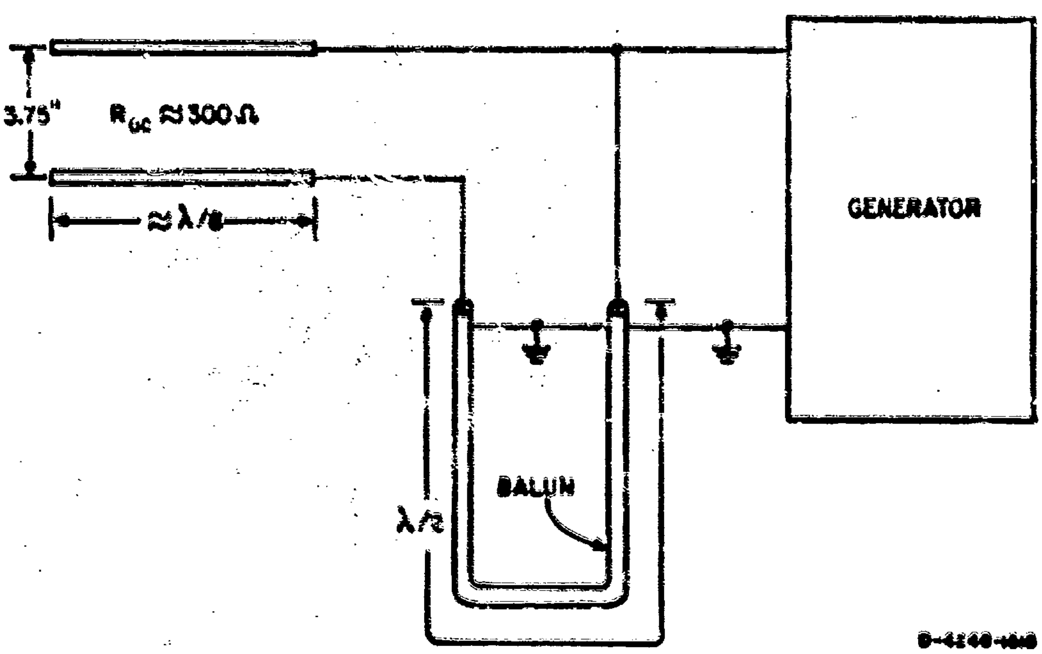

FIG. 14 BALANCED TWO-WIRE LINE

given in Table IV. This line was suspended 15 to 22 inches above a wooden table top, the greatest height for the widest line separation. It was far enough above the table that the table top had negligible effect on the measurements (see Sec. III-B). Since one side of the impedance bridge was at ground potential, it was necessary to use a balanced-to-unbalanced transformer (balun) for measurements with this line. A one-half wavelength section of RG-8/U coaxial transmission line (see Fig. 14) was used for this purpose. The impedance-transformation ratio through this balun transformer was 4 to 1.

Table IV

SPACINGS AND CHARACTERISTIC IMPEDANCE FOR TWO-WIRE LINE

Center-to-Center Spacing (in)	Characteristic Impedance, R_c (ohms)
2.90	270
3.75	300
9.20	400
12.00	440

The other measuring line was the image-plane line corresponding to one-half of the two-wire line (this line was also used for the foam measurements--see Fig. 10). Each of these lines was one-eighth of a wavelength long at the measurement frequency of 17 MHz. The measurements were made with a General Radio 1606 impedance bridge. The signal generator was a Hewlett-Packard Model 608D and the detector receiver was a Hewlett-Packard Model 417A.

The bridge accuracy was barely sufficient to measure the effect of a single scatterer or a pair of scatterers, and the spread of the data points is primarily due to our inability to make precise measurements. In fact, it was necessary to add a special slow-motion gear mechanism to the dials of the bridge to obtain enough resolution and repeatability for these tests. In spite of this limitation on the accuracy of a single measurement, enough measurements were made so that the susceptance is sufficiently accurate to show the various effects we are considering. Unfortunately, the scatter in the conductance points is so great that some of the trends are masked.

C. Equivalent Admittance of a Single Scatterer near an Open-Wire Transmission Line

The equivalent shunt admittances of selected scatterers placed in various configurations about a transmission line were measured. The scatterers consisted of wet and dry wooden bars,* aluminum cylinders, cut vegetation and finally, growing trees. All of the scatterers measured which were not trees or freshly cut parts of trees were cylinders or bars which to some extent could be used to simulate tree trunks or branches.

1. Effect of Longitudinal Position of Scatterer

The shunt admittance should be independent of the longitudinal position of the scatterer on the line except when the scatterer is in the fringing field near the open end of the line. However, the sensitivity, and hence the accuracy, of the measurement is much better when the scatterer is near a high voltage point. For our one-eighth wavelength line the only high voltage region is near the open end. To overcome this dilemma, we measured the admittances of several types of scatterers with each of the scatterers at several longitudinal positions near the open end of the line. From these values of admittance as the scatterer was progressively moved along the line, it was determined how far from the open end a scatterer need be so that the admittance would be relatively independent of the longitudinal position. For convenience in making the measurements and for measurements involving several scatterers, twenty positions with equal spacing (s=3/8 in) were marked off along the line, with position one corresponding to the sending end and position 20 corresponding to the termination end.

*Two types of dry wooden bars were used for these tests: air-dried bars and oven-dried bars. The water (moisture) content of the wet wooden bars is expressed in percent (by weight) relative to the oven-dried bars. The water content of the air-dried bars was estimated at about 9 percent relative to the oven-dried bars.

The results of those measurements of dry wooden bars, wet wooden bars, and aluminum cylinders are shown in Table V. The 150-ohm image-plane line was used, and the axis of the bar was at right angles to the image plane (Fig. 15). The values of admittances shown are the averages of several measurements with the same configuration. The point at 13-1/8 inches appears to be in error and a little bit high for both the No. 2 set of dry wood bars and the set of metal rods. The difference between Sets 1 and 2 in all cases can be attributed to slight changes in the measuring setup between the two sets of measurements. Nevertheless, the measurements indicate that consistent results are obtained if the scatterer is at least one line spacing from the open end. For the rest of the measurements involving one or two scatterers, the scatterers were kept at least one line spacing from the end.

2. Effect of Distance of Scatterer from Line

The 150-ohm image-plane line was used for these tests. The 24-1/2-in dry and wet wooden bars (1-1/2 in square) and 1/4-in-diameter aluminum rods were placed 4-3/8 in (position 19--see Fig. 15) from the open end of the line, and the equivalent shunt admittance of the scatterer was measured as the distance from the center line of the scatterer to the center line of the conductor was varied. Two orientations of scatterer were used: scatterers perpendicular to the image plane (as indicated in Fig. 15) and scatterers parallel to the image plane (see Fig. 16). The results of these measurements are summarized in Tables VI and VII for the two cases where the scatterers were perpendicular to the image plane and parallel to the image plane respectively.

3. Effect of Length of Scatterer

The tests on the effect of scatterer position around the line (described above in Secs. V-C-1 and V-C-2) were all made with scatterers 24-1/2 in long. It is the purpose of this section to investigate the effect of the length of scatterer for shorter scatterers, and to determine if the equivalent shunt admittance was relatively insensitive to scatterer length for the length used in the previous sections. For these tests, the 300-ohm two-wire line was used, and the scatterers were

Table V

EQUIVALENT ADMITTANCE OF SINGLE WOODEN SCATTERER VERSUS LONGITUDINAL POSITION ON TRANSMISSION LINE

Date of Measurement	Type of Scatterer	Distance from Open End of Line (in)	Distance of Scatterer from Conductor— ℄ to ℄ (in)	Measured Equivalent Shunt Admittance on Image-Plane Line (μmhos)	Equivalent Admittance of Scatterer on 300-ohm Two-Wire Line (μmhos)	Equivalent Shunt Capacitance (C) of Scatterer on 300-ohm Two-Wire Line (pF)	Loss Tangent,** δ = arc tan (1/ωRC)
December 1967	Dry Wooden Bar	0	1-3/4	0.06 + j12.20	0.03 + j6.10	0.057	0.004
	(9 percent WC)	4-3/8	1-3/4	0.06 + j12.20	0.03 + j6.10	0.057	0.004
	24-1/2" × 1-1/2"	8-3/4	1-3/4	0.06 + j12.20	0.03 + j6.10	0.057	0.004
	× 1-1/2"	13-1/8	1-3/4	0.06 + j11.80	0.03 + j5.80	0.054	0.004
March 1968	Dry Wooden Bar	0	1-3/4	0.06 + j12.27	0.03 + j6.14	0.057	0.004
	(9 percent WC)	4-3/8	1-3/4	0.06 + j13.23	0.03 + j6.62	0.061	0.004
	24-1/2" × 1-1/2"	8-3/4	1-3/4	0.06 + j13.62	0.03 + j6.81	0.063	0.004
	× 1-1/2"	13-1/8	1-3/4	0.06 + j15.18	0.03 + j7.59	0.071	0.004
December 1967	Wet Wooden Bar	0	1-3/4	0.1 + j24.8	0.05 + j12.40	0.117	0.004
	(33 percent WC)	4-3/8	1-3/4	0.1 + j26.1	0.05 + j13.05	0.123	0.004
	24-1/2" × 1-1/2"	8-3/4	1-3/4	0.1 + j26.8	0.05 + j13.45	0.127	0.004
	× 1-1/2"	13-1/8	1-3/4	0.1 + j27.9	0.05 + j13.80	0.130	0.004
March 1968	Wet Wooden Bar	0	1-3/4	0.1 + j21.34	0.05 + j10.77	0.100	0.004
	(34 percent WC)*	4-3/8	1-3/4	0.1 + j29.04	0.05 + j14.52	0.135	0.003
	24-1/2" × 1-1/2"	8-3/4	1-3/4	0.1 + j31.86	0.05 + j15.93	0.149	0.003
	× 1-1/2"	13-1/8	1-3/4	0.1 + j32.00	0.05 + j16.00	0.149	0.003
March 1968	Aluminum Rods	0	1-1/8	0.00 + j13.90	0.00 + j6.95	0.065	0.000
	1/4" diameter	4-3/8	1-1/8	0.21 + j22.32	0.11 + j11.16	0.104	0.009
	× 24-1/2"	8-3/4	1-1/8	0.21 + j22.45	0.11 + j11.23	0.105	0.009
		13-1/8	1-1/8	0.21 + j25.87	0.11 + j12.91	0.120	0.008

*The percent water content was calculated from the following equation:

$$WC = \frac{(\text{Weight after soaking} - \text{Weight before})}{\text{Weight before}} \times 100 \quad .$$

Before soaking, the wooden bars were dried in an oven until their change in weight with time became negligible.

**These values should be considered only as rough estimates of the loss tangent.

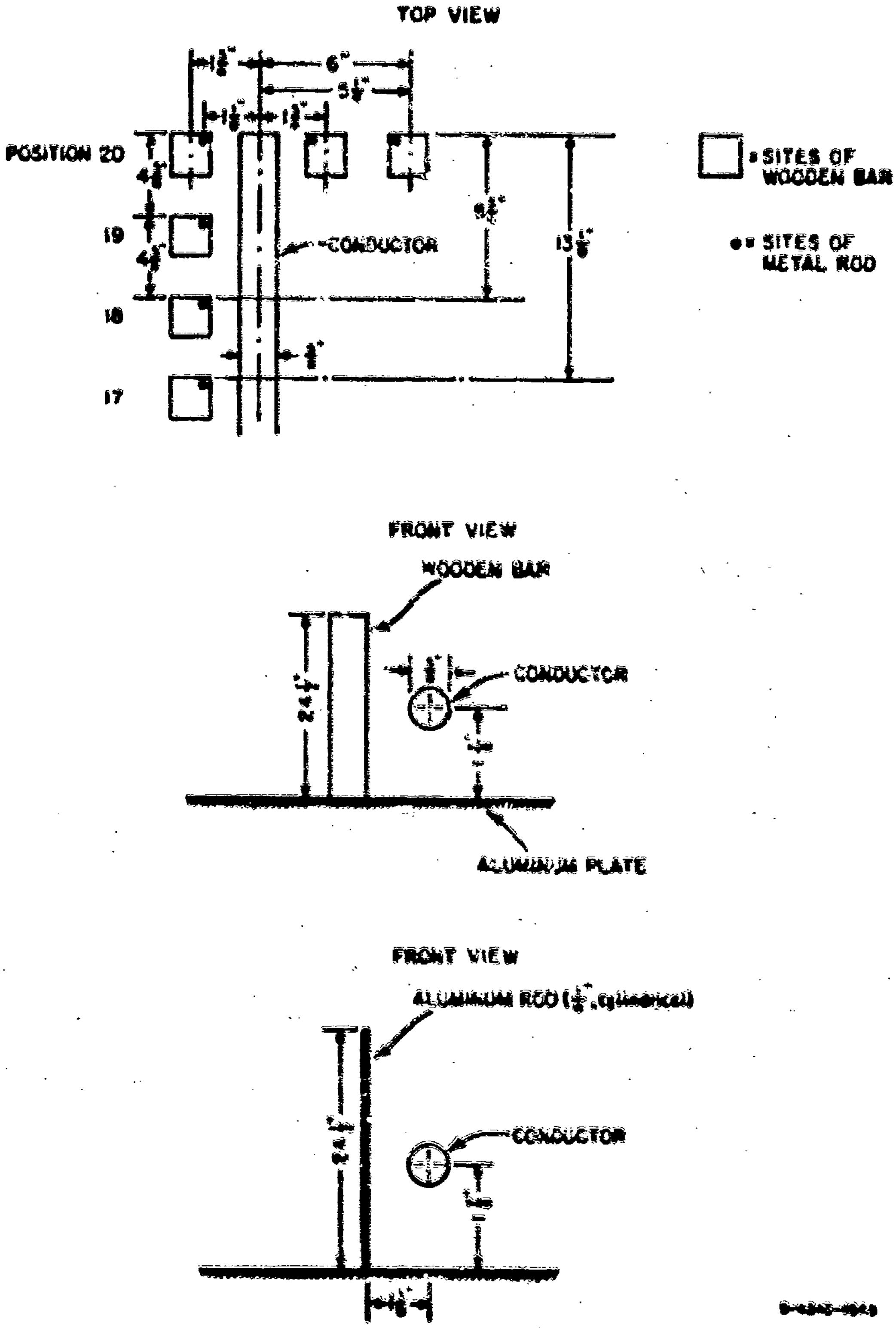

FIG. 16 SETUP FOR IMAGE-PLANE LINE MEASUREMENT OF SHUNT ADMITTANCE OF SINGLE SCATTERER PERPENDICULAR TO IMAGE PLANE (and perpendicular to line)

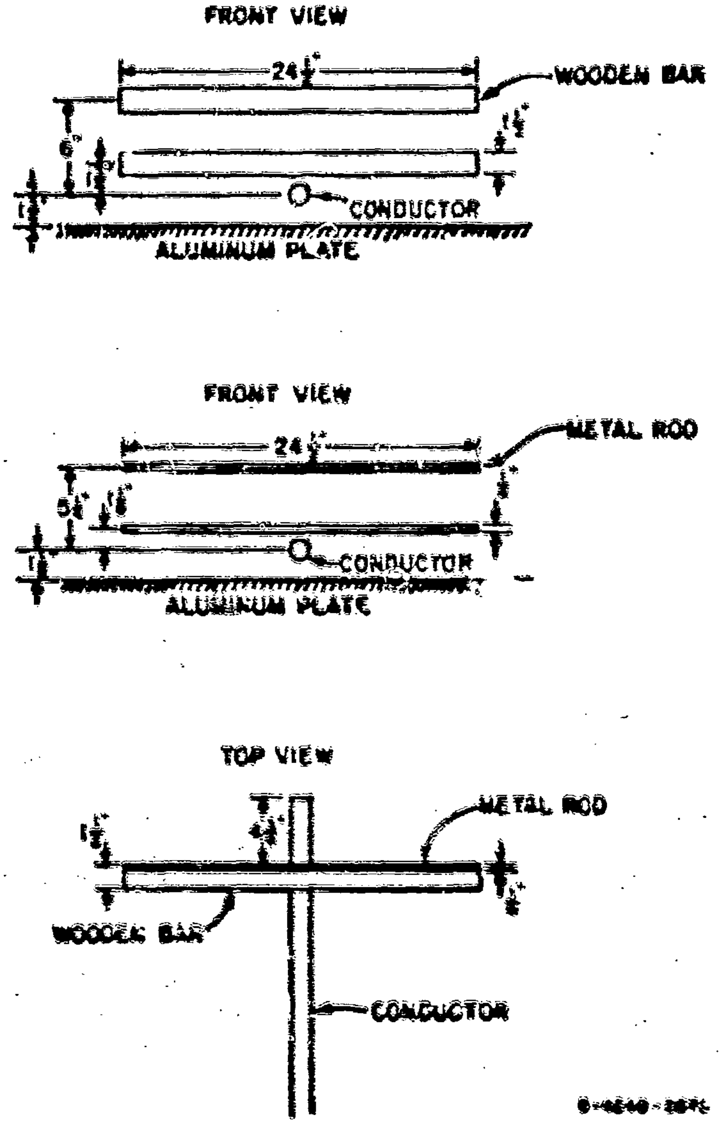

FIG. 36 SETUP FOR IMAGE-PLANE LINE MEASUREMENT OF SHUNT ADMITTANCE OF SINGLE SCATTERER PARALLEL TO IMAGE PLANE (but perpendicular to line)

Table VI

SHUNT ADMITTANCE VERSUS DISTANCE FROM LINE, BARS PERPENDICULAR TO IMAGE PLANE

Type of Scatterer	Distance of Scatterer from Conductor ℄ to ℄ (in)	Measured Equivalent Shunt Admittance on Image-Plane Line (mmhos)	Equivalent Admittance of Scatterer on 300-ohm Two-Wire Line (mmhos)	Equivalent Shunt Capacitance (C) of Scatterer on 300-ohm Two-Wire Line (pF)	Loss Tangent, δ = arc tan (1/ωRC)
Dry Wooden Bar (0 percent WC) 21-1/2" × 1-1/2" × 1-1/2"	1-3/4 6	0.89 + j6.36 0.94 + j0.78	0.45 + j4.16 0.47 + j0.39	0.039 0.003	0.106 1.211
Wet Wooden Bar (15 percent WC) 21-1/2" × 1-1/2" × 1-1/2"	1-3/4 6	1.81 + j24.01 0.66 + j2.76	0.95 + j12.46 0.33 + j1.38	0.116 0.012	0.076 0.228
Aluminum Rod 1/4" diameter × 21-1/2"	1-1/4 3-1/4	0.62 + j21.76 0.65 + j1.07	0.31 + j10.65 0.33 + j0.54	0.102 0.005	0.02 0.40

Table VII

SHUNT ADMITTANCE VERSUS DISTANCE FROM LINE, BARS PARALLEL TO IMAGE PLANE

Type of Scatterer	Distance of Scatterer from Conductor ℄ to ℄ (in)	Measured Equivalent Shunt Admittance on Image-Plane Line (mmhos)	Equivalent Admittance of Scatterer on 300-ohm Two-Wire Line (mmhos)	Equivalent Shunt Capacitance (C) of Scatterer on 300-ohm Two-Wire Line (pF)	Loss Tangent, δ = arc tan (1/ωRC)
Dry Wooden Bar (0 percent WC) 21-1/2" × 1-1/2" × 1-1/2"	1-3/4 6	0.80 + j7.12 0.94 + j1.55	0.45 + j2.56 0.47 + j0.76	0.023 0.007	0.176 0.004
Wet Wooden Bar (15 percent WC) 21-1/2" × 1-1/2" × 1-1/2"	1-3/4 6	1.92 + j20.90 0.40 + j2.45	0.86 + j10.45 0.80 + j1.23	0.09 0.01	0.091 0.342
Aluminum Rod 1/4" diameter × 21-1/2"	1-1/4 5-1/4	0.62 + j13.77 0.66 + j1.88	0.31 + j6.85 0.33 + j0.84	0.05 0.007	0.044 0.388

placed 4-3/8 in from the open end of the line and 1-3/4 in away from and orthogonal to one conductor of the line. Again 1-1/2-in-square dry and wet wooden bars and aluminum rods were used. Seven different scatterer lengths, from 4-3/8 in to 24-1/2 in, were measured, and the results are summarized in Table VIII. Figure 17 shows the equivalent shunt

Table VIII

EQUIVALENT SHUNT ADMITTANCE OF SCATTERER NEAR A 300-OHM TWO-WIRE TRANSMISSION LINE VERSUS LENGTH OF SCATTERER

Type of Scatterer	Length of Scatterer (in)	Equivalent Shunt Admittance on Two-Wire Line (µmhos)	Equivalent Shunt Capacitance of Scatterer (pF)	Loss Tangent at 17 MHz
Dry Wooden Bars	4-3/8	0.35 + j4.67	0.043	0.07
with Square	5-1/2	0.36 + j5.14	0.048	0.06
Cross Section	8-7/8	0.75 + j5.15	0.048	0.14
(9 percent WC)	11-1/4	0.75 + j5.60	0.052	0.13
1-1/2" X 1-1/2"	13-1/4	1.28 + j5.82	0.054	0.21
	22-1/2	1.28 + j6.00	0.056	0.21
	24-1/2	1.28 + j6.60	0.060	0.21
Wet Wooden Bars	4-3/8	0.20 + j4.98	0.046	0.04
with Square	5-1/2	0.20 + j5.76	0.053	0.03
Cross Section	8-7/8	0.20 + j6.52	0.061	0.03
(24 percent WC)	11-1/4	0.19 + j8.06	0.075	0.02
1-1/2" X 1-1/2"	13-1/4	0.19 + j10.37	0.097	0.01
	22-1/2	0.19 + j10.37	0.097	0.01
	24-1/2	0.19 + j10.45	0.097	0.01
Aluminum Rods	4-3/8	0.10 + j4.20	0.039	0.02
1/4" diameter	5-1/2	0.10 + j6.67	0.062	0.01
	8-7/8	0.10 + j8.61	0.080	0.01
	11-1/4	0.10 + j8.64	0.081	0.01
	13-1/4	0.10 + j8.97	0.084	0.01
	22-1/2	0.10 + j10.06	0.094	0.009
	24-1/2	0.10 + j10.06	0.094	0.009

capacitance of the scatterers as a function of scatterer length. Evidently the length of the scatterers used for the tests of the effect of longitudinal position was adequate.

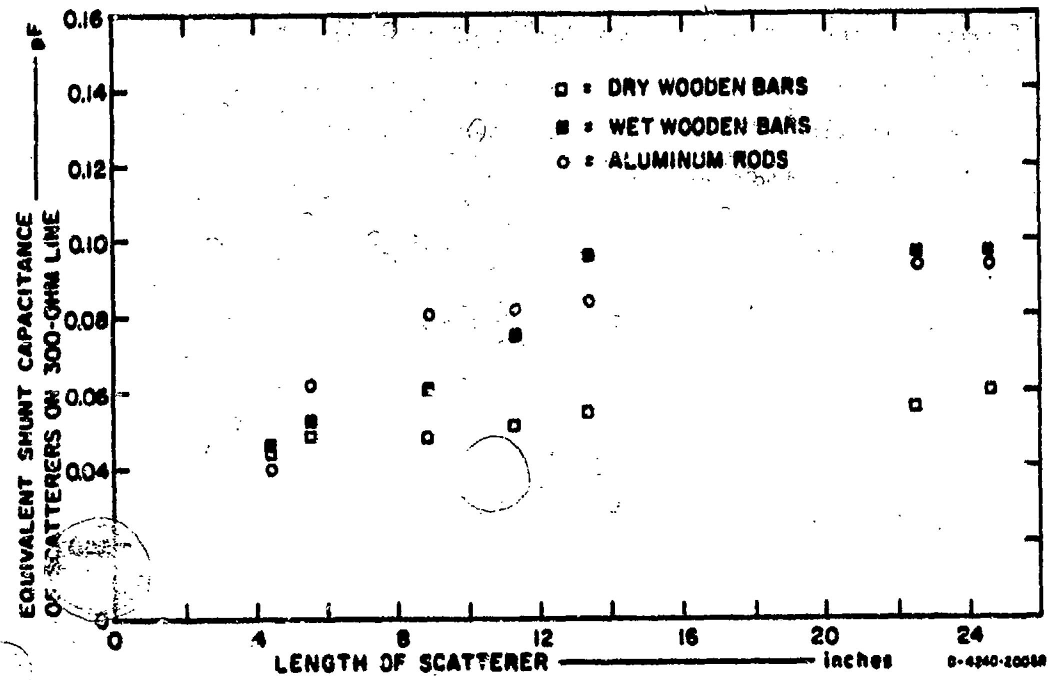

FIG. 17 MEASURED EQUIVALENT SHUNT CAPACITANCE AS A FUNCTION OF SCATTERER LENGTH

4. Effect of Electrical Properties of the Scatterer

Three types of scatterers have been used thus far: dry wood bars, wet wood bars, and aluminum rods. Some indication of the effect of conductivity can be obtained by examining the results already obtained, but it should be pointed out that the aluminum rods are of a different shape and size than the wooden bars. Consequently we will use wooden bars of the same size and shape (but with varying water content) to study further the effect of the intrinsic complex dielectric constant of the scatterer upon the equivalent shunt admittance of the scatterers observed with our 150-ohm image-plane line at 17 MHz.

For these tests, 1-1/2-in-square bars 24-1/2 in long were placed 4-3/8 in from the open end of the line. The bars were perpendicular to the line at position 19, and data were obtained with the bars at two different distances from the line. Immediately after the bridge measurement the water content was determined in percent relative to the dry weights obtained by oven drying at 60°C until the change of weight with time was negligible. The results of these tests are summarized in Table IX. An increase in equivalent shunt capacitance with increasing water content is observed. The equivalent shunt capacitance is plotted

Table IX

EQUIVALENT ADMITTANCE OF WOODEN BARS NEAR A 150-OHM IMAGE-PLANE TRANSMISSION LINE VERSUS MOISTURE CONTENT OF BARS

Water Content of Bars, WC (percent)	Distance ℄ of Scatterer to ℄ of Conductor (in)	Measured Equivalent Admittance of Scatterer on 150-ohm Line (μmhos)	Admittance Equivalent of Scatterer on 300-ohm Line (μmhos)	Equivalent Shunt Capacitance on 300-ohm Line (pF)
0.0	1-3/4	0.89 + j8.36	0.45 + j4.18	0.039
	6	0.94 + j0.78	0.47 + j0.39	0.003
8.5	1-3/4	2.54 + j12.94	1.27 + j6.47	0.060
	6	0.48 + j1.54	0.24 + j0.77	0.007
12.7	1-3/4	0.62 + j15.76	0.31 + j7.88	0.073
	6	0.66 + j1.08	0.33 + j0.54	0.005
25.0	1-3/4	1.90 + j24.92	0.95 + j12.46	0.116
	6	0.66 + j0.236	0.33 + j0.138	0.012
44.2	1-3/4	1.92 + j29.84	0.96 + j14.92	0.139
	6	0.44 + j3.70	0.22 + j1.85	0.017

as a function of water content in Fig. 18 for both scatterer spacings from the line conductor. The variation of effective shunt capacitance with water content is very linear for the 6-in spacing (with the exception of the value at 12.7 percent water content, which seems low), and a similar variation is apparent for the 1-3/4-in spacing. Also, values from the other tests involving wet bars have been plotted for the 1-3/4-in spacing. Dashed lines have been drawn in to illustrate these trends. These results are in agreement with those obtained with freshly cut willows in an earlier study (see Appendix of Ref. 8), where the variation of effective relative dielectric constant exhibited a linear variation with the weight (and, by inference, water content) of the willows as they dried out.

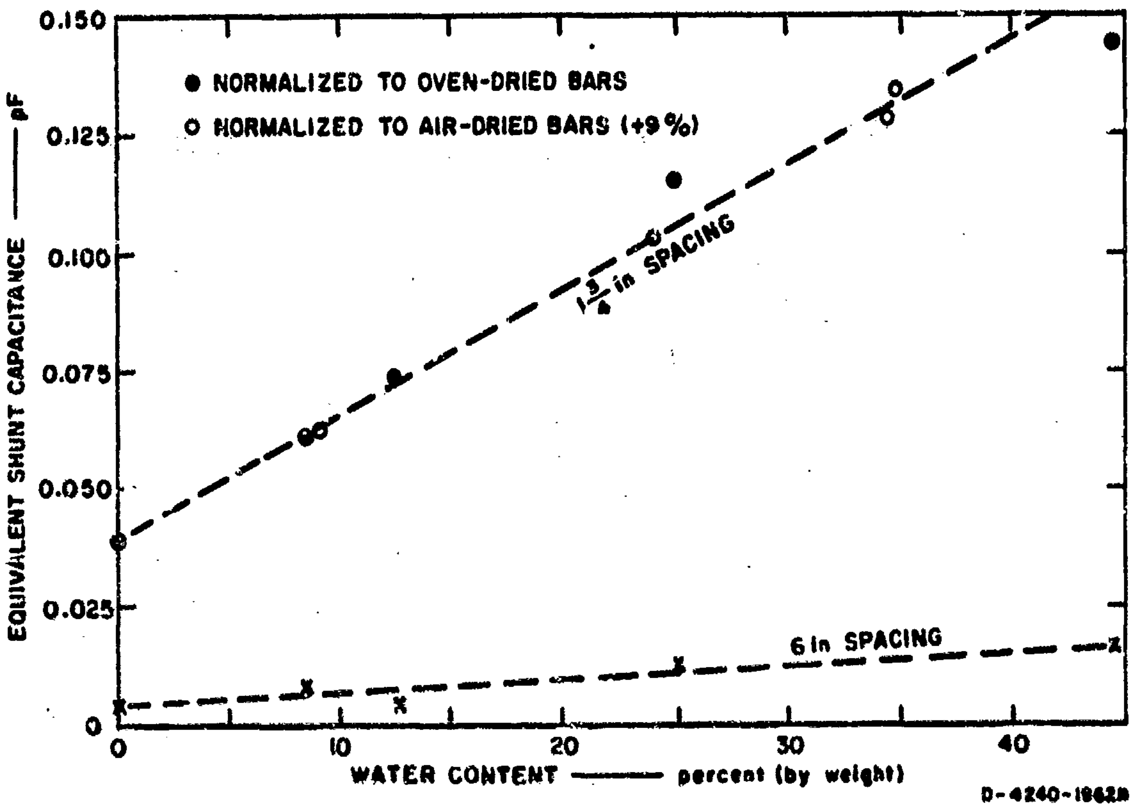

FIG. 18 EQUIVALENT SHUNT CAPACITANCE OF WOODEN BARS AS A FUNCTION OF WATER CONTENT

5. Equivalent Shunt Admittance of a Single Cut Pine Bough

The 440-ohm two-wire line was used in the laboratory to measure the equivalent shunt admittance of a single, freshly cut pine bough. The pine bough was fastened in an upright position to the wooden table used for the tests discussed in Sec. I-A-1-B, and data were obtained for three different configurations: line in plane parallel to table top with bough stem 12 in from nearest conductor, and line in plane perpendicular to table top (i.e., in plane parallel to bough stem) with bough stem 12 in from nearest conductor. The bough stem was always 10 in from the end of the line (between positions 17 and 18). These configurations are illustrated in the sketches in Fig. 19. The data obtained during these measurements are summarized in Table X.

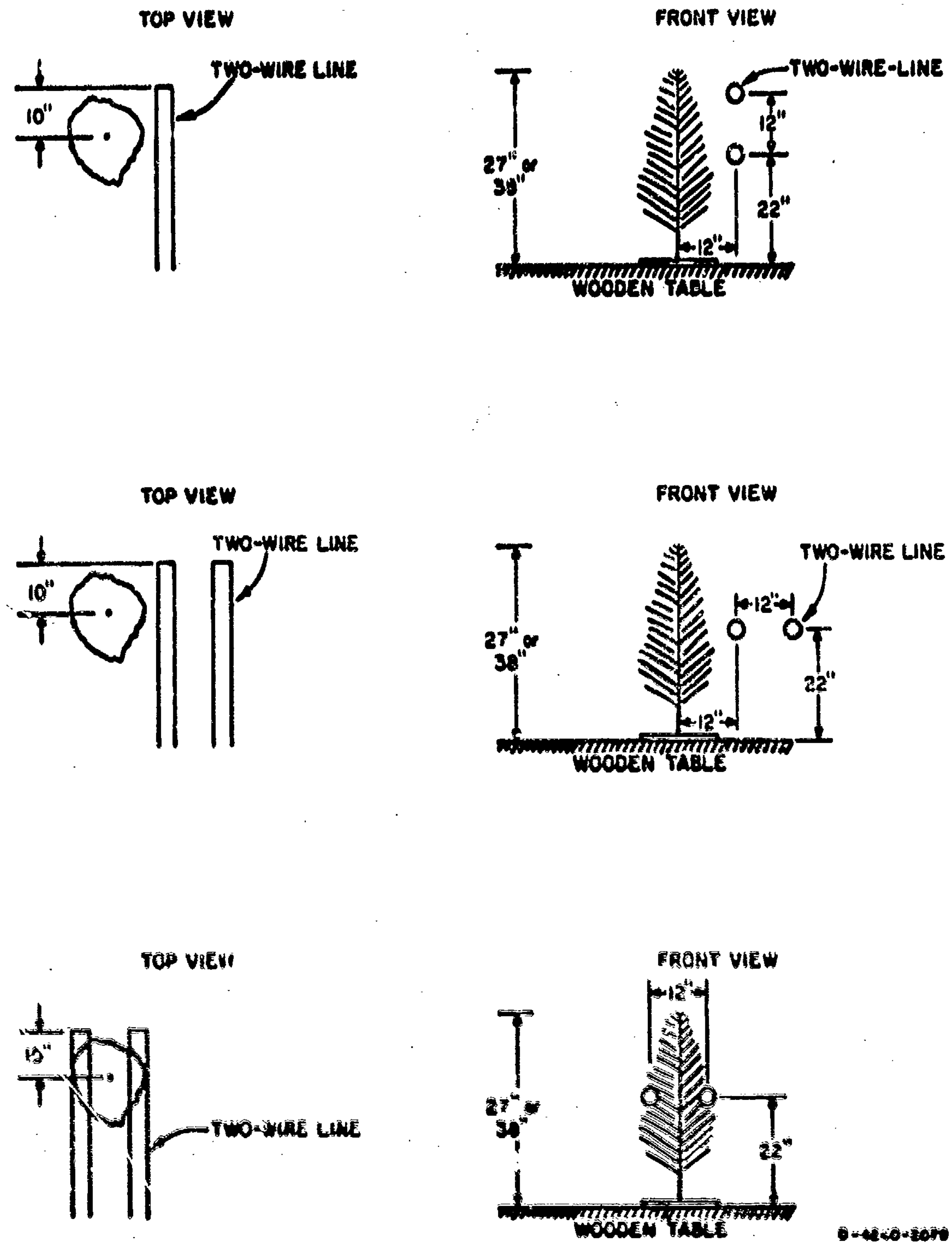

FIG. 19 TEST SETUP FOR MEASUREMENTS ON SINGLE PINE BOUGH

Table X

EQUIVALENT SHUNT ADMITTANCE OF SINGLE PINE BOUGH

Measurement Configuration	Height of Bough (in)	Equivalent Shunt Admittance (μmhos)	Equivalent Shunt Capacitance, C (pF)	Loss Tangent
A	27 38	0.23 + j6.32 0.92 + j9.47	0.059 0.088	0.036 0.097
B	27 38	0.24 + j5.21 0.61 + j8.59	0.048 0.080	0.046 0.070
C	27	0.66 + j7.95	0.074	0.082

6. Equivalent Shunt Admittance of Living Oak Trees

Following the laboratory tests described in the preceding section, the 440-ohm two-conductor line was taken to the field to obtain data on a living tree. Two small oak trees (see Fig. 20) about 15 and 25 ft high (breast-height diameters about 4 in and 5-1/2 in respectively) which were conveniently located near the laboratory were selected for these tests, and the line was set up in a manner similar to that described for the tests on the cut pine boughs (see Fig. 21 for setup at the small-tree site). The results of these tests are summarized in Table XI.

7. Summary of Results on Measurements of Equivalent Shunt Admittance of Single Scatterers

We have observed that the equivalent circuit of a single scatterer which is short relative to the wavelength of the test signal is always a lossy capacitor--never an inductor. The value of the equivalent capacitance depends upon the length of the scatterer, its electrical properties (as indicated by water content in the case of wooden scatterers), its position radially from the line, and its orientation (whether the line is parallel to or perpendicular to the plane containing the scatterer). Provided the scatterer is not located in the fringing

(a) 15-ft TREE

(b) 25-ft TREE

TA-8863-5

FIG. 20 PHOTOGRAPHS OF TREES USED FOR SINGLE-TREE MEASUREMENTS

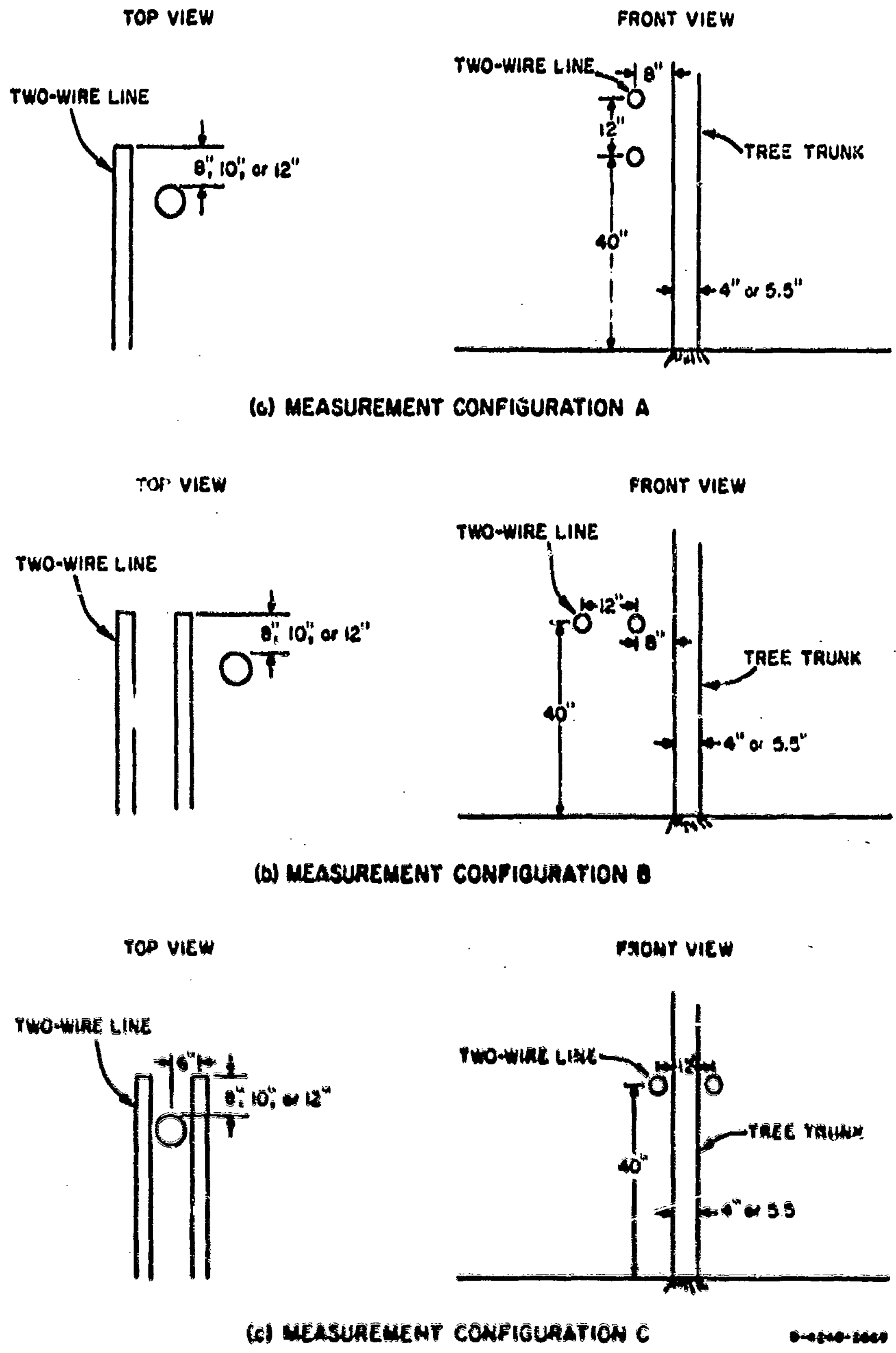

FIG. 21 MEASUREMENT SETUP FOR ISOLATED-TREE TESTS

Table XI

EQUIVALENT SHUNT ADMITTANCE OF ISOLATED SMALL OAK TREES

Measurement Configuration	Tree Height (ft)	Distribution of Trunk from End of Line (in)	Equivalent Shunt Admittance (μmhos)	Equivalent Shunt Capacitance, C (pF)	Loss Tangent $\delta = 1/\omega RC$
A	15	0	1.21 + j6.98	0.065	0.173
	15	10	3.18 + j10.55	0.100	0.300
	15	12	3.28 + j10.58	0.101	0.310
	25	0	2.19 + j10.49	0.097	0.221
	25	8	1.30 + j12.86	0.119	0.101
	25	10	2.59 + j12.68	0.118	0.202
	25	12	2.60 + j13.03	0.121	0.198
B	15	10	0.26 + j8.45	0.079	0.030
	25	10	0.50 + j9.81	0.091	0.051
C	15	8	0.39 + j9.41	0.088	0.041
	15	10	0.39 + j9.94	0.093	0.039
	15	12	0.40 + j10.23	0.095	0.039
	25	8	1.03 + j12.78	0.120	0.086
	25	10	1.04 + j13.30	0.125	0.077

fields near the open end of the line, however, the equivalent shunt admittance is relatively independent of its position longitudinally along the line. This concludes our study of the effects of single scatterers. Let us now turn our attention to the effects of more than one scatterer.

D. Mutual Impedance and Coupling Effects

In the one-dimensional model which we are using to find the equivalent dielectric constant of a distribution of scatterers we expect to neglect the mutual coupling between the scatterers and consider only the coupling of the individual scatterers to the transmission line. This coupling to the transmission line can be taken into account in the model by an equivalent shunt admittance for each scatterer. In the preceding section we have been considering this equivalent admittance and finding how it changes with various parameters which affect it. We now need to determine whether we are justified in neglecting mutual coupling effects when more than one scatterer is present or if we need to modify the equivalent circuits of the scatterers to account for mutual coupling.

Measurements were made with pairs of dry wooden bars, pairs of wet wooden bars, and pairs of aluminum rods to investigate mutual coupling effects. Two sets of measurements were made, one with the two scatterers in a plane perpendicular to both the conductors and the image plane, and the other with the two scatterers in a plane perpendicular to the image plane but parallel to the conductors. In both cases, the scatterers were perpendicular to the image plane (see Fig. 15). The results of these measurements are shown in Tables XII and XIII, respectively. Only the susceptance is given since the accuracy with which it can be determined with our measurement equipment is much better than that with which the conductance can be measured. Moreover, the conductance was much smaller than the susceptance and may be considered negligible for the purpose of these tests on mutual coupling.

The results of the tests with both scatterers in a plane perpendicular to the transmission line are given in Table XII. Column 5, headed "Equivalent Shunt Susceptance," shows the measured values for

Table XII

MUTUAL COUPLING TESTS WITH SCATTERERS IN PLANE PERPENDICULAR TO 150-OHM IMAGE-PLANE LINE

Type of Scatterer	Number of Scatterers Measured Simultaneously	Scatterer Position*	Distance from ℄ of Conductor to ℄ of Scatterer (in)	Equivalent Susceptance, B (μmhos)	Difference** (μmhos)
Dry Wooden Bars	1	19	1-3/4	9.7	0.0
(0 percent MC)	1	19	6	3.0	
24-1/2" × 1-1/2" × 1-1/2"	2	19	1-3/4 and 6	12.7	
Wet Wooden Bars	1	19	1-3/4	25.1	0.3
(34.2 percent MC)	1	19	6	3.2	
24-1/2" × 1-1/2" × 1-1/2"	2	19	1-3/4 and 6	28.6	
Aluminum Rods	1	19	1-3/4	14.1	1.2
1/4" diameter × 24-1/2"	1	19	5-1/4	1.0	
	2	19	1-3/4 and 5-1/4	16.3	

*See Fig. 15 for description of scatterer positions.

**This is the difference between the susceptance measured for the pair of scatterers and the sum of the two susceptances measured for the individual scatterers.

Table XIII

MUTUAL COUPLING TESTS WITH SCATTERERS IN PLANE PARALLEL TO 150-OHM IMAGE-PLANE LINE

Type of Scatterer	Number of Scatterers Measured Simultaneously	Scatterer Position*	Distance from ℄ of Conductor to ℄ of Scatterer (in)	Measurement Equivalent Susceptance, B (µmhos)	Computed Susceptance (µmhos)	Difference** (µmhos)
Dry Wooden Bars	1	17	1-3/4	15.1		
(9 percent MC)	1	18	1-3/4	13.5		
24-1/2" × 1-1/2" × 1-1/2"	1	19	1-3/4	13.2		
	2	17 and 18	1-3/4	917.0	913.4	+3.6
	2	18 and 19	1-3/4	618.8	614.7	+4.1
	2	17 and 19	1-3/4	913.6	913.1	+0.5
Aluminum Rods	1	17	1-1/8	23.8		
1/4" diameter × 24-1/2"	1	18	1-1/8	18.8		
	1	19	1-1/8	15.6		
	2	17 and 18	1-1/8	929.1	92[illegible].4	+1.7
	2	18 and 19	1-1/8	623.6	622.3	+1.3
	2	17 and 19	1-1/8	922.7	924.2	-1.5

*See Fig. 15 for description of scatterer positions.

**This is the difference between the measured susceptance of the line plus two scatterers (from the point of the scatterer nearer the sending end of the line) and the corresponding value computed from the measured equivalent susceptances of the individual scatterers.

each scatterer alone, and for the pair. The difference between the result for the pair and the sum of the individual susceptances is shown in Column 6. The differences are so small that they lie in the experimental error range, except possibly the result for the aluminum rod which shows a small but measurable difference.

The results of the tests with the scatterers perpendicular to the line but in a plane parallel to the line (see Table XIII) are somewhat more difficult to interpret. Here we cannot simply take the difference of the measured results for one and two scatterers to determine mutual coupling effects because the equivalent susceptance of the section of the line between the scatterers (essentially due to the capacitance per unit length for our relatively low-loss line) must be taken into account.

The measured equivalent susceptances for the individual scatterers (given in Column 5) are the values appropriate for use as lumped-constant equivalents at the position of the scatterer down the line. The measured equivalent susceptances for the pairs of scatterers represent the lumped-circuit equivalent of the line plus scatterers as seen at the scatterer closer to the sending end of the line looking toward the load end of the line (which was an open circuit for these tests). The value of equivalent susceptance seen at this point was computed for the case of two scatterers from the measured values for the individual scatterers under the assumptions of no mutual coupling and a perfectly conducting line. Therefore, the difference between this computed value and the observed value with both scatterers present is a measure of the mutual effect. Unfortunately, the line susceptance is much greater than the susceptance of any individual scatterer and we must rely upon the difference of two large numbers for our estimate of the mutual effect.

For the aluminum rods this difference is about 10 percent of the value of the susceptances of the individual scatterers and it may be concluded that mutual coupling is negligible in this case. Indeed, the observed differences are near the limit of the accuracy of our measurements. For the wooden bars, the mutual effect is significant when the bars are in adjacent positions as expected, but the effect appears negligible when the bars are separated by only one position. Perhaps the increase in the magnitude of the apparent mutual coupling of the wood bars over that of the aluminum rods when the scatterers are in adjacent positions may be explained in part by the larger size of the bars which, for a fixed spacing (see Fig. 15), places the bars physically closer together. The separation of the wooden bars in adjacent positions ($\approx\lambda/240$ at 17 MHz) is only about twice the width of a single bar, whereas the separation of the aluminum rods in adjacent positions is about sixteen times the diameter of a single rod.

The results of these measurements with pairs of scatterers appear to justify the assumption that the [illegible] coupling is negligible in most practical cases (i.e., excep[illegible] scatterers are <u>very</u> close together), and that the principal [illegible] the coupling of the individual scatterers to the transmission line.

E. <u>Many Scatterers Randomly Distributed about a Transmission Line</u>

1. <u>Methods of Approach</u>

Our objective was to determine the feasibility of representing a forest as a dielectric medium and of measuring the dielectric properties of this medium by means of transmission-line probes. We have already discussed the effect of individual scatterers and have concluded that each scatterer of any of the shapes and sizes (short compared to the wavelength of the test signal) investigated could be represented by a shunt capacitance with an associated shunt conductance placed across the transmission line at the position of the scatterer. We now need to consider the case of many scatterers randomly distributed about the transmission line, as trees in a forest would be, and see whether we can represent a region with many discrete scatterers as if it were filled with a continuous medium characterized by a dielectric constant with associated loss factors. In other words, we are going to make a model of the forest using wooden bars or metal cylinders as trees and determine the effective dielectric constant of the model by means of a transmission line probe.

In carrying out this part of the investigation we approached the problem in each of two ways. First, we placed scatterers randomly about the transmission line, rolling dice to see whether or not a "tree" should be at each position of a two-dimensional grid. We then measured the input impedance of the line with the termination open circuited and again with the termination short circuited, and (using the equations of Sec. II) calculated the effective dielectric constant, permeability and loss tangent. This process was repeated five times (see Fig. 22 for the actual scatterer positions used) and the results were averaged. These average values are termed measured values. Our second approach to the

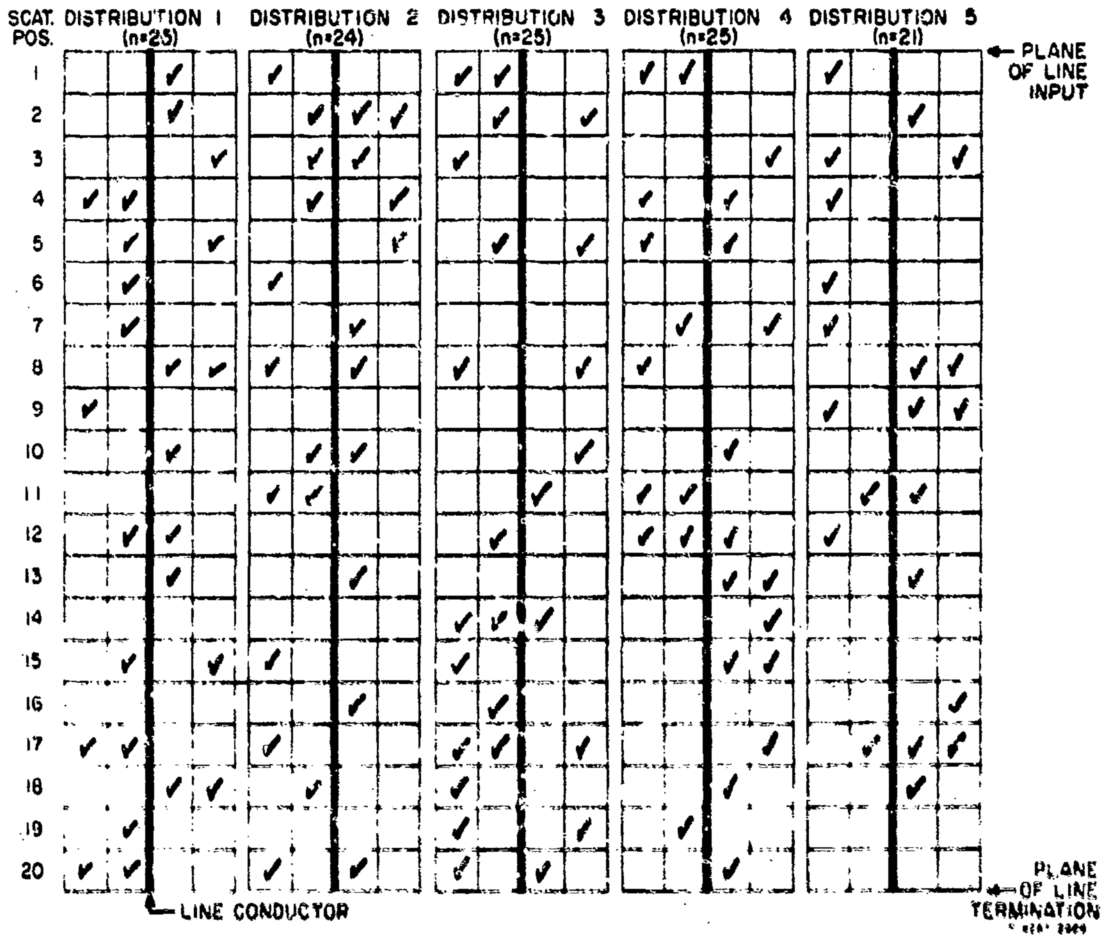

FIG. 22 RANDOM DISTRIBUTIONS OF SCATTERERS USED FOR MEASUREMENTS

multiple-scatterer problem was based on previous measurements, but it involved computation only. In the latter case, we constructed a distribution of sizes of lossy capacitors from the measured results for single scatterers and used a random-number generator to decide what size capacitor to place at each of the uniformly spaced intervals along a hypothetical transmission line. We then calculated the input impedance of the hypothetical line when open and short circuited and again used the equations of Sec. II to convert to the electrical parameters of the medium around the line. The process was repeated ten times, and average values, which we call calculated values, were obtained. The remainder of this section will deal with a comparison of such measured and calculated values for various example cases.

2. 17-MHz Tests with Image-Plane Line

Tests were made with the λ/8 image-plane line on the dry wood (9 percent WC) and wet wood bars (≈25 percent WC) and aluminum rods used in the earlier tests. For these tests the scatterers were set up perpendicular to the image plane. The details of the line spacing and the scatterer spacings are pictured as insets on the figures showing the calculated and measured values.

a. Dry Wood Bars

For the first tests on the dry wood bars, the center of the transmission-line conductor was positioned 4.6 in above the aluminum plate which forms the image plane. The measured values are summarized in Table XIV and the calculated values are given in Table XV. The average values of the real parts of the relative complex dielectric constant and complex permeability are plotted as a function of the number of scatterers (i.e., scatterers per wavelength) in Fig. 33.

The conductor then was lowered so that its center was 1.452 in above the aluminum plate and measurements were repeated. Tables XVI and XVII summarize these results; the average values of the real parts of the complex relative dielectric constant and permeability are plotted in Fig. 34 as a function of the number of scatterers.

Table XIV

ELECTRICAL CONSTANTS WITH DRY WOOD BARS MEASURED

WITH 200-OHM IMAGE-PLANE LINE

Random Distribution Number	Number of Scatterers n	Relative Dielectric Constant ϵ_r'	Relative Permeability, $\mu_r = \mu_r' - j\mu_r''$	Loss Tangent δ
1	25	1.080	0.994 - j0.002	0.0082
2	24	1.090	0.990 - j0.000	0.0079
3	25	1.057	0.994 - j0.002	0.0055
4	25	1.076	0.997 - j0.003	0.0062
5	21	1.063	0.994 - j0.000	0.0062
Average	24	1.080	0.994 - j0.001	0.0068

Table XV

ELECTRICAL CONSTANTS WITH DRY WOOD BARS CALCULATED

FOR 200-OHM IMAGE-PLANE LINE

Number of Scatterers n	Relative Dielectric Constant ϵ_r'	Relative Permeability $\mu_r = \mu_r' - j\mu_r''$	Loss Tangent δ
10	1.040	1.001 - j0.000	0.0023
20	1.060	1.001 - j0.000	0.00431
25	1.064	1.006 - j0.000	0.0055
30	1.114	1.003 - j0.000	0.0067

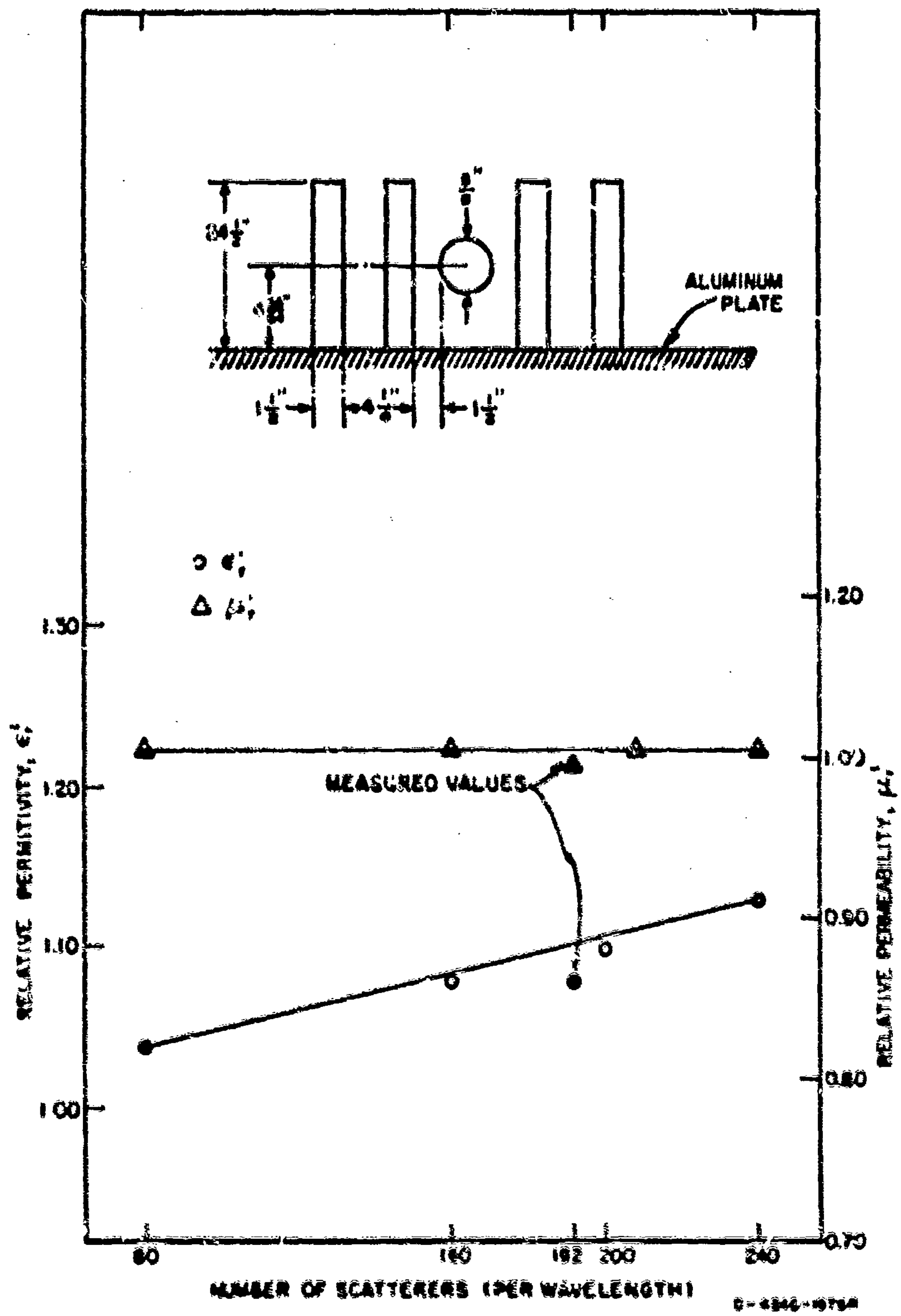

FIG. 23 EFFECTIVE ELECTRICAL CONSTANTS OF VOLUME CONTAINING DRY WOOD BARS--CALCULATED AND MEASURED WITH 200-ohm IMAGE-PLANE LINE

Table XVI

ELECTRICAL CONSTANTS WITH DRY WOOD BARS MEASURED WITH 135-OHM IMAGE-PLANE LINE

Random Distribution Number	Number of Scatterers n	Relative Dielectric Constant ϵ_r'	Relative Permeability, $\mu_r = \mu_r' - j\mu_r''$	Loss Tangent δ
1	25	1.039	1.016 - j0.002	0.0011
2	24	1.059	1.016 - j0.001	0.0025
3	25	1.038	1.020 - j0.002	0.0014
4	25	1.030	1.026 - j0.003	0.0015
5	21	1.034	1.016 - j0.001	0.0025
Average	24	1.041	1.019 - j0.002	0.0018

Table XVII

ELECTRICAL CONSTANTS WITH DRY WOOD BARS CALCULATED FOR 135-OHM IMAGE-PLANE LINE

Number of Scatterers n	Relative Dielectric Constant ϵ_r'	Relative Permeability $\mu_r = \mu_r' - j\mu_r''$	Loss Tangent δ
10	1.021	1.000 - j0.000	0.0048
20	1.045	1.002 - j0.000	0.010
25	1.058	1.001 - j0.000	0.013
30	1.066	1.000 - j0.000	0.015

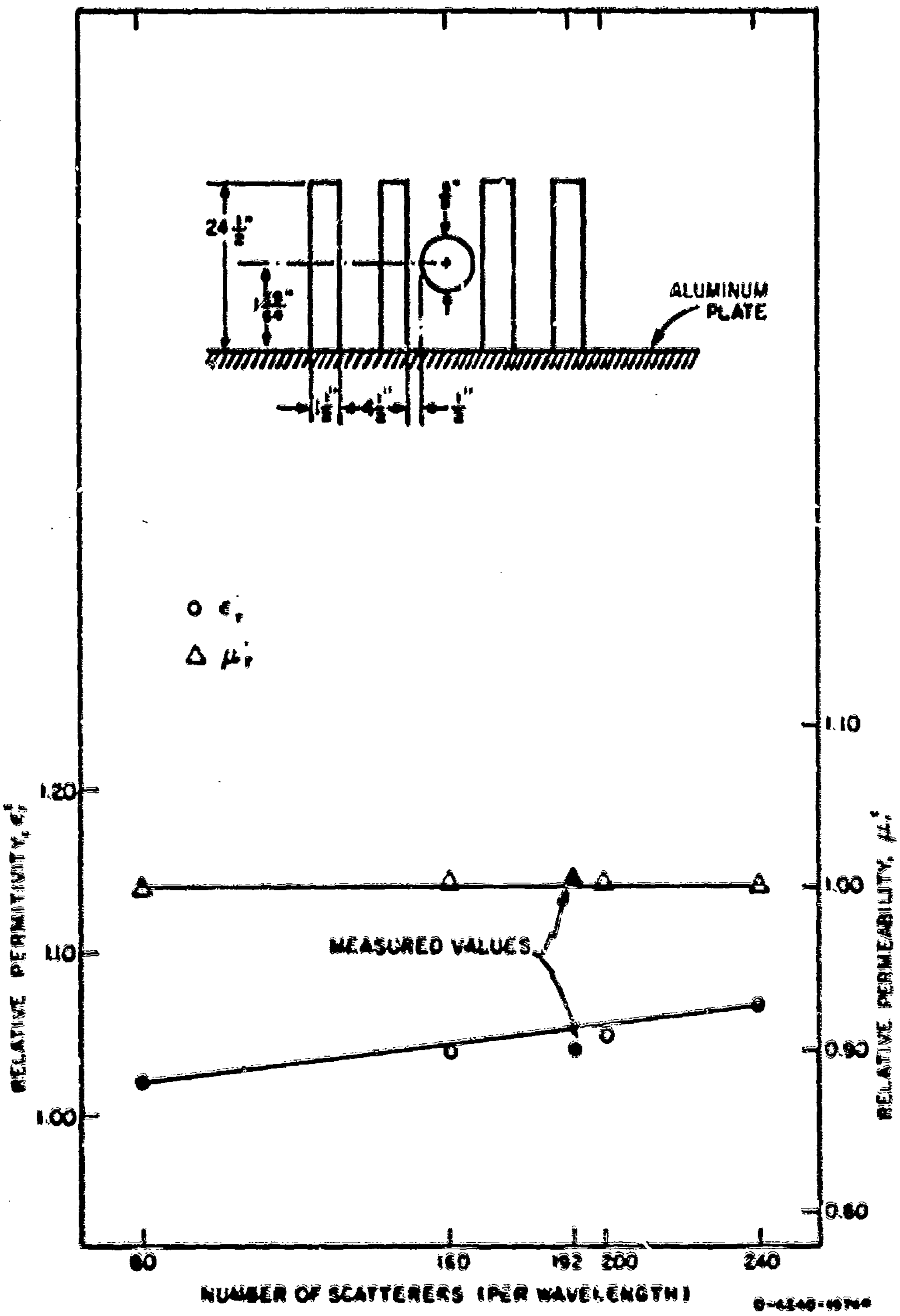

FIG. 24 EFFECTIVE ELECTRICAL CONSTANTS OF VOLUME CONTAINING DRY WOOD BARS--CALCULATED AND MEASURED WITH 135-ohm IMAGE-PLANE LINE

b. Wet Wood Bars

Wet bars (moisture content 20 percent by weight) were used as scatterers with the center of the transmission-line conductor at 1.375 in above the aluminum plate. Data were obtained with both 80 and 160 scatterers per wavelength; the results are summarized in Table XVIII (measured values) and in Table XIX (calculated values). These data are plotted in Fig. 25.

Table XVIII

ELECTRICAL CONSTANTS WITH WET WOOD BARS MEASURED WITH 150-OHM IMAGE-PLANE LINE

Random Distribution Number	Number of Scatterers n	Relative Dielectric Constant ϵ_r'	Relative Permeability, $\mu_r = \mu_r' - j\mu_r''$	Loss Tangent δ
1	10	1.064	0.992 - j0.002	0.009
1	20	1.111	0.992 - j0.002	0.012
2	10	1.077	0.997 - j0.002	0.012
2	20	1.099	0.997 - j0.002	0.010
3	10	1.062	0.989 + j0.001	0.011
3	20	1.111	0.989 + j0.001	0.009
4	10	1.047	0.966 + j0.000	0.010
4	20	1.119	0.966 + j0.000	0.011
5	10	1.079	0.990 + j0.000	0.016
5	20	1.137	0.990 + j0.000	0.012
Average	10 20	1.066 1.115	0.990 - j0.000 0.990 - j0.000	0.010 0.011

c. Metal Rods

For the first of these tests, the center of the conductor was placed 1.875 in above the aluminum plate, the 1/8-in-diameter aluminum rods were positioned perpendicular to the aluminum plate. The

Table XIX

ELECTRICAL CONSTANTS WITH WET WOOD BARS CALCULATED

FOR 150-OHM IMAGE-PLANE LINE

Number of Scatterers n	Relative Dielectric Constant ϵ_r'	Relative Permeability $\mu_r = \mu_r' - j\mu_r''$	Loss Tangent δ
10	1.075	1.000 - j0.000	0.010
20	1.136	1.000 - j0.000	0.017

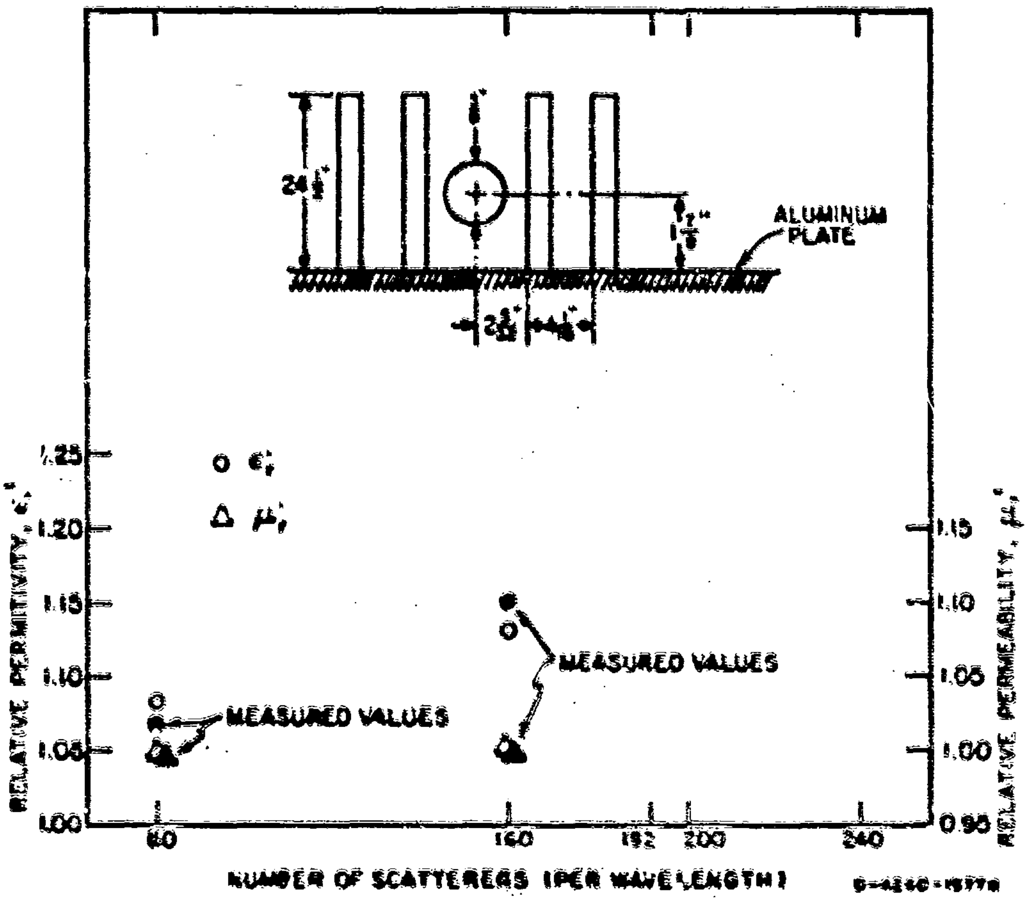

FIG. 25 EFFECTIVE ELECTRICAL CONSTANTS OF VOLUME CONTAINING WET WOOD BARS--CALCULATED AND MEASURED WITH 150-ohm IMAGE-PLANE LINE

results are summarized in Table XX (measured values) and in Table XXI (calculated values). Figure 26 shows these results along with a sketch of the measurement setup.

Table XX

ELECTRICAL CONSTANTS WITH METAL RODS PERPENDICULAR TO ZERO-POTENTIAL PLANE MEASURED WITH 150-OHM IMAGE-PLANE LINE

Random Distribution Number	Number of Scatterers n	Relative Dielectric Constant ϵ_r'	Relative Permeability, $\mu_r = \mu_r' - j\mu_r''$	Loss Tangent δ
1	25	1.197	1.101 - j0.0034	0.00256
2	24	1.165	1.100 - j0.0047	0.00283
3	25	1.171	1.104 - j0.0022	0.00249
4	25	1.148	1.107 - j0.0024	0.00371
5	21	1.160	1.100 - j0.0020	0.00267
Average	24	1.168	1.105 - j0.0028	0.00285

Table XXI

ELECTRICAL CONSTANTS WITH METAL RODS PERPENDICULAR TO ZERO-POTENTIAL PLANE CALCULATED FOR 150-OHM IMAGE-PLANE LINE

Number of Scatterers n	Relative Dielectric Constant ϵ_r'	Relative Permeability $\mu_r = \mu_r' - j\mu_r''$	Loss Tangent δ
10	1.046	1.001 - j0.001	0.00284
20	1.095	1.002 - j0.004	0.00576
25	1.111	1.001 - j0.000	0.00631
30	1.142	1.003 - j0.000	0.00825

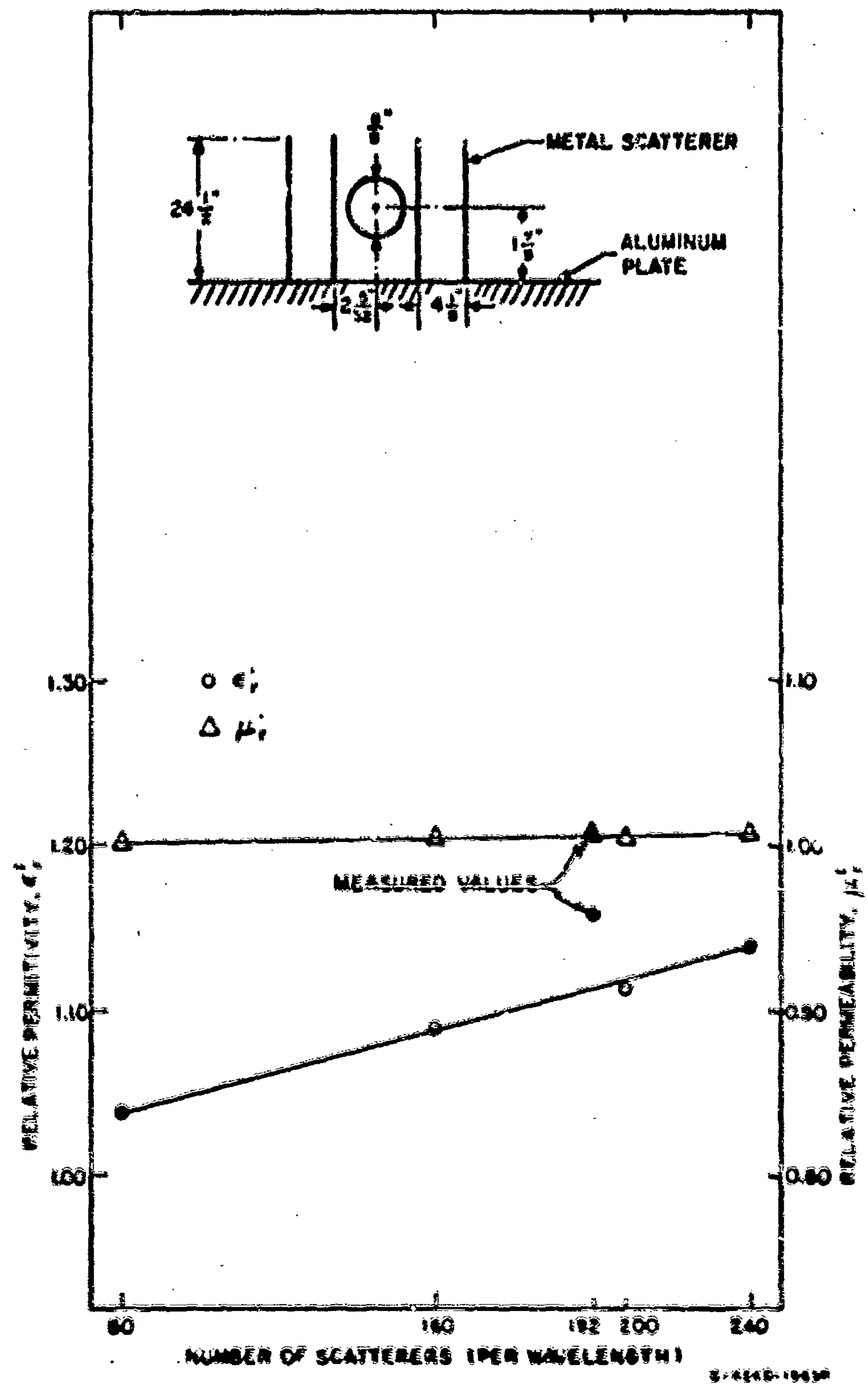

FIG. 20 EFFECTIVE ELECTRICAL CONSTANTS OF VOLUME CONTAINING METAL RODS PERPENDICULAR TO ALUMINUM PLATE—CALCULATED AND MEASURED WITH 150-ohm IMAGE-PLANE LINE

These tests were repeated with the aluminum rods parallel to the aluminum plate but still perpendicular to the transmission-line conductor (which remained at 1.875 in above the aluminum plate). Tables XXII and XXIII summarize the measured and calculated results respectively, and Fig. 27 shows the average values of the real part of the complex relative dielectric constant and permeability as a function of the number of scatterers per wavelength.

Table XXII

ELECTRICAL CONSTANTS WITH METAL RODS PARALLEL TO IMAGE PLANE MEASURED WITH 150-OHM IMAGE-PLANE LINE

Random Distribution Number	Number of Scatterers n	Relative Dielectric Constant ϵ_r'	Relative Permeability, $\mu_r = \mu_r' - j\mu_r''$	Loss Tangent δ
1	25	1.064	0.978 − j0.001	0.0025
2	24	1.057	0.974 − j0.001	0.0025
3	25	1.071	0.993 − j0.001	0.0025
4	25	1.067	0.994 − j0.002	0.0021
5	21	1.076	1.008 − j0.002	0.0023
Average	24	1.066	0.990 − j0.001	0.0024

Table XXIII

ELECTRICAL CONSTANTS WITH METAL RODS PARALLEL TO IMAGE PLANE CALCULATED FOR 150-OHM IMAGE-PLANE LINE

Number of Scatterers n	Relative Dielectric Constant ϵ_r'	Relative Permeability $\mu_r = \mu_r' - j\mu_r''$	Loss Tangent δ
10	1.017	1.0035 − j0.000	0.00095
20	1.036	1.001 − j0.000	0.00199
25	1.050	0.993 − j0.000	0.00255
30	1.055	1.002 − j0.000	0.00263

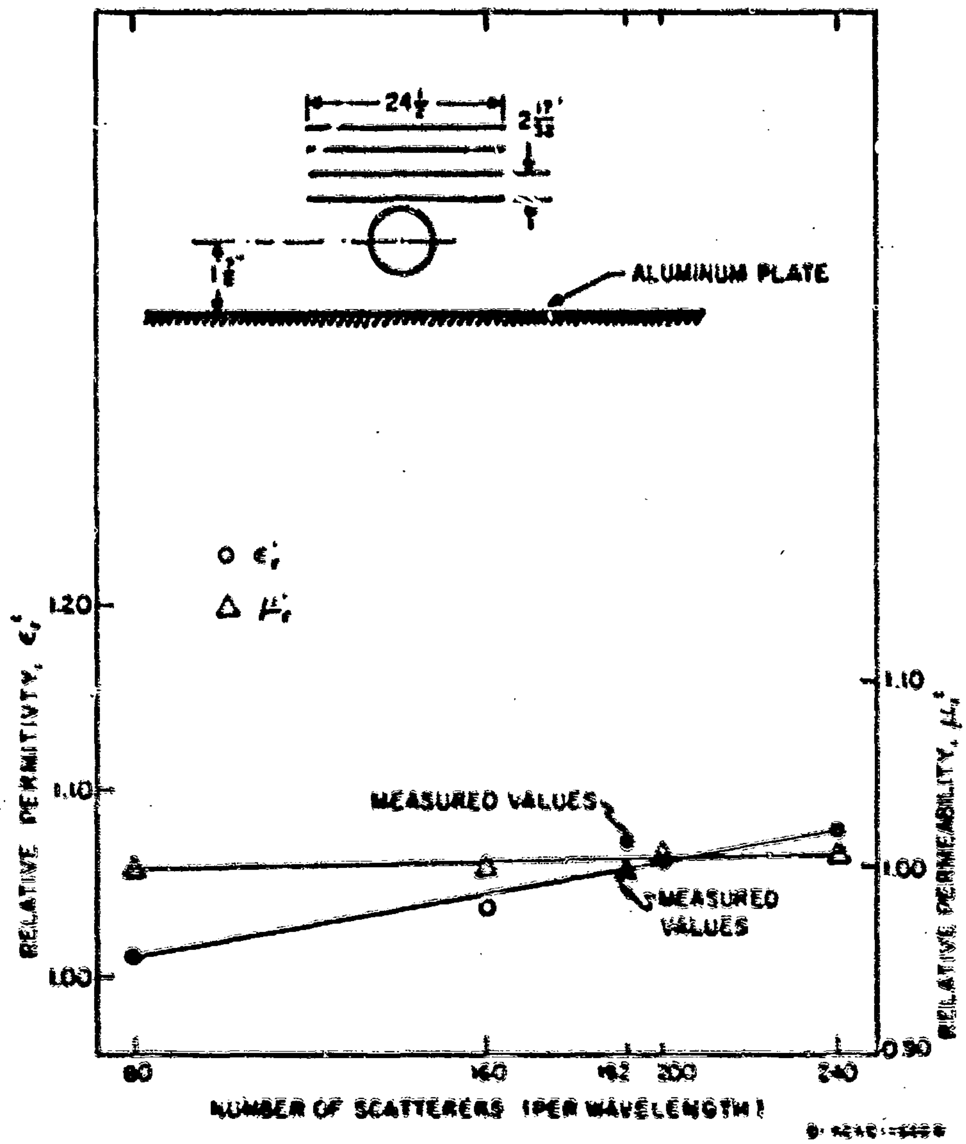

FIG. 27 EFFECTIVE ELECTRICAL CONSTANTS OF VOLUME CONTAINING METAL RODS PARALLEL TO ALUMINUM PLATE--CALCULATED AND MEASURED WITH 150-ohm IMAGE-PLANE LINE

3. 17-MHz Tests with 300-Ohm Two-Conductor Line

Tests also were made with the $\lambda/8$ two-conductor line on the dry wood, wet wood, and aluminum rod scatterers. For these tests the scatterers were positioned perpendicular to the line as shown on the inserts on the figures showing the calculated and measured results.

a. Dry Wood Bars

The measured and calculated values are summarized in Tables XXIV and XXV. The average values of the real parts of the complex relative dielectric constant and permeability are shown in Fig. 28 as a function of the number of scatterers per wavelength.

Table XXIV

ELECTRICAL CONSTANTS WITH DRY WOOD BARS MEASURED WITH 300-OHM TWO-WIRE LINE

Random Distribution Number	Number of Scatterers n	Relative Dielectric Constant ϵ_r'	Relative Permeability, $\mu_r = \mu_r' - j\mu_r''$	Loss Tangent δ
1	25	1.074	0.987 − j0.013	0.016
2	24	1.059	0.992 − j0.013	0.016
3	25	1.101	0.975 − j0.015	0.017
4	25	1.060	0.984 − j0.013	0.017
5	21	1.051	0.998 − j0.015	0.017
Average	24	1.071	0.990 − j0.016	0.017

b. Wet Wood Bars

The measured and calculated values for the bars with 15 percent water content by weight are summarized in Tables XXVI and XXVII respectively. The average values of the real part of the complex relative dielectric constant and permeability are shown in Fig. 29 as a function of the number of scatterers per wavelength. Values are also

Table XXV

ELECTRICAL CONSTANTS WITH DRY WOOD BARS CALCULATED

FOR 300-OHM TWO-WIRE LINE

Number of Scatterers n	Relative Dielectric Constant ϵ'_r	Relative Permeability $\mu_r = \mu'_r - j\mu''_r$	Loss Tangent δ
10	1.011	1.004 - j0.000	0.0035
20	1.036	1.000 - j0.000	0.007
25	1.060	1.003 - j0.000	0.009
30	1.079	1.000 - j0.000	0.010

shown on Fig. 29 for bars with 8 percent water content for the case of 160 scatterers per wavelength.

c. Metal Rods

Measured and calculated values are summarized in Tables XXVIII and XXIX. The average values of the real parts of the complex relative dielectric constant and permeability are shown in Fig. 30 as a function of the number of scatterers per wavelength.

4. Discussion of Results of Laboratory Multiple-Scatterer Tests

In general there was quite good agreement between the values of the effective complex relative dielectric constant and complex relative permeability of the region filled with scatterers calculated on the basis of representing the short scatterers as effective lossy shunt capacitances on the transmission line and the average values actually measured with the lines in the laboratory. This agreement further encourages us to consider estimating these quantities for an actual forest from forest measuration data (i.e., distribution of tree sizes and number of trees per unit area or nearest-neighbor distance data) together with the measured effect of a single tree (i.e., scatterer). Such forest measuration data are available for selected forests in Thailand.[illegible] It would remain only to determine by measurement the equivalent circuit of

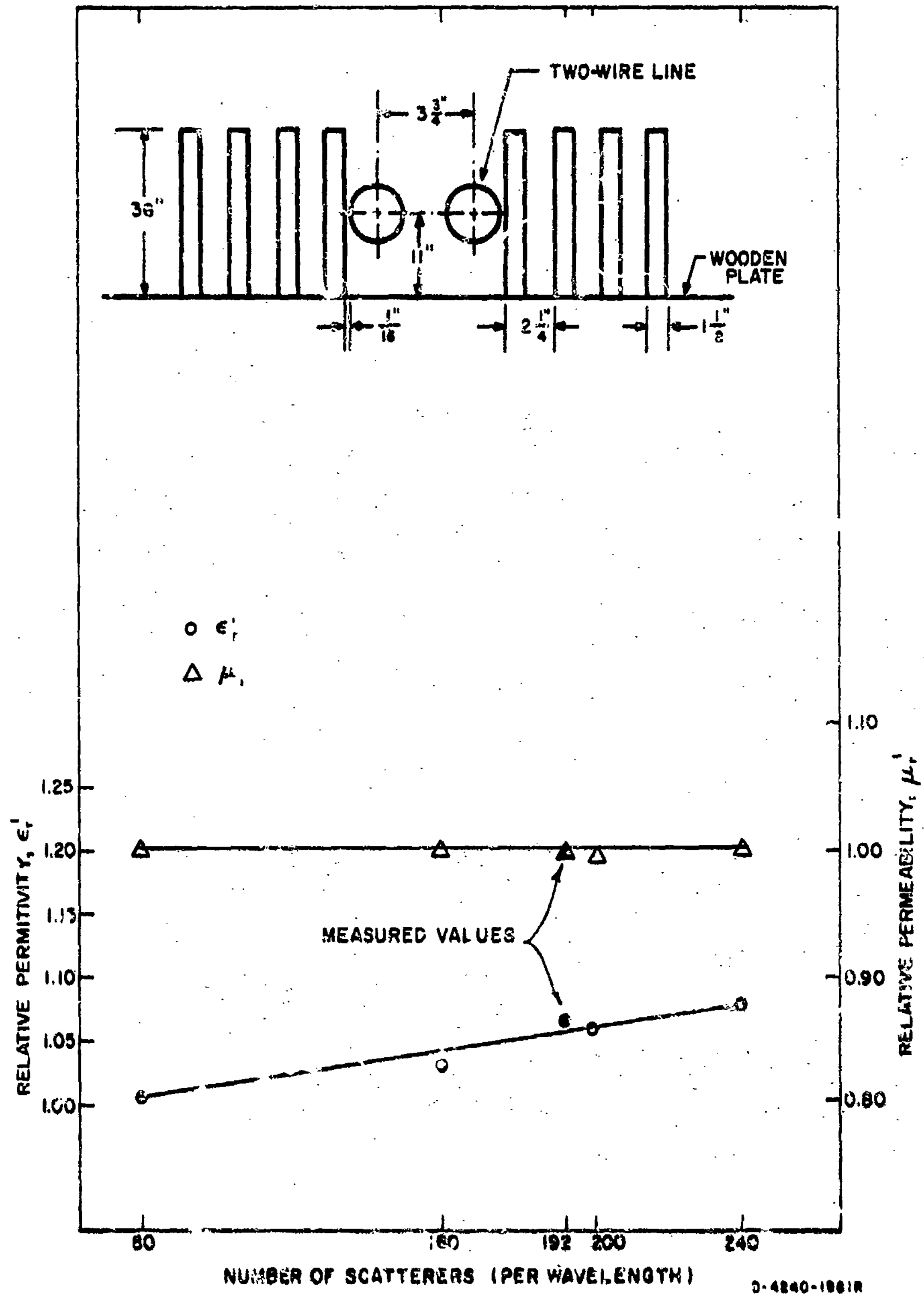

FIG. 28 EFFECTIVE ELECTRICAL CONSTANTS OF VOLUME CONTAINING DRY WOOD BARS--CALCULATED AND MEASURED WITH 300-ohm TWO-WIRE LINE

Table XXVI

ELECTRICAL CONSTANTS WITH WET (15 PERCENT WC) WOOD BARS
MEASURED WITH 300-OHM TWO-WIRE LINE

Random Distribution Number	Number of Scatterers n	Relative Dielectric Constant ϵ_r'	Relative Permeability, $\mu_r = \mu_r' - j\mu_r''$	Loss Tangent δ
1	25	1.105	1.000 - j0.011	0.025
2	24	1.090	0.998 - j0.011	0.032
3	25	1.118	0.998 - j0.015	0.028
4	25	1.120	1.012 - j0.015	0.028
5	21	1.099	1.009 - j0.014	0.025
Average	24	1.107	1.000 - j0.013	0.025

Table XXVII

ELECTRICAL CONSTANTS WITH WET (15 PERCENT WC) WOOD BARS
CALCULATED FOR 300-OHM TWO-WIRE LINE

Number of Scatterers n	Relative Dielectric Constant ϵ_r'	Relative Permeability $\mu_r = \mu_r' - j\mu_r''$	Loss Tangent δ
10	1.040	1.003 - j0.000	0.006
20	1.079	0.999 - j0.000	0.012
25	1.110	1.005 - j0.000	0.017
30	1.171	1.000 - j0.000	0.019

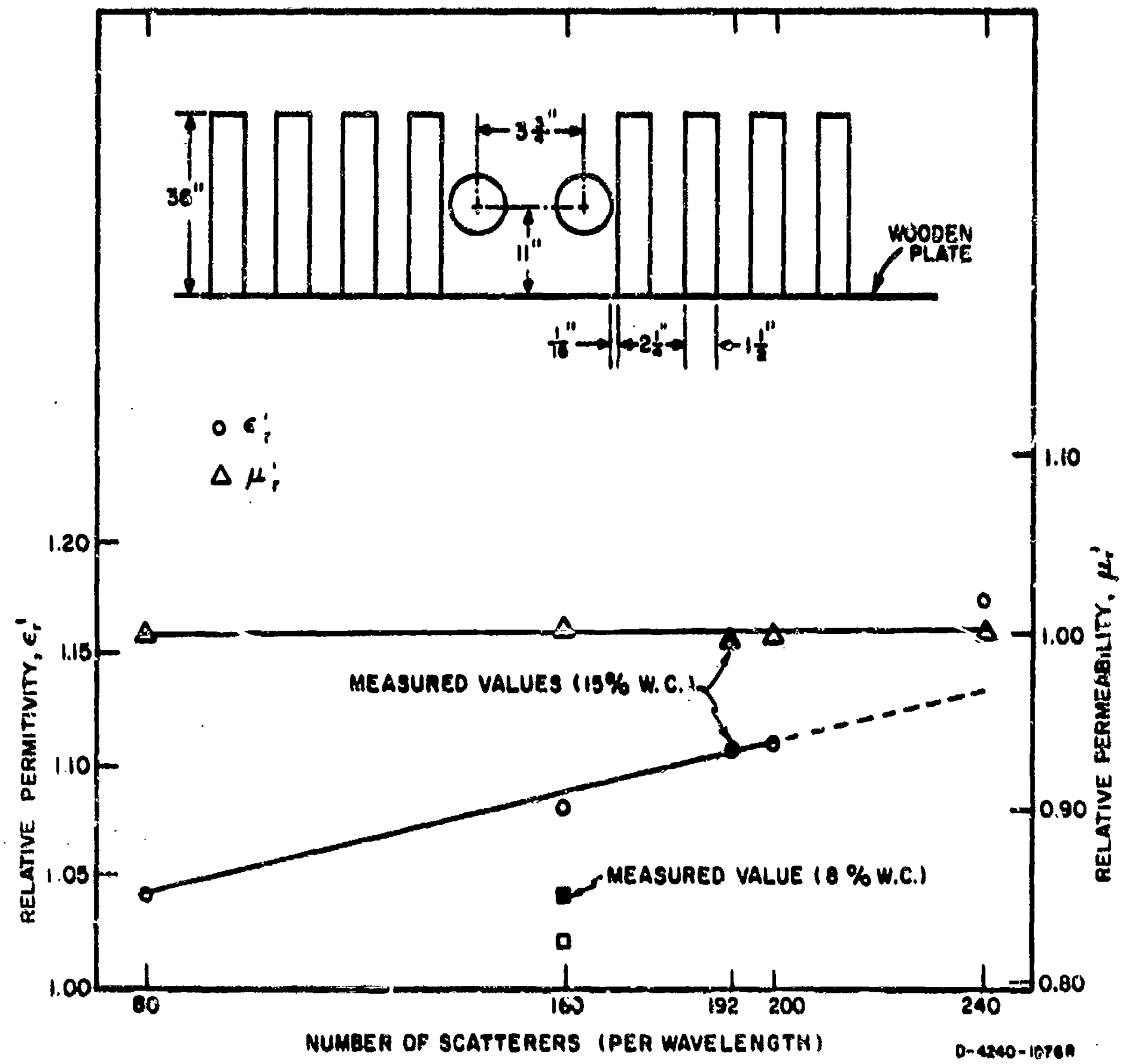

FIG. 30 EFFECTIVE ELECTRICAL CONSTANTS OF VOLUME CONTAINING WET WOOD BARS--CALCULATED AND MEASURED WITH 300-ohm TWO-WIRE LINE

Table XXVIII

ELECTRICAL CONSTANTS WITH METAL RODS MEASURED WITH 300-OHM TWO-WIRE LINE

Random Distribution Number	Number of Scatterers n	Relative Dielectric Constant ϵ_r'	Relative Permeability $\mu_r = \mu_r' - j\mu_r''$	Loss Tangent δ
1	25	1.064	0.999 - j0.013	0.015
2	24	1.063	0.992 - j0.012	0.015
3	25	1.081	0.997 - j0.013	0.015
4	25	1.061	1.004 - j0.013	0.015
5	21	1.098	0.992 - j0.012	0.016
Average	24	1.073	0.997 - j0.013	0.016

Table XXIX

ELECTRICAL CONSTANTS WITH METAL RODS CALCULATED FOR 300-OHM TWO-WIRE LINE

Number of Scatterers n	Relative Dielectric Constant ϵ_r'	Relative Permeability $\mu_r = \mu_r' - j\mu_r''$	Loss Tangent δ
10	1.027	1.002 - j0.000	0.002
20	1.057	0.998 - j0.000	0.005
25	1.064	1.001 - j0.000	0.006
30	1.082	1.004 - j0.000	0.006

the trees as a function of tree size, shape, and distance from the line of interest (such as was done for the oak trees in Sec. V-C-6) in order to generate the required set of equivalent lossy capacitors. These equivalent circuits could then be used, along with the technique presented above, to calculate the effective electrical properties of the forest considered as a lossy dielectric slab.[3] These values could then

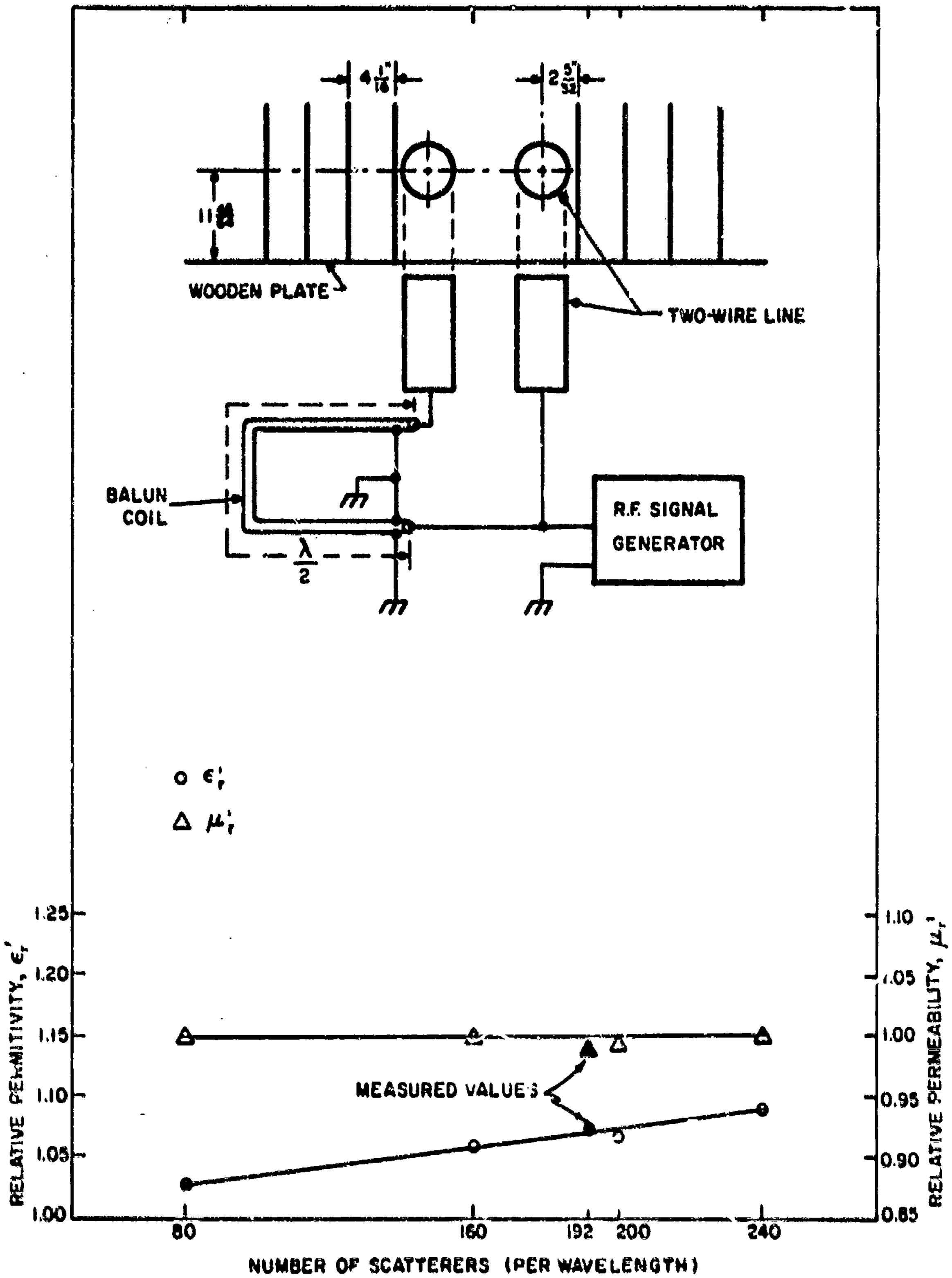

D-4240-1082R

FIG. 30 EFFECTIVE ELECTRICAL CONSTANTS OF VOLUME CONTAINING METAL RODS--CALCULATED AND MEASURED WITH 300-ohm TWO-WIRE LINE be compared with actual values of the slab constants as determined by open-wire transmission-line measurement.[5,8] This technique is illustrated in Sec. VI.

5. Results of Measurements with Transmission Lines in Living Vegetation in South Carolina

Data already have been taken under this contract with transmission lines in forests in the western part of the U.S.[8,9,10] and in Thailand.[11,12,13] The purpose of this section is to present and discuss some results obtained more recently in living vegetation in South Carolina.

The $\lambda/8$ two-conductor line was used in clumps of small pines (see Figs. 31 and 32) and camellia bushes (see Fig. 33) to measure at 17 MHz the relative dielectric constant, loss tangent, and complex relative permeability of the volume containing the living vegetation. The data (see Table XXX) were obtained with a 440-ohm line (5/8-in conductor diameter and 12-in spacing) on a cool (48°F), cloudy spring day. The relative humidity was 75 percent. Two line orientations were used: plane of line parallel to ground and plane of line perpendicular to ground.

The values of complex dielectric constant obtained with the line parallel to the ground compare with typical values obtained in the earlier forest measurements reported in Refs. 8 and 13. It may be noted that the values of the real part of the complex dielectric constant obtained with the line perpendicular to the ground are somewhat higher than the values obtained with the line parallel to the ground, indicating that the vegetation is anisotropic as observed with the line. This is in contrast to earlier results where the line orientation produced essentially similar results, and also in conflict with the study on anisotropy presented in Sec. IV of this report. Presumably this apparent observed anisotropy in ϵ_r' results from the small number of samples averaged to give the values shown in Table XXX. The observed values for the loss tangent appear more isotropic--as expected for a line with R_c as high as 440 ohms (see Fig. 13)--whereas the actual values of loss tangent in forests probably are anisotropic.[4,5,15]

TA-8843-6

FIG. 31 SIX-ft PINE TREES AND APPROXIMATE LINE POSITION

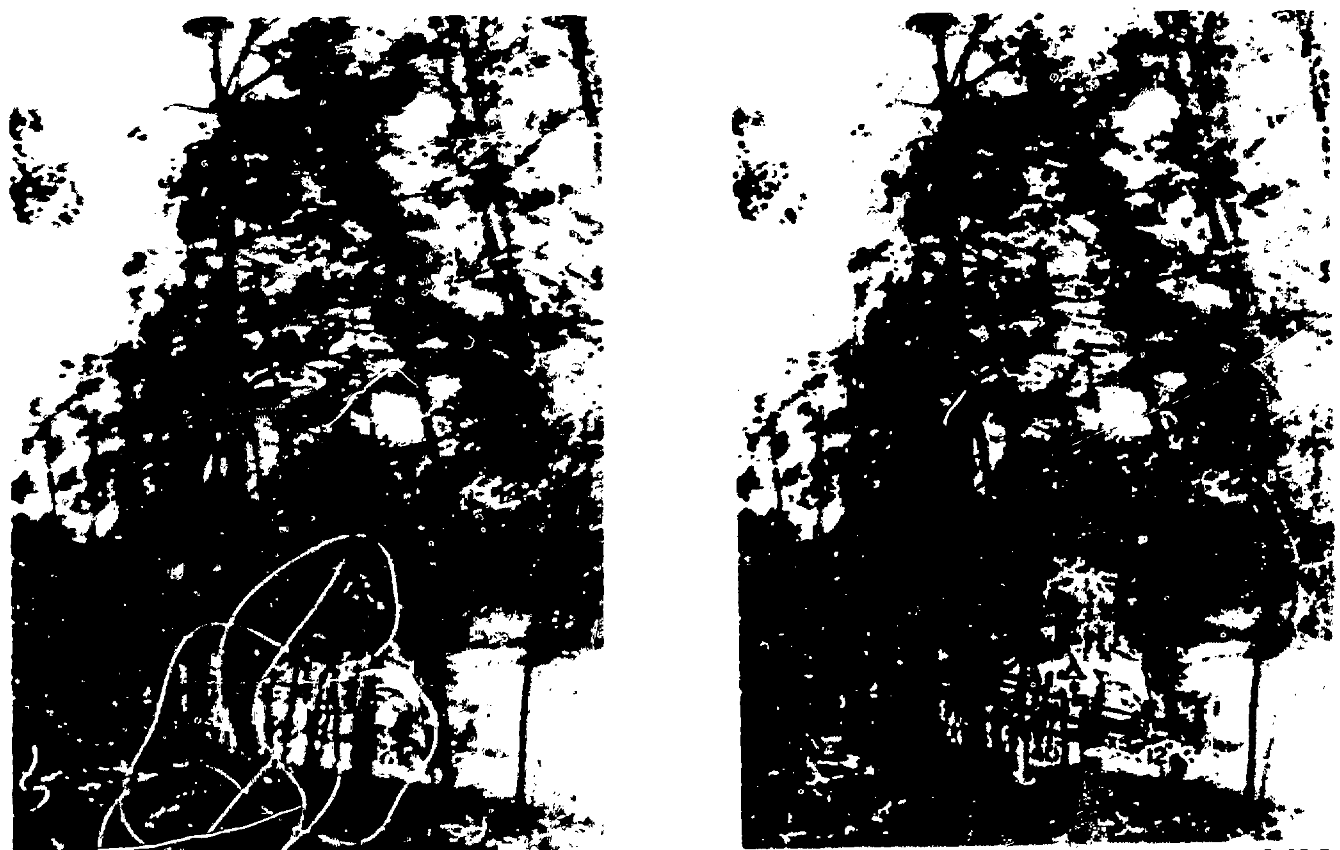

TA-8863-7

FIG. 32 TEN-ft PINE TREES AND APPROXIMATE LINE POSITION

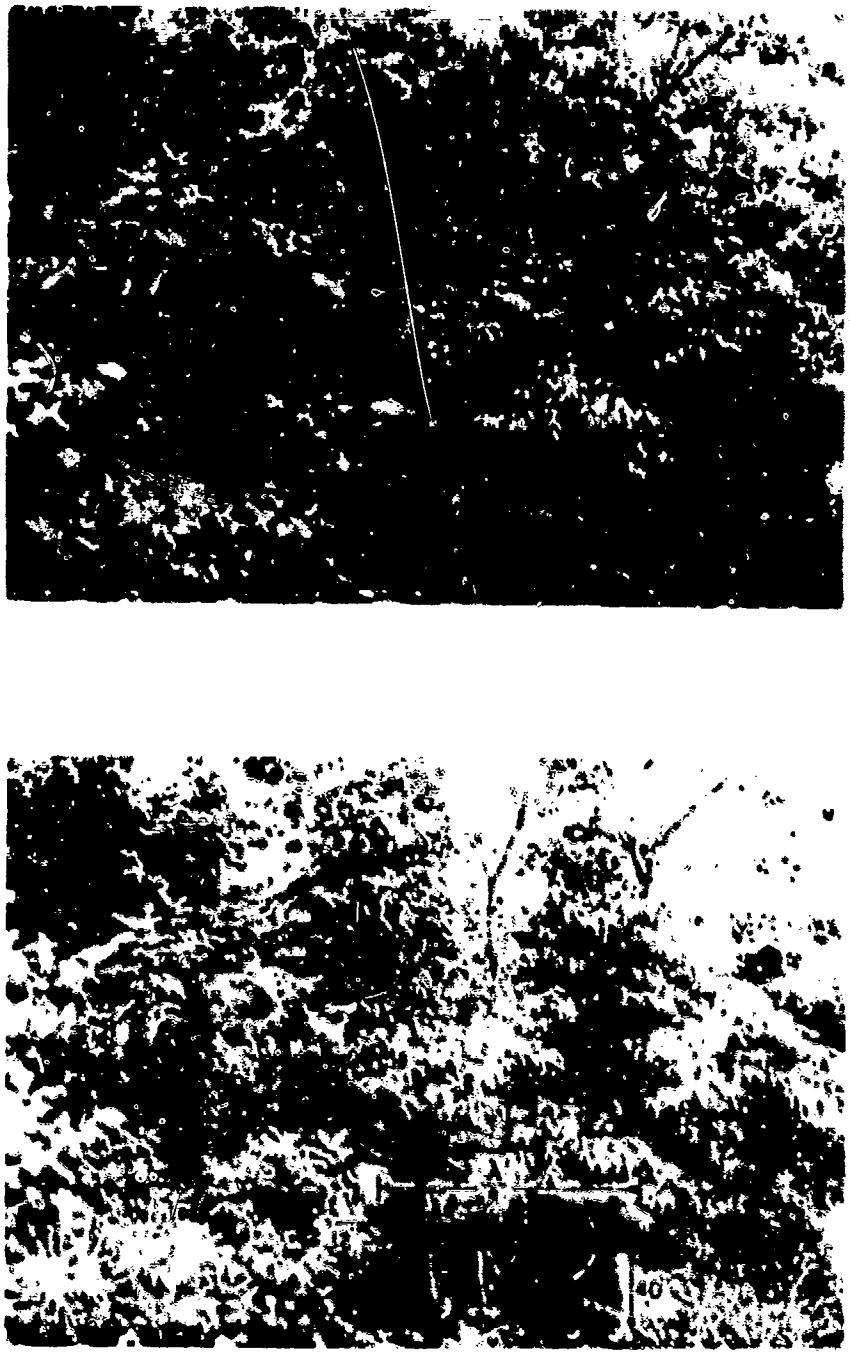

TA-8863-8

FIG. 33 TEN-ft CAMELLIA TREES AND APPROXIMATE LINE POSITION

Table XXX

FIELD MEASUREMENT OF ACTUAL FOREST EFFECTIVE ELECTRICAL PROPERTIES WITH 440-OHM TWO-WIRE LINE ($\lambda/8$) AT 17 MHz IN SOUTH CAROLINA

Type of Forest	Average Height of Tree (ft)	Average Number of Trees per Acre	Orientation of Two-Wire Line	Distance of Line from Ground (ft)	Relative Dielectric Constant ϵ_r'	Relative Permeability $\mu_r = \mu_r' - j\mu_r''$	Loss Tangent at 17 MHz
Camellia	10	400	plane of two-wire line parallel to ground	3	1.084	1.063 - j0.003	0.03
Pine	6	600		3	1.051	1.008 - j0.003	0.04
Pine	10	800		3	1.071	1.035 - j0.003	0.03
Camellia	10	400	plane of two-wire line perpendicular to ground	3*	1.12	1.002 - j0.002	0.04
Pine	6	600		3*	1.07	1.000 + j0.002	0.04
Pine	10	800		3*	1.14	0.990 - j0.002	0.03

*This dimension was measured from the lower conductor to ground.

The observed values of relative permeability also agree reasonably well with previous observations.[13] The one observed value of μ_r' in Table XXX less than one may be considered unity to within the accuracy of the measurement (see also Appendix E for a discussion of measurement errors caused by incomplete spatial sampling such as avoiding the placement of a tree trunk at the OWL input).

VI CONCLUSIONS AND RECOMMENDATIONS

A. Conclusions

(1) It was determined theoretically and verified experimentally that the maximum effective sensing volume for a 300-ohm line is a cylinder (of radius approximately 1-1/2 times the line spacing) placed symmetrically around the line and approximately the length of the line.* Of course, the region of greatest sensitivity is nearest the conductors in the vicinity of voltage maxima.

(2) Open wire lines (OWL's), except possibly very low-impedance lines (R_c < 100 ohms), are not very useful in resolving anisotropy of the medium into which the line is inserted.

(3) Single scatterers such as trees near an OWL may be modeled as lossy shunt capacitors. The capacitance is a function of the geometry (i.e., tree size, shape, and proximity to the line). The measurements of equivalent shunt conductance were not as accurate as the capacitance measurements, but the limited results obtained indicate that the loss tangent of the equivalent capacitor is relatively insensitive to scatterer position. These results on the effects of scatterers are important regarding the theory of RF transmission lines passing near trees as well as for the modeling of wave propagation in forests.

(4) A forest can be considered to consist of an ensemble of such scatterers distributed along the transmission

---

*The concept of a sensing radius or volume is imprecise, but nevertheless it is of some usefulness in visualizing how the line samples the electrical properties of a vegetated region line. When the equivalent circuit of a single scatterer (tree) as a function of the geometry is known and when the distribution of tree sizes and shapes is known for a given forest, then these data can be used to compute the effective macroscopic electric constants for a forest considered as a lossy dielectric slab.

(5) Therefore, OWL probes are useful for estimating the macroscopic electrical properties of a volume containing living vegetation--even when significant scatterers (e.g., tree trunks) are present--although the results of OWL measurements must be interpreted with care in this latter case and in other cases where anisotropy may be significant.

B. Recommendations

Conclusions (4) and (5) should be checked by experiment as follows:

(1) The statistical distribution of tree heights, diameters and spacings should be determined for a given forest.

(2) The equivalent circuits for representative example trees of this forest should be measured as a function of proximity to an OWL (or OWL's).

(3) The effective macroscopic electric constants for the slab should be calculated for many cases using the random program discussed in Sec. V and an estimate of the actual slab properties inferred from an average of these results.

(4) These constants should then be used in a forest-slab model to predict antenna height-gain and path-loss functions.

(5) Then, an OWL probe should be used to measure the effective slab constants in the actual forest and a comparison made with the average values computed using the random program.

(6) The height-gain and path-loss functions should be recalculated using electrical constants computed from the actual OWL measurements.

(7) The height-gain and path-loss functions then should be measured and compared with those calculated using both inferred and measured slab constants.

If the suggested comparisons prove successful, then a significant step will have been taken toward relating the type of forest descriptions currently being made by environmental scientists[18] to the needs of researchers in the field of radio propagation and communication.

Appendix A

DERIVATION OF RELATIVE POWER DENSITY

Preceding page blank

Appendix A

DERIVATION OF RELATIVE POWER DENSITY

For a TEM wave, the power density S is given by

$$S = K(\nabla\varphi)^2$$

where K is a constant, φ is a scalar potential function satisfying

$$\nabla^2\varphi = 0$$

and

$$\frac{\partial\varphi}{\partial S} = 0$$

on the surface S of the conductors.

In order to find the power density around the open two-wire line, we first consider the power density in the region between the conductors of a coaxial line.

Using polar coordinates r and θ, we have

$$\nabla^2\varphi = \frac{1}{r}\frac{\partial}{\partial r}\left(r\frac{\partial\varphi}{\partial r}\right) + \frac{1}{r^2}\frac{\partial^2\varphi}{\partial\theta^2} = 0 \quad .$$

Because of symmetry, φ is independent of θ. The above equation reduces to

$$\frac{1}{r}\frac{d}{dr}\left(r\frac{d\varphi}{dr}\right) = 0$$

$$r\frac{d\varphi}{dr} = C$$

$$\varphi = C\ln r + D$$

where C and D are constants.

Preceding page blank

Since the boundary of the conductors is defined by $r = a$ and $r = b$, the condition

$$\frac{\partial\varphi}{\partial s} = 0$$

on the surface S of the conductors was satisfied automatically when we chose φ to be a function of r only.

$$(\nabla\varphi)^2 = \nabla\varphi \cdot \nabla\varphi$$

$$= \hat{r}\,\frac{C}{r} \cdot \hat{r}\,\frac{C}{r}$$

$$= \frac{C^2}{r^2} \quad .$$

The power density S becomes

$$S = K(\nabla\varphi)^2$$

$$= \frac{KC^2}{r^2}$$

$$= \frac{A}{r^2}$$

where $r^2 = u^2 + v^2$, and u, v are rectangular coordinates.

The total power flowing down the line is

$$P_o = 2\pi \int_{r_o}^{1} P(u,v)\,r\,dr$$

$$= 2\pi A \ln\left(\frac{1}{r_o}\right) \quad .$$

We normalize S so that

$$P = \frac{S}{P_o}$$

where P is the normalized power density; then

$$P = \frac{1}{2\pi \ln\left(\frac{1}{r_o}\right)} \cdot \frac{1}{r^2}$$

$$= \frac{B}{r^2}$$

where

$$B = \frac{1}{2\pi \ln\left(\frac{1}{r_o}\right)} \quad .$$

But the characteristic impedance of the coaxial line is

$$R_{c\ coax} = \frac{\zeta}{2\pi} \ln\left(\frac{1}{r_o}\right)$$

and that of the open two-wire line is known to be

$$R_{cTw} = 2\ R_{c\ coax} \quad .$$

B is therefore given by

$$B = \frac{\zeta}{2\pi^2\ R_{cTw}} \quad .$$

Now under the transformation to the coaxial line given by

$$W = \frac{Z - 1}{Z + 1}$$

where $W = u + iv$, $Z = x + iy$, the power density $p(x,y)$ in z-plane is related to $p(u,v)$ in w-plane by (see Appendix B)

$$p(x,y) = \left(\nabla_{xy} v\right)^2\ p(u,v)$$

$$= \left[\left(\frac{\partial v}{\partial x}\right)^2 + \left(\frac{\partial v}{\partial y}\right)^2\right] \cdot \frac{B}{u^2 + v^2} \quad .$$

From the transformation we defined, we have

$$u = \frac{x^2 + y^2 - 1}{(x + 1)^2 + y^2}$$

$$v = \frac{2y}{(x + 1)^2 + y^2} \quad .$$

Substituting in the above expression for p(x,y), we have

$$p(x,y) = \frac{4B}{\left(x^2 + y^2 - 1\right)^2 + 4y^2} \quad .$$

For a contour of constant power density, let

$$p(x,y) = p_k$$

and

$$D^2 = \frac{4B}{p_k} \quad .$$

Then,

$$\left(x^2 + y^2 - 1\right)^2 + 4y^2 = D^2 \quad .$$

At x = 0, y = 0, we have

$$p_k = 4B$$

and

$$D = 1 \quad .$$

So, if we take D = 1 contour as 0-dB contour, then the power in dB based on D = 1 contour as reference is given by

$$p = 10 \log_{10} \frac{1}{D} \quad .$$

Appendix B

EQUIVALENCE OF POWER FLOW IN THE COMPLEX z AND w PLANES

Appendix B

EQUIVALENCE OF POWER FLOW IN THE COMPLEX z AND w PLANES

It is known that for the TEM wave, the power density S is proportional to $(\nabla\varphi)^2$, that is,

$$S = K(\nabla\varphi)^2$$

where K is a constant, φ is a scalar potential function satisfying

$$\nabla^2\varphi = 0$$

and

$$\frac{\partial\varphi}{\partial S} = 0$$

on the surface S of the conductors. Let the mapping $Z = F(w)$, where $z = x + iy$, and $w = u + iv$, be conformal; then Cauchy-Riemann equations apply; that is,

$$\frac{\partial x}{\partial u} = \frac{\partial y}{\partial v}$$

and

$$\frac{\partial x}{\partial v} = -\frac{\partial y}{\partial u} \quad .$$

The equations for metric coefficients are known to be

$$\begin{aligned} \partial_{uv} &= \partial_{vu} \\ &= \frac{\partial x}{\partial u}\frac{\partial x}{\partial v} + \frac{\partial y}{\partial u}\frac{\partial y}{\partial v} \\ &= \frac{\partial x}{\partial u}\frac{\partial x}{\partial v} - \frac{\partial x}{\partial u}\frac{\partial x}{\partial v} \\ &= 0 \end{aligned}$$

Preceding page blank

$$\partial_{uu} = \left(\frac{\partial x}{\partial u}\right)^2 + \left(\frac{\partial y}{\partial u}\right)^2$$

$$= \left(\frac{\partial x}{\partial v}\right)^2 + \left(\frac{\partial y}{\partial v}\right)^2$$

$$= \partial vv \quad .$$

The gradient of φ is therefore given by

$$\nabla\varphi = \hat{x}\,\frac{\partial\varphi}{\partial x} + \hat{y}\,\frac{\partial\varphi}{\partial y}$$

$$= \frac{\hat{u}}{\left(\partial_{uu}\right)^{1/2}}\,\frac{\partial\varphi}{\partial u} + \frac{\hat{v}}{\left(\partial_{uu}\right)^{1/2}}\,\frac{\partial\varphi}{\partial v}$$

$$= \frac{1}{\left(\partial_{uu}\right)^{1/2}}\left[\hat{u}\,\frac{\partial\varphi}{\partial u} + \hat{v}\,\frac{\partial\varphi}{\partial v}\right]$$

and

$$(\nabla\varphi)^2 = \nabla\varphi \cdot \nabla\varphi$$

$$= \left(\frac{\partial\varphi}{\partial x}\right)^2 + \left(\frac{\partial\varphi}{\partial y}\right)^2$$

$$= \frac{1}{\partial_{uu}}\left[\left(\frac{\partial\varphi}{\partial u}\right)^2 + \left(\frac{\partial\varphi}{\partial v}\right)^2\right] \quad .$$

So we have

$$\left(\nabla_{xy}\varphi\right)^2 = \frac{1}{\partial_{uu}}\left(\nabla_{uv}\varphi\right)^2$$

under the conformal mapping.

The relation between the area element dA_{xy} in the z-plane and dA_{uv} in the w-plane is found to be

$$\partial_{uu} = \left(\frac{\partial x}{\partial u}\right)^2 + \left(\frac{\partial y}{\partial u}\right)^2$$

$$= \left(\frac{\partial x}{\partial v}\right)^2 + \left(\frac{\partial y}{\partial v}\right)^2$$

$$= \partial vv \quad .$$

The gradient of φ is therefore given by

$$\nabla\varphi = \hat{x}\,\frac{\partial\varphi}{\partial x} + \hat{y}\,\frac{\partial\varphi}{\partial y}$$

$$= \frac{\hat{u}}{\left(\partial_{uu}\right)^{1/2}}\,\frac{\partial\varphi}{\partial u} + \frac{\hat{v}}{\left(\partial_{uu}\right)^{1/2}}\,\frac{\partial\varphi}{\partial v}$$

$$= \frac{1}{\left(\partial_{uu}\right)^{1/2}}\left[\hat{u}\,\frac{\partial\varphi}{\partial u} + \hat{v}\,\frac{\partial\varphi}{\partial v}\right]$$

and

$$(\nabla\varphi)^2 = \nabla\varphi \cdot \nabla\varphi$$

$$= \left(\frac{\partial\varphi}{\partial x}\right)^2 + \left(\frac{\partial\varphi}{\partial y}\right)^2$$

$$= \frac{1}{\partial_{uu}}\left[\left(\frac{\partial\varphi}{\partial u}\right)^2 + \left(\frac{\partial\varphi}{\partial v}\right)^2\right] \quad .$$

So we have

$$\left(\nabla_{xy}\varphi\right)^2 = \frac{1}{\partial_{uu}}\left(\nabla_{uv}\varphi\right)^2$$

under the conformal mapping.

The relation between the area element dA_{xy} in the z-plane and dA_{uv} in the w-plane is found to be

$$dA_{xy} = dxdy$$

$$= \left(\partial_{uu}\partial_{uu}\right)^{1/2} dudv$$

$$= \partial_{uu} dudv$$

$$= \partial_{uu} \, dA_{uv}$$

and the power in each plane is

$$P_{xy} = S_{xy} dA_{xy} = \left[K\left(\nabla_{xy}\varphi\right)^2\right] dA_{xy}$$

$$P_{uv} = S_{uv} dA_{uv} = \left[K\left(\nabla_{uv}\varphi\right)^2\right] dA_{uv}$$

where P_{xy}, S_{xy}, and P_{uv}, S_{uv} are the power and the power density in the z-plane and the w-plane through the respective area elements.

Since

$$\left[K\left(\nabla_{xy}\varphi\right)^2\right] dA_{xy} = \left[K \frac{1}{\partial_{uu}} \left(\nabla_{uv}\varphi\right)^2\right] \partial_{uu} dA_{uv}$$

$$= \left[K\left(\nabla_{uv}\varphi\right)^2\right] dA_{uv}$$

we conclude that

$$P_{xy} = P_{uv}$$

which says that under the conformal mapping the power in any area of the z-plane is the same as the power in the equivalent area of the w-plane.

Appendix C

DERIVATION OF EQUATION USED FOR COMPUTING PROPAGATION CONSTANT AND PHASE VELOCITY

Preceding page blank

Appendix C

DERIVATION OF EQUATION USED FOR COMPUTING PROPAGATION CONSTANT AND PHASE VELOCITY

In this appendix we derive an expression for the propagation constant of a T-M wave on a two-wire transmission line partly filled with dielectric (see Figure C-1).

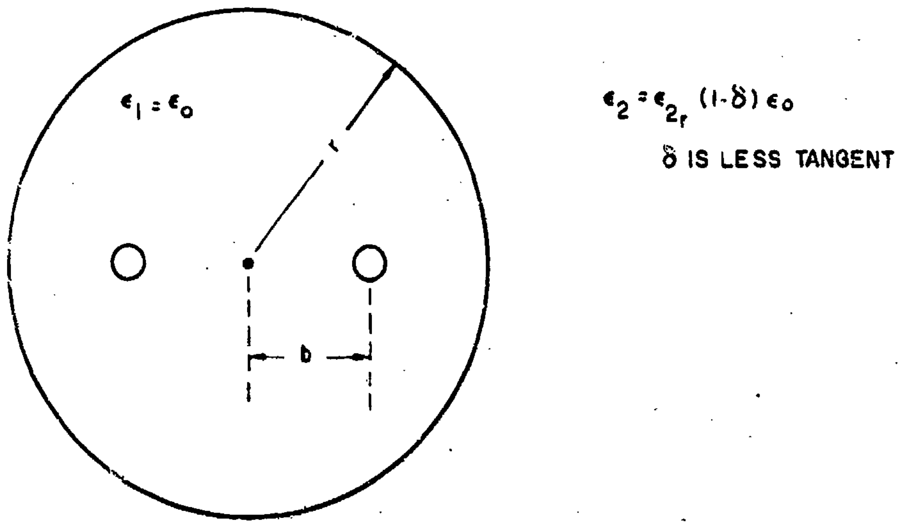

FIG. C-1 TRANSMISSION LINE GEOMETRY

We wish to find an approximation to the propagation constant for the quasi TEM wave on a two-wire transmission line that has, along its length, two dielectric materials (we are assuming one to be empty space, but this is not necessary). The boundary between the two dielectric materials is everywhere parallel to the conductor surfaces--i.e., parallel to the z-axis. In finding the propagation constant we will consider the case where the line is terminated in its characteristic impedance so that we have only a wave propagating in the positive z direction.

We will assume (or define) the power flow through any surface, closed or open, to be given by

Preceding page blank

$$P = \mathrm{Re}\int_{\Sigma} \hat{n} \cdot \overline{S} d\sigma \quad ,$$

where $\hat{n}$ is the unit normal to the surface and

$$\overline{S} = \frac{1}{2} \overline{E} \times \overline{H}^{*} \quad .$$

In particular, the power flow d… n open wire line is

$$P_o = \mathrm{Re}\int_0^{2\pi}\int_0^{\infty} \hat{z} \cdot \overline{S} \; r \, dr \, d\theta \quad .$$

Now consider, briefly, the TEM wave on the air-filled line with the same conductor configuration. For the lossless case, $\overline{E}$ and $\overline{H}$ are in phase and $\overline{S}$ is real.

$$\hat{z} \cdot \overline{S} = \frac{|\overline{E}|^2}{2\zeta_o} = \frac{\zeta_o |\overline{H}|^2}{2} \quad .$$

Hence

$$P_o = \frac{\zeta_o}{2}\int_0^{2\pi}\int_0^{\infty} |\overline{H}|^2 \, r \, dr \, d\theta \quad .$$

Note also that

$$\tilde{H} \cdot \overline{H} = \overline{H} \cdot \overline{H}^{*} e^{-2j\nu_v z}$$

where the reference phase is taken at the point $z = 0$.

If we partly fill the line with a dielectric whose dielectric constant is of the order of magnitude of unity the H field will not change very much. We will, therefore, compute the propagation constant for the partly filled line from the TEM H field in the air filled line.

In either region of the partly filled line the transverse component of $\bar{E}$ is perpendicular to $\bar{H}$, and $\bar{H}$ is related to $\bar{E}$ by

$$\bar{H} = \frac{j\omega\epsilon}{\gamma}\,\hat{z} \times \bar{E} \quad ,$$

where

$$\gamma = \alpha + j\beta$$

is the propagation constant we wish to find.

Thus

$$\hat{z} \cdot \bar{E} \times \bar{H} = \frac{\gamma}{j\omega\epsilon}\,\bar{H} \cdot \bar{H} = \frac{\gamma}{j\omega\epsilon}\,|\bar{H}|^2 e^{-2j\beta z} \quad .$$

Now let

$$v = \int_0^{2\pi}\int_0^{\infty} \hat{z} \cdot \bar{E} \times \bar{H}\ r\,dr\,d\theta$$

which, upon substitution of the foregoing result, becomes

$$v = \frac{\gamma e^{-2j\beta z}}{j\omega}\int_0^{2\pi}\int_0^{\infty} \frac{1}{\epsilon}\,|H|^2 r\,dr\,d\theta \quad .$$

Note also that $v \doteq P_t e^{-2j\beta z}$, where P_t is the power flowing on the partly filled line. Since both $\bar{E}$ and $\bar{H}$ vary as $e^{-\gamma z}$

$$v \propto e^{-2\gamma z}$$

and

$$\frac{dv}{dz} = -2\gamma v \quad ,$$

Therefore,

$$\gamma = -\frac{1}{2}\frac{\frac{dv}{dz}}{v} .$$

To find dv/dz start with the identity

$$\int_v \nabla \cdot \bar{E} \times \bar{H} dv = \oint_\Sigma \hat{n} \cdot \bar{E} \times \bar{H} d\sigma ,$$

where v is the volume outside of the conductors in a section of transmission line of length, h, and may extend radially to infinity. The integral over the cylindrical surface bounding the transmission line approaches zero as $r \to \infty$, hence

$$\left[\int_o^{2\pi}\int_o^{\infty} \hat{z} \cdot \bar{E} \times \bar{H} r dr d\theta\right]_{z+h} - \left[\int_o^{2\pi}\int_o^{\infty} \hat{z} \cdot \bar{E} \times \bar{H} r dr d\theta\right]_z$$

$$= \int_v \nabla \cdot \bar{E} \times \bar{H}_{dv} - \int_{\text{conductor surface}} \hat{n} \cdot \bar{E} \times \bar{H} d\sigma .$$

When we divide by h and take the limit as $h \to o$ we obtain

$$\frac{dv}{dz} = \int_o^{2\pi}\int_o^{\infty} \nabla \cdot \bar{E} \times \bar{H} r dr d\theta - \int_c \hat{n} \cdot \bar{E} \times \bar{H} dS .$$

The integral on the contour around the surface of the conductors

$$\int_c \hat{n} \cdot \bar{E} \times \bar{H} ds = \int_c \bar{E} \cdot \bar{H} \times \hat{n} ds ,$$

and on the conductor surface

$$\bar{H} \times \hat{n} = \bar{J}_s = \hat{z} J_s ,$$

where $\bar{J}_s$ is the surface current density. Now

$$E_z = Z_s J_s \quad ,$$

where

$$Z_s = R_s + jX_s = (1 + j)\sqrt{\frac{\omega\mu}{2\sigma}}$$

is the surface impedance and σ is the conductivity.

Hence

$$\int_c \hat{n} \cdot \bar{E} \times \bar{H}\, ds = (1 + j)R_s e^{-2j\beta z} \int_c |J_s|^2 ds$$

and

$$\frac{dv}{dz} = \int_0^{2\pi}\int_0^{\infty} \nabla \cdot \bar{E} \times \bar{H} r\,dr\,d\theta - (1 + j)e^{-2j\beta z} R_s \int_c |J_s|^2 ds \quad .$$

If we use the vector identity

$$\nabla \cdot \bar{E} \times \bar{H} = \bar{H} \cdot \nabla \times \bar{E} - \bar{E} \cdot \nabla \times \bar{H}$$

and substitute from Maxwell's equations

$$\nabla \times \bar{H} = j\omega\epsilon\bar{E}$$

$$\nabla \times \bar{E} = j\omega\mu\bar{H}$$

we obtain

$$\nabla \cdot \bar{E} \times \bar{H} = -j\omega\{\mu\bar{H} \cdot \bar{H} + \epsilon\bar{E} \cdot \bar{E}\} \quad .$$

When we assume

$$|\bar{E}_z| \ll |\bar{E}|$$

and use the relationship

$$\bar{H} = \frac{j\omega\epsilon}{\gamma} \nabla \times \bar{E}$$

we obtain

$$\nabla \cdot \bar{E} \times \bar{H} \doteq -j\omega e^{-2j\beta z}\left\{\mu - \frac{\gamma^2}{\omega^2 \epsilon}\right\}|H|^2 \quad .$$

If we now let Σ_1 be the cross section surface over the air-filled region, and Σ_2 be that over the dielectric-filled region, we find

$$\frac{dv}{dz} = -j\omega \left[\left(\mu - \frac{\gamma}{\omega\epsilon_o}\right)\int_{\Sigma_1} |H|^2 d\sigma + \left(\mu - \frac{\gamma}{\omega^2 \epsilon_2}\right)\int_{\Sigma_2} |H|^2 d\sigma\right] e^{-2j\beta z}$$

$$- (1 + j) R_s \int_c |J_s|^2 ds e^{-2j\beta z}$$

and

$$\gamma = \frac{1}{2} \frac{j\omega\left[\mu \int_{\Sigma_1+\Sigma_2} |H|^2 d\sigma - \frac{\gamma}{\omega^2 \epsilon_o} \int_{\Sigma_1} |H|^2 d\sigma - \frac{\gamma}{\omega^2 \epsilon_2} \int_{\Sigma_2} |H|^2 d\sigma\right]}{\frac{\gamma}{j\omega\epsilon_o}\int_{\Sigma_1} |H|^2 d\sigma + \frac{\gamma}{j\omega\epsilon_2}\int_{\Sigma_2} |H|^2 d\sigma}$$

$$+ (1 + j) \frac{\frac{Rs}{2}\int_c |J_s|^2 ds}{P_t} \quad .$$

If we define the attenuation constant due to the power dissipated in the conductors in the usual way, then the last term on the right is $(1 + j)\alpha_c$, i.e.,

$$\alpha_c = \frac{\frac{Rs}{2}\int_c |J_s|^2 ds}{P_t}$$

where P_t is the power carried in the wave traveling in the positive z direction on the partly filled line.

Since we are assuming the H field on the partly dielectric filled line to be the same as that on a line with air as a dielectric, we can think of the integrals in the expression as the fractions of the power flowing in the corresponding regions of the air-filled line; thus,

$$P_1 = \frac{\delta}{2} \int_{\Sigma_1} |H|^2 d\sigma$$

$$P_2 = \frac{\delta}{2} \int_{\Sigma_2} |H|^2 d\sigma$$

and

$$P_o = P_1 + P_2 \quad .$$

If we now divide both the numerator and the denominator of the first term on the right by P_o and write

$$\frac{P_1}{P_o} = P$$

and

$$\frac{P_2}{P_o} = 1 - P$$

we obtain

$$\gamma^2 - 2(1 + j)\alpha_c \gamma = \frac{-k_o^2}{P + \frac{1}{\epsilon_{2r}}(1 - P)} \quad .$$

In this expression ϵ_{2r} may be complex:

$$\epsilon_{2r} = \epsilon'_{2r}(1 - j\delta) \quad ,$$

where δ is the loss tangent of the dielectric material in region 2.

If the power loss due to the conductors is negligibly small, so that

$$\alpha_c \doteq 0 \quad ,$$

then the above equation reduces to

$$\gamma^2 = \frac{-k_o^2}{P + \frac{1}{\epsilon_{2r}}(1 - P)} \quad .$$

We can solve this equation for ϵ_{2r} to yield

$$\epsilon_{2r} = \frac{-\gamma^2(1 - P)}{k_o^2 + \gamma^2 P} \quad .$$

As a check on the validity of the above expression for γ we can compare the result obtained from it with the propagation constant for the transverse magnetic mode in a special case that is relatively easy to solve. The coaxial transmission line with a coaxial dielectric sheath around the center conductor and an air space between that and the outer conductor is such a case. When we make the small argument approximations in the Bessel functions obtained in this solution, the two results are identical. We note also that this simple case can be approximated by assuming that the capacitance per unit length is equivalent to that obtained by connecting those of the two regions in series and that the conductance per unit length is that for the air-filled line. This approximation also yields the identical result for γ.

Appendix D

DERIVATION OF RELATIVE POWER DENSITY IN BOTH x AND y POLARIZATIONS

Preceding page blank

Appendix D

DERIVATION OF RELATIVE POWER DENSITY IN BOTH x AND y POLARIZATIONS

For a TEM wave the electric field intensity $\vec{E}$ is given by

$$\vec{E} = -\varphi_z \nabla_{uv} F$$

where φ_z is a function only of z, and F is a function of u, v satisfying

$$\nabla^2_{uv} F = 0$$

and

$$\frac{\partial F}{\partial S} = 0$$

on the surface S of the conductors.

Let u, v be the bipolar coordinates.[14] Then we find

$$F = Au$$

$$\vec{E} = A\varphi_z \left(\frac{\cosh u - \cos v}{C}\right)\hat{u}$$

$$\hat{u} = \frac{1 - \cosh u \cos v}{\cosh u - \cos v}\hat{x} - \frac{\sinh u \sin v}{\cosh u - \cos v}\hat{y}$$

so,

$$\vec{E} = \frac{A\varphi_z}{C}(1 - \cosh u \cos v)\,\hat{x} - \frac{A\varphi_z}{C}(\sinh u \sin v)\,\hat{y} \quad .$$

The ratio of the y component of $\vec{E}$ to the x component, $|E_y|/|E_x|$, is

$$\frac{|E_y|}{|E_x|} = \frac{\sinh u \sin v}{\cosh u \cos v - 1} \quad .$$

Preceding page blank

Now,

$$x = \frac{c \sinh u}{\cosh u - \cos v}$$

$$y = \frac{c \sin v}{\cosh u - \cos v} \quad .$$

Using the additional identities

$$\sin^2 v + \cos^2 v = 1$$

$$\cosh^2 u - \sinh^2 u = 1$$

we can solve for sin v, cos v, sinh u, and cosh u in terms of x, y. This results in,

$$\sin v = \frac{2cy}{\sqrt{\left(x^2 + y^2 - c^2\right)^2 + (2cy)^2}}$$

$$\cos v = \frac{(x^2 + y^2 - c^2)}{\sqrt{\left(x^2 + y^2 - c^2\right)^2 + (2cy)^2}}$$

$$\sinh u = \frac{2cx}{\sqrt{\left(x^2 + y^2 - c^2\right)^2 + (2cy)^2}}$$

$$\cosh u = \frac{(x^2 + y^2 + c^2)}{\sqrt{\left(x^2 + y^2 - c^2\right)^2 + (2cy)^2}} \quad .$$

Substituting the above expressions in the expression for $|E_y|/|E_x|$, we find

$$\frac{|E_y|}{|E_x|} = \left|\frac{2xy}{x^2 - y^2 - c^2}\right| \quad .$$

Normalizing the coordinates with c, we have

$$\frac{|E_y|}{|E_x|} = \left|\frac{2xy}{x^2 - y^2 - 1}\right|$$

$$\frac{|E_y|^2}{|E_x|^2} = \frac{4x^2y^2}{\left(x^2 - y^2 - 1\right)^2} \quad .$$

Since the power density P_x and P_y in x- and y-polarization, respectively, are given by

$$P_x = \frac{|E_x|^2}{2\zeta}$$

$$P_y = \frac{|E_y|^2}{2\zeta}$$

we have,

$$\frac{P_y}{P_x} = \frac{|E_y|^2}{|E_x|^2} = \frac{4x^2y^2}{\left(x^2 + y^2 - 1\right)^2} \quad , \qquad \text{(D-1)}$$

The relation between the total power density P and P_x, P_y for the TEM wave is found to be

$$P = P_x + P_y \quad .$$

It i known that

$$P = \frac{4B}{\left(x^2 + y^2 - 1\right)^2 + 4x^2y^2}$$

where

$$B = \zeta/2\pi \bar{r}^2 a_{ctw}$$

Normalizing the coordinates with c, we have

$$\frac{|E_y|}{|E_x|} = \left| \frac{2xy}{x^2 - y^2 - 1} \right|$$

$$\frac{|E_y|^2}{|E_x|^2} = \frac{4x^2y^2}{\left(x^2 - y^2 - 1\right)^2} \quad .$$

Since the power density P_x and P_y in x- and y-polarization, respectively, are given by

$$P_x = \frac{|E_x|^2}{2\zeta}$$

$$P_y = \frac{|E_y|^2}{2\zeta}$$

we have,

$$\frac{P_y}{P_x} = \frac{|E_y|^2}{|E_x|^2} = \frac{4x^2y^2}{\left(x^2 + y^2 - 1\right)^2} \quad . \qquad \text{(D-1)}$$

The relation between the total power density P and P_x, P_y for the TEM wave is found to be

$$P = P_x + P_y \quad .$$

It is known that

$$P = \frac{4B}{\left(x^2 + y^2 - 1\right)^2 + 4x^2y^2}$$

where

$$B = \zeta/2\pi^2 R_{ctw}$$

so,

$$P_x + P_y = \frac{4B}{\left(x^2 + y^2 - 1\right)^2 + 4x^2y^2} \quad . \qquad \text{(D-2)}$$

Solving (D-1) and (D-2) simultaneously, we get

$$P_y = \frac{16Bx^2y^2}{\left[\left(x^2 + y^2 - 1\right)^2 + y^2\right]^2}$$

$$P_x = \frac{4B\left(x^2 + y^2 - 1\right)^2}{\left[\left(x^2 + y^2 - 1\right)^2 + 4x^2y^2\right]^2} \quad .$$

1. The Plot of P_x

For a contour of constant P_x, let

$$P_x = P_{xk} = \text{constant}$$

and

$$D_x^2 = \frac{4B}{P_{xk}}$$

then

$$\frac{\left[\left(x^2 + y^2 - 1\right)^2 + 4x^2y^2\right]^2}{\left(x^2 + y^2 - 1\right)^2} = D_x^2 \quad .$$

The power in dB is given by

$$P_x = 10 \log_{10} \frac{1}{D_x} \quad .$$

2. The Plot of P_y

For a contour of constant P_y, let

$$P_y = P_{yk} = \text{constant}$$

and

$$D_y^2 = \frac{4B}{P_{yk}}$$

then

$$\frac{\left[(x^2 + y^2 - 1)^2 + 4x^2y^2\right]^2}{4x^2y^2} = D_y^2 \quad .$$

The power in dB is given by

$$P_y = 10 \log_{10} \frac{1}{D_y} \quad .$$

Appendix E

ANALYSIS OF ADDED CAPACITANCE ON A TRANSMISSION LINE TO APPROACH A GIVEN EFFECTIVE DIELECTRIC CONSTANT

Preceding page blank

Appendix E

ANALYSIS OF ADDED CAPACITANCE ON A TRANSMISSION LINE TO APPROACH A GIVEN EFFECTIVE DIELECTRIC CONSTANT

The following computations were made as a check on the validity of representing a transmission line with discrete capacitive scatterers (shunt capacitors) as a line with a higher dielectric constant and no shunt capacitors.

For the TEM wave on a two-conductor transmission line:

the voltage, $$V = \int_{\text{conductor 1}}^{\text{conductor 2}} \bar{E}\cdot\overline{dr} \quad ,$$

the total current, $$I = \oint_{\text{conductor 1 or 2}} \bar{H}\cdot\overline{ds} \quad ,$$

and the charge per unit length $$q = \oint_{\text{conductor 1 or 2}} \hat{n}\cdot\bar{D}ds \quad .$$

Since

$$\hat{n} \times \bar{E} = 0$$

and $$\hat{n}\cdot\bar{H} = 0$$

at the conductor surface, and since

$$|E| = \zeta|H|$$

where

ζ = the modulus of the impedance of the medium

and

$$\bar{D} = \epsilon\bar{E}$$

$$I = \frac{1}{\zeta}\oint_{\text{conductor 1}} |E|ds$$

Preceding page blank

$$q = \epsilon \int_{\text{conductor 1}} |E|\, ds$$

Therefore, the characteristic impedance

$$R_c = \frac{V}{I} = \sqrt{\frac{\mu_r}{\epsilon_r}}\, \zeta \frac{V}{\int_{\text{conductor 1}} |E|\, ds}$$

and the capacitance per unit length is

$$C = \frac{q}{V} = \frac{\epsilon_r \epsilon_o}{V} \int_{\text{conductor 1}} |E|\, ds \quad .$$

The added capacitance per unit length due to increasing the dielectric constant from 1 to ϵ_r is

$$C' = \frac{(\epsilon_r - 1)\epsilon_o}{V} \int_{\text{conductor 1}} |E|\, ds \quad .$$

Now suppose we place n capacitors per wavelength (λ) on an air dielectric line, each capacitor having a capacitance

$$C_s = \frac{\lambda C'}{n} \quad .$$

Then, as n increases, the equivalent dielectric constant should approach ϵ_r and the relative permeability should approach unity.

On the air line, each shunt capacitor has a normalized admittance,

$$Y_s = j2\pi f C_s R_{c(air)}$$

where

$$f = \text{frequency, in Hz}$$

$$Y_s = j\frac{2\pi f \lambda}{n} C' R_{c(air)}$$

$$Y_s = j\frac{2\pi V_o}{n}(\epsilon_r - 1)\,\epsilon_o \zeta_o$$

where

$$V_o = \text{phase velocity in air}$$

$$Y_s = j\frac{2\pi}{n}(\epsilon_r - 1) \quad .$$

In our computation we let C_s have a small loss factor, δ, such that

$$\epsilon_r = \epsilon'_r\,(1 - j\delta) \quad .$$

For computations with equally spaced uniform-size capacitors two circuits were used (see Figure E-1).

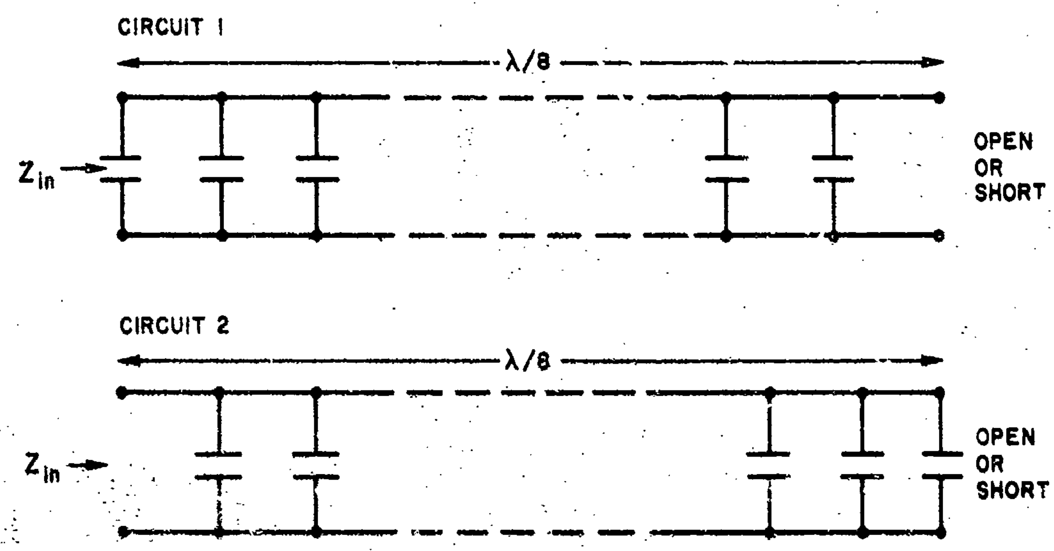

FIG. E-1 EQUIVALENT CIRCUITS FOR CAPACITIVELY LOADED TRANSMISSION LINE

Example computations of ϵ'_r and μ'_r were made using equally spaced uniform-size capacitors in Circuits 1 and 2 for the case:

$$\epsilon_r = 1.2(1 - j0.05)$$

$$n = a \cdot 24 \qquad\qquad a = 1 \text{ to } 20 \quad .$$

The results are plotted in Figure E-2. Notice that when the number of capacitors (scatterers) per wavelength is large that both circuits yield

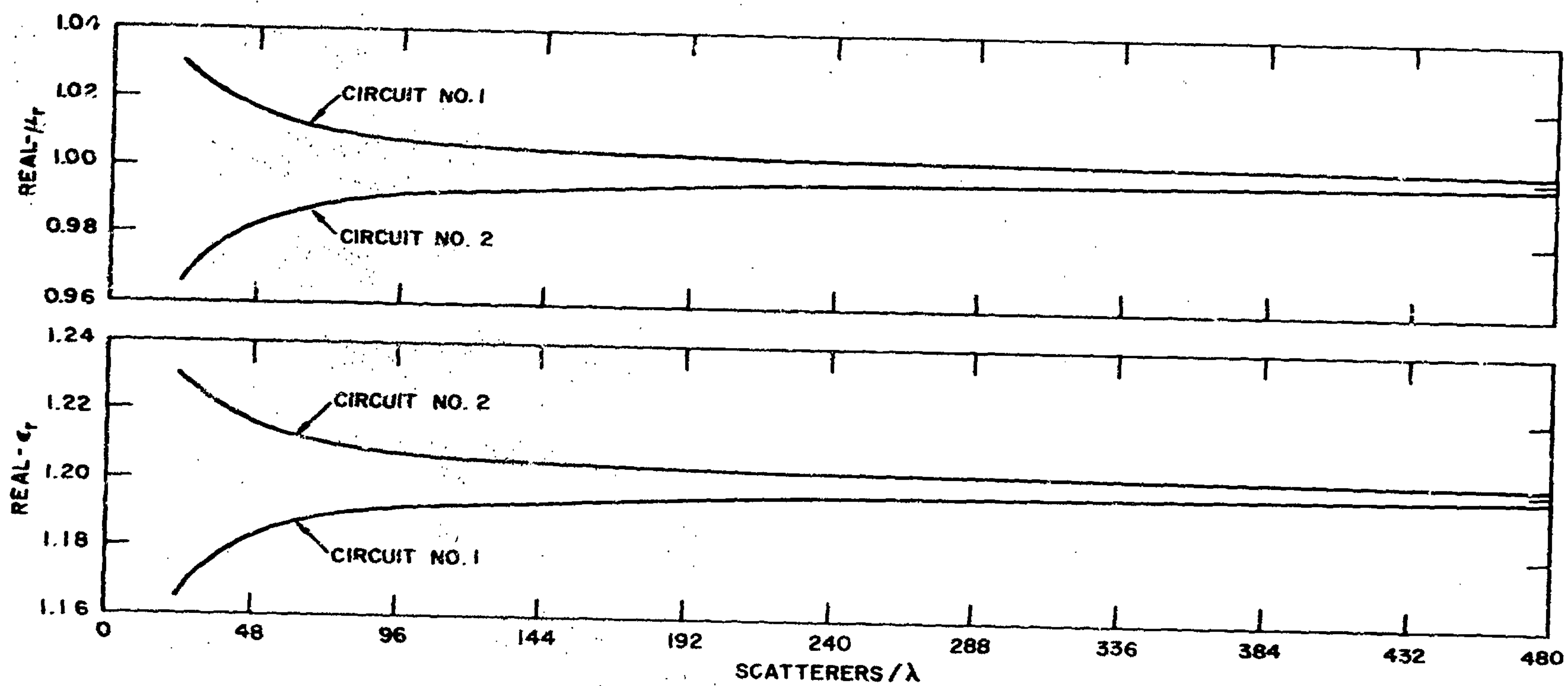

FIG. E-2 RELATIVE PERMEABILITY AND PERMITTIVITY vs. THE NUMBER OF CAPACITORS (SCATTERERS) PER WAVELENGTH the same (and correct) answer. On the other hand, when the number of scatterers is small, both circuits exhibit a bias. Circuit 2, more nearly the case in actual field measurements described in Ref. 13, where the vegetation was cleared from around the bridge input to the line,* yields results slightly high for ϵ_r' and slightly low for μ_r'. Notice that, for a given number of scatterers, the value of either ϵ_r' or μ_r' obtained by averaging the results from Circuits 1 and 2 is the correct value to use in the slab model. This implies that, because of incomplete spatial sampling (i.e., never having a tree trunk right at the bridge input), the average of the observed values of μ_r' given in Ref. 13 should be somewhat less than unity--and indeed such was the case. Nevertheless, contrary to the discussion in Ref. 13, the true value of μ_r' in the forest being measured probably was unity, and the assumption $\mu_{r1}' = 1$ should be used in forest-slab-model computations. In addition, the true value of ϵ_{r1}' probably always was greater than (or equal to) unity. Finally, future measurements should include complete spatial sampling relative to the geometry of the scatterers.

Computations also were made for the case of random scatterer size and location. For the random-size scatterers, the average value of Y was set equal to Y_s above. Except for increased spread of the computed data points, essentially the same conclusion was reached: Namely, that a transmission line with discrete scatterers placed along it can be represented as a line immersed in a scatterer-free region of higher dielectric constant--provided there is a sufficient number of scatterers present (per wavelength) down the line.

---

*Private communication, H. W. Parker.

REFERENCES

1. D. J. Pounds and A. H. LaGrone, "Considering Forest Vegetation as an Imperfect Dielectric Slab," Report 6-53, Contract AF 19(604)-8038, Project 4603, The Electrical Engineering Research Laboratory, University of Texas, Austin, Texas (1963), UNCLASSIFIED, AD-410 836.

2. John Taylor, "A Note on the Computed Radiation Patterns of Dipole Antennas in Dense Vegetation," Special Technical Report 16, Contract DA 36-039 AMC-00040(E), SRI Project 4240, Stanford Research Institute, Menlo Park, California (February 1966), UNCLASSIFIED, AD-487 495.

3. D. L. Sachs and P. J. Wyatt, "A Conducting-Slab Model for Electromagnetic Propagation within a Jungle Medium," Technical Memorandum 376 and Internal Memorandum IMR-471, Defense Research Corporation, Santa Barbara, California (1966). [Also appears in Radio Science, Vol. 3 (New Series), No. 2, pp. 125-134 (February 1968).]

4. D. L. Sachs, "A Conducting Slab Model for Electromagnetic Propagation within a Jungle Medium II," Internal Memorandum IMR-471, Defense Research Corporation, Santa Barbara, California (30 September 1966).

5. Theodor Tamir, "On Radio-Wave Propagation in Forest Environments," IEEE Trans. on Antennas and Propagation, Vol. AP-15, No. 6, pp. 806-817 (November 1967).

6. James R. Wait, "Radiation from Dipoles in an Idealized Jungle Environment," Radio Science, Vol. 2 (New Series), No. 7, pp. 747-750 (July 1967).

7. Ching-Chun Han, "The Measurement of Electrical Properties of a Forest," Master Thesis, Department of Electrical Engineering, University of South Carolina, Columbia, South Carolina (1967).

8. H. W. Parker and G. H. Hagn, "Feasibility Study of the Use of Open-Wire Transmission Lines, Capacitors, and Cavities to Measure the Electrical Properties of Vegetation," Special Technical Report 13, Contract DA 36-039 AMC-00040(E), SRI Project 4240, Stanford Research Institute, Menlo Park, California (August 1966), UNCLASSIFIED, AD-489 294.

9. G. H. Hagn, H. W. Parker, and E. L. Younker, "Research-Engineering and Support for Tropical Communications," Semiannual Report 5, covering the period 1 April through 30 September 1965, Contract DA 36-039 AMC-00040(E), SRI Project 4240, Stanford Research Institute, Menlo Park, California (May 1966), UNCLASSIFIED, AD-486 466.

Preceding page blank

10. G. H. Hagn, E. L. Younker, and H. W. Parker, "Research-Engineering and Support for Tropical Communications," Semiannual Report 6, covering the period 1 October 1965 through 31 March 1966, Contract DA 36-039 AMC-00040(E), SRI Project 4240, Stanford Research Institute, Menlo Park, California (June 1966), UNCLASSIFIED, AD-653 608.

11. E. L. Younker, G. H. Hagn, and H. W. Parker, "Research-Engineering and Support for Tropical Communications," Semiannual Report 7, covering the period 1 April through 30 September 1966, Contract DA 36-039 AMC-00040(E), SRI Project 4240, Stanford Research Institute, Menlo Park, California (September 1966), UNCLASSIFIED, AD-653 615.

12. E. L. Younker, G. H. Hagn, and H. W. Parker, "Research-Engineering and Support for Tropical Communications," Semiannual Report 8, covering the period 1 October 1966 through 31 March 1967, Contract DA 36-039 AMC-00040(E), SRI Project 4240, Stanford Research Institute, Menlo Park, California (May 1967), UNCLASSIFIED, AD-675-459.

13. H. W. Parker and Withan Makarabhiromya, "Electric Constants Measured in Vegetation and in Earth at Five Sites in Thailand," Special Technical Report 43, Contract DA 36-039 AMC-00040(E), SRI Project 4240, Stanford Research Institute, Menlo Park, California (December 1967), UNCLASSIFIED, AD-674-740.

14. Hugh H. Skilling, Electric Transmission Lines (McGraw-Hill Book Co., Inc., New York, New York, 1951).

15. G. H. Hagn, G. E. Barker, H. W. Parker, J. D. Hice, and W. A. Ray, "Preliminary Results of Full-Scale Pattern Measurements of Simple VHF Antennas in a Eucalyptus Grove," Special Technical Report 19, Contract DA 36-039 AMC-00040(E), SRI Project 4240, Stanford Research Institute, Menlo Park, California (January 1966), UNCLASSIFIED, AD-484 239.

16. D. G. Neal, "Statistical Description of the Forests of Thailand," MRDC Report 67-019, Miliary Research and Development Center, Bangkok, Thailand (May 1967).